

**Sediment Suspension as a Control on Light Availability in a Coastal Lagoon**

Sarah Elizabeth Lawson  
Decatur, Georgia

B.A. Eckerd College, 2000

A Thesis presented to the Graduate Faculty of the University of Virginia in Candidacy for  
the Degree of Master of Sciences

Department of Environmental Sciences

University of Virginia  
January, 2004

---

---

---

---

## Abstract

Light availability is an important control on the productivity and distribution of seagrass. However, prevalent methods of examining light availability, fair weather monitoring or in-situ continuous recorders, can not adequately represent the spatial and temporal variability of light attenuation. In many systems, light attenuation is controlled by suspended sediment which will vary as a result of currents and waves. A process based modeling approach linking waves and currents to light availability overcomes the limitations of other methods of studying light attenuation. This approach was used in a shallow coastal lagoon, Hog Island Bay, on the Eastern Shore of Virginia. Hog Island Bay is an appropriate study site for this work because of a local extinction of *Zostera marina* (eelgrass) in the 1930's and current attempts at restoration.

Light availability in Hog Island Bay was approached through characterization of the bed sediments, modeling and field data of the hydrodynamics, field and lab work relating light attenuation to water column components, and modeling of the amount of light available at the sediment surface by modeling sediment suspension. The bed sediments in Hog Island Bay are generally fine-grained with the average grain size of 85% of the modeled area less than 125  $\mu\text{m}$ . The average grain size shows a trend of landward fining and the sediments show characteristic of flocculated transport. The hydrodynamics of Hog Island Bay are strongly responsive to wind forcing, with bottom stresses from wind driven waves dominant for 88% of the modeled area for a November 2002 model period and 56% of the modeled area for an August 2000 model period. November is typically a windier month than August because of the areas dominant storm type, the Nor'easter. Both current speeds and wave stresses also show a dependence on

depth. Light attenuation was dependent solely on total suspended solids concentration based on the field data. However, lab data showed that attenuation was also dependent on sediment size, with finer sediment attenuating more light. While total suspended solids concentration dominates the bulk attenuation, the spectral pattern of attenuation in Hog Island Bay was controlled by dissolved organic matter and chlorophyll. Based on the modeled average light availability at the sediment surface, 22% more of the modeled area was suitable habitat for seagrass in August 2000 than in November 2002. The main difference between these two modeled periods was wind speed, with higher wind speeds in November 2002. This result shows that meteorological forcing can be an important control on light availability at the sediment surface.

**Acknowledgements**

Thanks to my committee members, Karen McGlathery, Pat Wiberg and Jay Zieman for guidance and advice; David Fugate and Joel Carr for modeling work; Randy Carlson, Philip Smith, Jason Restein and Kathleen Overman for field assistance; Brenda Lam and David New for lab and field help; the McG lab group and grad students for everything; and the NSF VCR/LTER program and the Department of Environmental Sciences at UVA for financial support.

**Table of contents**

Abstract	1
Acknowledgements	3
Table of contents	4
Introduction	5
Sediment characteristics	15
Hydrodynamics	36
Light attenuation	58
Sediment suspension	83
Conclusion	101
References	104
Appendix	110

# Chapter 1: Introduction

Shallow coastal lagoons are common along the low to moderate energy coastlines of the southeastern Atlantic coast of the United States (Stickney 1984). These lagoons are typically dominated by benthic primary producers because most of the sediment surface is within the photic zone. The shallow depth also makes the sediment susceptible to wave suspension, which can lead to high light attenuation in the water column limiting primary productivity, particularly for species with high light requirements, such as seagrasses. Studies linking physical sediment transport processes and light attenuation are limited in number (e.g., Hanlon et al 1998, Olesen 1996), but represent an important step in understanding controls on light availability. This study will examine light attenuation in Hog Island Bay as a result of sediment suspension from waves, tides, and wind-induced currents and will link these physical processes to potential seagrass distribution.

Hog Island Bay is a shallow embayment in the Virginia Coast Reserve Long Term Ecological Research (VCR-LTER) site on the Atlantic side of the Delmarva Peninsula (Fig. 1). Since the 1930's, Hog Island Bay, as well as lagoons to the north and south, has undergone a major state change from a seagrass-dominated system to an algae-dominated system. The combined effects of a wasting disease and hurricane led to local extinction of eelgrass (*Zostera marina*) throughout the VCR until recently when eelgrass began recolonizing some of the bays. Following the extinction of eelgrass, anecdotal evidence indicates an increase in turbidity, which may be attributed to the loss of the sediment stabilizing effects of the seagrass and the decline of oyster populations. This

change in the trophic base impacts the entire system because it influences nutrient cycling (e.g., Sfriso and Marcomini 1997, Viaroli et al 1996, McGlathery et al in press) and higher trophic levels (e.g., Norkko et al 2000, Lepont et al 2000, Sfriso et al 2001).

Decreased light availability may limit the potential spatial extent of seagrass recolonization in Hog Island Bay. Light has been suggested as a limiting factor in seagrass distribution in Indian River Lagoon, FL (Kenworthy and Fonseca 1996, Gallegos and Kenworthy 1996) and the York River, VA, (Moore and Wetzel 2000, Moore et al 1997) where light availability was shown to be a stronger factor controlling seagrass success than nutrient enrichment and any concurrent epiphyte responses (Moore and Wetzel 2000). Even short term high turbidity events can affect the viability of seagrass beds (Longstaff et al 1999; Longstaff and Dennison 1999; Moore et al 1997). A decrease in biomass was seen as early as 3-6 days after a reduction in light availability (Longstaff et al 1999), with complete plant death resulting from month long shading for *Zostera marina L.* (Moore et al 1997) and *Halophila ovalis* (Longstaff and Dennison 1999, Longstaff et al 1999). *Halodule pinofilia* did not have biomass loss for the first 38 days of shading, but complete die-off was expected after 100 days (Longstaff and Dennison 1999).

This study will examine sediment suspension as a control on light availability in a shallow system. Numerous studies have examined the effects of light attenuation on seagrass and many studies have examined the conditions necessary for the suspension of marine sediments. However, few studies have linked these two areas together, examining both the causes and consequences of suspended sediments in a shallow coastal system. Most data currently available on light attenuation is based on fair weather monitoring,

which can miss high turbidity events, or on continuous light recorders, which capture fluctuations in light availability, but only represent a limited area. Physical process modeling overcomes the limitations and can give insight into both the frequency and causes of periodic low-light events that could affect the extent of seagrass recolonization and can expand field data spatially and temporally. The light requirements of seagrass have been well-defined but further work is needed to relate these light requirements to the processes such as sediment suspension that regulate light availability.

### **Approach**

The questions underlying this research are what are the controls on light attenuation in Hog Island Bay and how do these controls vary across the lagoon and throughout the year. This project examines sediment suspension and light attenuation through a combination of fieldwork and modeling. The fieldwork consists of measurements of light profiles, suspended sediment profiles, velocity profiles and sediment bed characteristics in Hog Island Bay. The modeling portion includes a hydrodynamic model, a wave model, a sediment suspension model, and an empirical equation relating water quality to light attenuation. The modeling portion is calibrated using the field data and allows examination of high wind events and extension of the field data temporally and spatially.

### **Objectives**

The objectives of this thesis were to:

- 1) Map the sediment characteristics of Hog Island Bay

- 2) Determine the relative importance of waves and currents for sediment transport (temporally and spatially)
- 3) Determine the effects of sediment and phytoplankton on light availability and quality
- 4) Determine the extent of light attenuation (temporally and spatially) based on seasonal estimates of phytoplankton biomass and measured and modeled values of suspended sediment transport.

### **Review of relevant literature**

The importance of light as a control on seagrass has been demonstrated in field and mesocosm studies. Duarte (1991) found that globally the depth limit of seagrass colonization was related to the diffuse attenuation coefficient for downwelling light ( $K_d$ ) by a log linear relationship. Decreasing seagrass biomass with increasing depth is also related to light attenuation (Duarte 1991). Dennison et al (1993) introduced the concept of using submerged aquatic vegetation (SAV) as an integrating light meter because the distribution of SAV is dependent on the average light availability. The light available to seagrasses is dependent on the depth of water and the concentration of water column components. An increase in nutrients, which can lead to an increase in phytoplankton, or an increase in suspended sediments will limit seagrass habitat to shallower depths. Mesocosm experiments using neutral density screens to reduce light availability showed a significant effect of light availability on seagrass growth and morphology (Short et al 1995). Physiological responses of seagrasses to light limitation, typically by adaptations that increase light harvesting ability such as an increase in biomass allocation to leaves,

have also been seen in other studies (Olesen and Sand-Jensen 1993, Enriquez et al 1995). Seagrasses are sensitive not only to the average light conditions, but also to short term variability in light availability. Moore et al (1997) observed a die-off of transplanted eelgrass at a York River site that experienced a month-long period of high turbidity due to increased particulate matter. Cabello-Pasini et al (2002) found a decrease in leaf sugar and starch contents after a three week period of light limitation caused by winter storms, indicating a decrease in the health of the plants.

Because light is a dominant control on the distribution of seagrass, extensive research has been done on the controls on light attenuation. Gallegos and Kenworthy (1996) created an equation to predict the spectral light availability at depth in the Indian River Lagoon, FL, based on turbidity, chlorophyll concentration and dissolved colored organic matter (also called gilvin and represented by the light absorption of a filtered sample at 440 nm). Turbidity was the dominant control on light availability, though dissolved organic matter was important seasonally. The calculated values of spectral light availability were within 15% of observed values (Gallegos and Kenworthy 1996). Gallegos (2001) examined three approaches to modeling the diffuse attenuation coefficient ( $K$ ) as defined by Beer's law: Monte Carlo modeling of the radiative transfer equations, integration of wavelength specific  $K$  from wavelength and concentration specific absorption and scattering coefficients, and linear partitioning of  $K$ . The linear model, the simplest model, predicted values of  $K$  with a 3-4% error after application of a correction factor suggested by Gordon (1989) (Gallegos 2001). Gordon (1989) suggested multiplying  $K$  by the cosine of the underwater zenith angle to remove effects of the light field. The diffuse attenuation coefficient is considered an apparent optical property

because it depends on the characteristics of the light field, such as angle of incidence, in addition to the characteristics of the medium (Kirk 1983), but the correction from Gordon (1989) allows modeling of  $K$  as an inherent optical property, dependent solely on the water column components. Similar approaches have been taken to determine the effects of water column components on optical properties in many places, including Otago shelf waters, New Zealand (Pfannkuche 2002), lakes of the Mackenzie delta (Squires and Lesack 2003), and the North Sea (Wild-Allen et al 2002).

A few studies have begun the process of linking waves and tides, two dominant physical forcing mechanisms in coastal areas, to light availability for seagrass. Dring and Lüning (1994) found a dependence of light available at the sediment surface on the spring-neap tidal cycle based on continuous records of light at two depths. The greatest light availability was recorded when low tides occurred at midday; the lowest light availability was recorded when high tides occurred at midday. The difference between light availability during spring and neap tides was not explained solely by the difference in water depth indicating that attenuation during the spring tides must be greater than during neap tides. The proposed explanation for this difference was sediment suspension because of higher spring tide velocities, but this was not quantified (Dring and Lüning 1994). Koch and Beer (1996) also related tides to light availability and seagrass distribution by examining the effects of tidal range on habitat suitability. They defined the upper limit of seagrass growth as the spring low water line, because seagrasses are susceptible to dessication if exposed, and the lower limit as the greatest depth receiving adequate irradiance. The effect of changes in water quality was shown to be heightened

in areas with large tidal ranges where seagrasses were limited to a very small range of depths (Koch and Beer 1996).

In addition to tides, the importance of wind-driven events for SEAGRASS has been demonstrated. Olsen (1996) related particulate inorganic matter concentration to both wave orbital velocity and secchi depth using linear relationships. This study created an empirical relationship between waves and light attenuation; it was one of the first to relate explicitly a physical forcing mechanism to light attenuation. Hanlon et al (1998) also related wind speed to light attenuation in Lake Okeechobee, FL and noted higher correlations in areas with fine grained bottom sediments. Cabello-Pasini et al (2002) found that an increase in the attenuation coefficient coincident with winter storms led to a die-off of seagrass on the open coast in a site in Baja California, Mexico, though plants in the adjacent, more protected, lagoon survived. The short-term variability in photosynthetic characteristics of the seagrass at these sites indicated the need for higher frequency of monitoring light availability (Cabello-Pasini et al 2002).

The work of Blom et al (Blom et al 1994, Blom et al 1992, Vanduin et al 1992) in shallow Dutch lakes provides the clearest antecedent for this study. They combined a 2-dimensional sediment suspension model (STRESS-2d), which accounts for differential transport of sediment fractions, (Blom et al 1992) with a light attenuation model (CLEAR) to examine the temporal and spatial patterns of light attenuation in Lake Marken (Vanduin et al 1992). Both models were calibrated with field data and the combination of the models was used to examine light availability under different wind conditions (Vanduin et al 1992). Blom et al (1994) also found that low settling velocity, high organic content particles controlled light attenuation and larger particles could

largely be disregarded. These studies examined only wind-induced suspension, mostly by waves. The current study takes a similar approach, but adds the effects of tides.

This thesis is divided into four sections addressing light attenuation in Hog Island Bay. The first section examines the sediment characteristics and their spatial patterns in the lagoon. The sediment bed characteristics determine what is available for suspension and what stresses are required to suspend sediments. The hydrodynamics of Hog Island Bay are examined next. Waves, tides, and wind-induced currents control the magnitude and frequency of sediment suspension events. To relate modeled and measured values of sediment suspension to light availability, the relationship between sediment concentration and light attenuation is then established. Chapter 4 uses data from Hog Island Bay to examine how suspended sediment, chlorophyll and dissolved organic carbon affect light quantity and quality at depth. The next chapter presents a numerical model to determine suspended sediment concentration as a function of wind and tides and to calculate percent light available at the sediment surface. This model incorporates the results of the first three chapters and extends field data in space and time to give a dynamic picture of light availability in Hog Island Bay. Several measures of light availability are used to characterize potentially suitable areas for seagrass recolonization.

### **Study site**

Hog Island Bay is a part of the Virginia Coast Reserve Long Term Ecological Research (VCR-LTER) site on the Eastern Shore of Virginia. Hog Island Bay is a back barrier lagoon behind Hog Island one of the many barrier islands on the Atlantic side of the Delmarva peninsula. Much of the lagoon is bordered by *Spartina alterniflora*

marshes both on the mainland and Hog Island. The shallow depths in Hog Island Bay make it potential habitat for seagrass and susceptible to wind suspension of sediments. The bathymetry of the area is dominated by the Machipongo Channel which runs roughly north-south and exits the lagoon between Hog and Cobb Islands. A second channel, the North Channel runs roughly east-west and exits the lagoon north of Cobb Island. These channels are surrounded by sub-tidal flats and a few intertidal relic oyster reefs. The lagoon historically supported abundant populations of oysters and seagrass. Primary productivity in the lagoon is now dominated by microalgae and macroalgae, particularly *Ulva lactuca* and *Gracilaria tikvahiae*. About 50% of the bay is less than 1 meter deep at mean low water. There is no significant source of freshwater input and the tidal range is 1 m (Fig. 1).

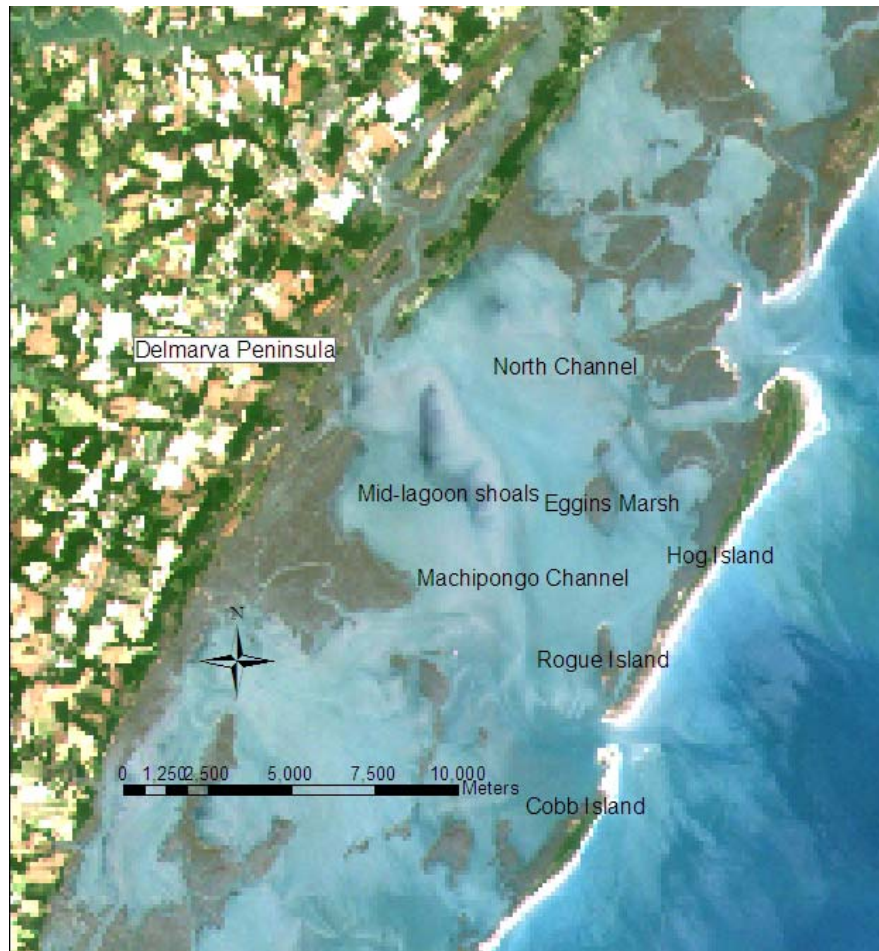


Fig.1 Map of study site.

## Chapter 2: Sediment characteristics

A study of the effects of sediment suspension must begin with the sediment bed, the source of sediment. Sediment grain size is a dominant control on critical shear stress, the stress required to mobilize bed sediments (e.g., Miller et al 1977) and on settling velocity (e.g., Dietrich 1982, Baba and Komar 1981). Through these parameters, sediment grain size determines both the mode of transport and vertical distribution of transported sediment. While the critical shear stress for all sediment sizes in a mixed-size bed may be similar (Wiberg and Smith 1987), fine sediment will be preferentially transported in suspension, where it can contribute to water column light attenuation. The amount of fine sediment at the bed surface and its characteristic settling velocity are then important considerations for light attenuation. The amount of fine sediment in a system also affects nutrient transport across the sediment-water interface (Huettel et al 2003), oxygen dynamics (Rasheed et al 2003), colonization by consumers (Meise and Stehlik 2003) and the growth and success of SAV, possibly through the above mechanisms (Terrados et al 1998, Bach et al 1998, Koch 2001).

Beds comprised of fine sediments are generally cohesive, requiring larger stresses for sediment suspension than size alone would suggest. In addition, the aggregation or flocculation of fine particles mediates the influence of particle size on sediment transport because many particles are not transported as single grains. Aggregation results in lower densities, higher concentrations of organic matter (Fennessy et al 1994, Dyer 1986), and higher settling velocities than single particles (McAnally and Mehta 2002, Krank and

Milligan 1992, Hill et al 2000). Flocculation of suspended sediment can affect water clarity (Hayakawa et al 2003) and contaminant transport (Milligan and Loring 1997, Drake et al 2002). Because of these effects, flocculation must be considered in systems with fine sediment. Sediment grain size characterization is important to this study because it describes the nature and amount of sediment available for suspension.

## **Methods**

### *Field methods*

Bed sediment samples were collected during two sampling efforts August-September, 2001 and June-July, 2002 (Fig. 1). Samples taken in 2001 focused on the area along the Machipongo Channel (blue), while samples taken in 2002 examined variation across the channel (yellow and red). The samples at the five locations shown in purple were taken to compare the two sampling methods used. Seven randomly selected sample locations from 2001 were re-sampled in 2002 to determine any change in sediment characteristics. All samples were taken using either an Ekman-style grab sampler (Fig. 1 yellow, purple and blue symbols) or hand-held acrylic coring tubes (Fig. 1 red and purple symbols) sectioned at 2cm intervals in the field. For both sampling methods, triplicate samples were taken at each location and a handheld GPS was used to record position.

### *Lab methods*

Sediment grain size for the grab samples and all depth intervals of the cores was determined by a combination of wet sieving (sand) and analysis on the

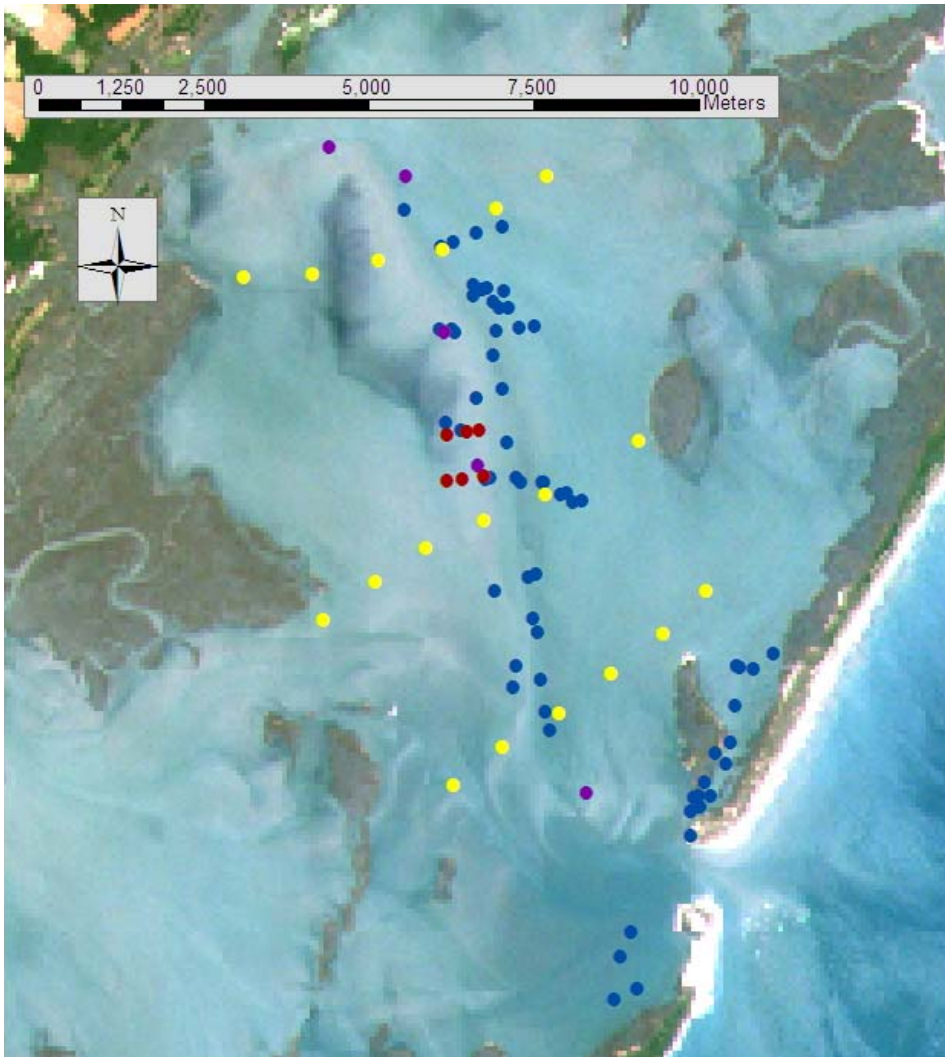


Fig 1 Location of sediment samples. The different colors represent different sampling periods. Samples in blues were taken using an Ekman-style grab sampler in August–September 2001. Samples in yellow and red were taken in June–July 2002, with samples in yellow taken using an Ekman-style grab sampler and samples in red taken using a hand-held acrylic coring tube. Samples in purple were taken with both the hand-held coring tubes and the Ekman grab sampler and were taken in July 2002.

Sedigraph 5100 particle size analyzer (silt and clay). The sediment-water mixture left after wet-sieving was allowed to settle for at least two days before excess water was siphoned off to achieve the necessary concentration for analysis on the Sedigraph (about 2.5 g dry weight of sediment per 100 ml of water). Samples were treated with 5 ml of bleach for at least 12 hours to remove organic matter (Gaffey and Bronniman 1993). On the day of analysis, 5 ml of 50% sodium hexametaphosphate solution was added to each sample as a dispersant. The sample was then dispersed sonically for 10 minutes using a Fischer sonic dismembranator immediately prior to analysis on the Sedigraph. Organic content was determined for all sediment samples by combustion of a bulk sample at 500° C for 8 hours (Murdoch and McKnight 1991).

#### *Data Analysis*

A continuous surface of mean bed sediment grain size was created using the GRID module of ARC-INFO. The data were interpolated using inverse distance weighted interpolation to create a grid with 200 m by 200 m cells, covering most of Hog Island Bay. This method of interpolation was chosen because it constrains the values to those observed, unlike spline interpolation which fits a line to the data and can therefore project values beyond those observed. Only data from the top 2 cm of the cores were included in the interpolation. This approach allowed examination of the percent of area characterized by different sediment sizes and provided the grain size data necessary for the sediment resuspension calculations described in Chapter 5.

Two sediment size characteristics, mean grain size and standard deviation, were calculated based on a base-two logarithmic scale, the phi scale. Sediment grain size in phi ( $\phi$ ) was calculated as

$$\phi = 2^{-D_{mm}}$$

Average sediment grain size of a sample was then calculated as a weighted average.

$$\phi_{avg} = \frac{\sum(\%W_i * \phi_i)}{\sum(\%W_i)}$$

where  $\phi_{avg}$  is the average grain size,  $\%W_i$  is the percent by weight in each size class, and  $\phi_i$  is the average diameter of the size class.

The standard deviation, or the sorting of the sediment size distribution, ( $\sigma$ ) was calculated as

$$\sigma_\phi = \frac{\sum(\%W_i * (\phi_{avg} - \phi_i)^2)}{\sum(\%W_i)}$$

(Dyer 1986). The standard deviation is indicative of the range of sizes present and can be suggestive of flocculated deposition.

### **Results and discussion:**

In general, Hog Island Bay sediments are fine grained. Based on the grid interpolated from the Ekman grab samples and the top 2 cm of the core samples, eighty-five percent of the area had an average grain size of fine sand (125-250 microns) or finer (Fig 2 and 3). The most prevalent size class is from 63- 88 microns, in the very-fine sand class (Fig 2). In general, the coarsest sediment is found near the inlet and the finest sediment is found near the mainland and the mid-lagoon area (Fig 3).

Sediment grain size in Hog Island Bay decreased with distance from the inlet (Fig. 4,  $r^2=0.54$ ,  $p < 0.0001$ ,  $n = 77$ ). Distance along the channel for a sediment sample was calculated by determining the distance from the inlet to the point in the channel nearest the location of the sediment sample. The four samples nearest the inlet were located behind Cobb Island and were left out of the regression because the transport at these locations is altered by local channels behind the islands. Points further from the

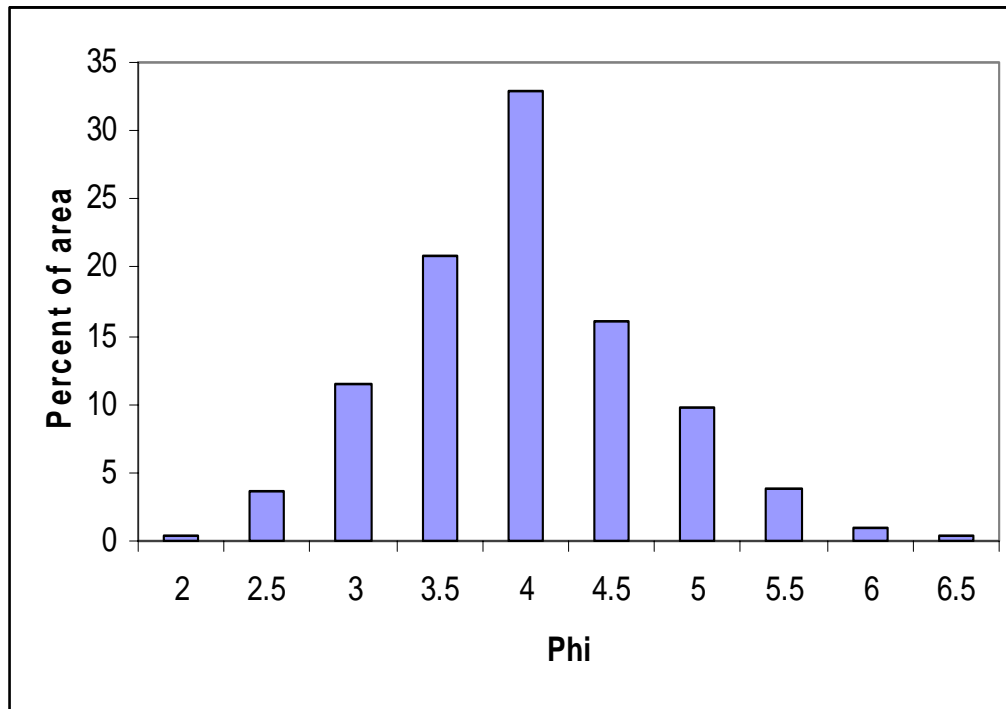


Fig 2. Spatial distribution of average sediment size in Hog Island Bay determined from the interpolated data. Phi sizes 2, 4, 6 correspond to diameters of 250, 63, and 16 microns, respectively.

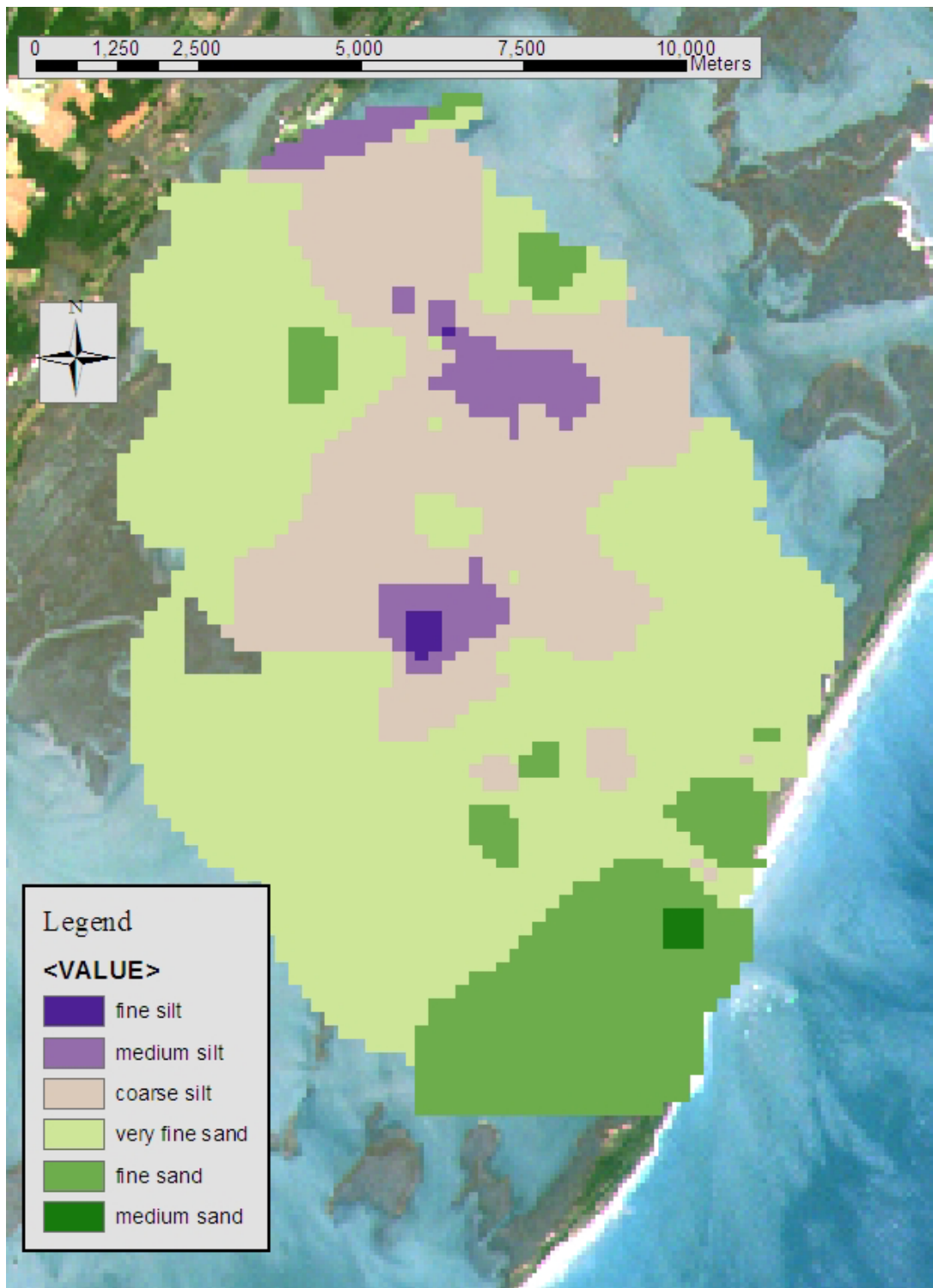


Fig 3 Average grain size in Hog Island Bay, interpolated from the sediment sample locations shown in Fig 1.

channel did not show greater deviation from the best fit line, indicating that the channel dominated water motion and therefore sediment grain size in the lagoon. No sediment samples were actually taken in the channel because of equipment limitations. Landward fining of sediment is common in estuarine systems because of gravitational circulation or a tidal asymmetry caused by narrowing at the head (Dyer 1986, Nichols and Biggs 1985, Dronkers 1986, Aubrey 1986). This tendency for landward transport was first noted by Postma (1954, 1961 cited in Dronkers 1986) and is based on a higher critical shear stress for suspension of fine sediment than for transport or deposition and differences in the settling fluxes during high and low water.

The influence of the channel on grain size was also seen in the across-channel data. The greatest changes in grain size typically occurred near the channel (Fig. 5) with deposition of fine material at the edge of the channel. Grain size remained constant for over two kilometers before fining. The water depth in this area was also relatively constant. The finer sediment samples were all located near marsh areas where the water velocity may be slowed. The sediment grain size seems to be consistent across the flats framed by fining at the edge of the channel and the edge of the marshes.

The three outlier points from this pattern (Fig. 5 and 6) all had finer sediment than other points of similar distance from the channel. The finer sediment may be related to lower current velocities because of some sheltering. A relationship between sediment characteristics and maximum current velocities has been noted for intertidal flats (Le Hir et al 2000). The outlier point in the north transect appeared to be sheltered by the shoal to its east. While the channel seemed to be the dominant control on sediment grain size, smaller features, such as the mid-lagoon shoals, also affected sediment size with coarser

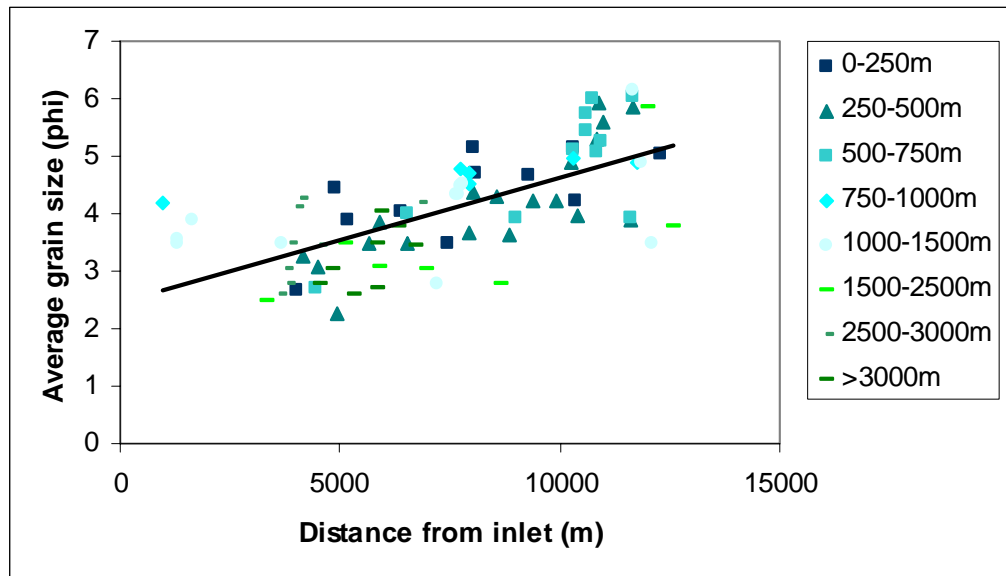


Fig. 4. Distance along the channel versus average size in phi. The different symbols in the graph represent different distances from the channel.

sediments behind the shoals (Fig. 7, red symbols in Fig 1). The change in depth may result in greater wave stress on top of the shoals, or a decrease in current velocity resulting in deposition of fine material as water moves from the channel over the shoals.

Sediment from cores taken in Hog Island Bay (Fig 1, purple symbols) showed minor changes in size with depth (Fig. 8). The cores taken in the northern part of the lagoon (Fig 8 a and b) showed a decrease in fine material near the surface, while the cores taken in the southern part of the lagoon, closer to the inlet, (Fig 8 c, d, and e) showed either no change or an increase in fine material. Cores from the third site are the only ones that showed an increase in clay and silt near the surface. These cores were taken near the mid-lagoon shoals, and may indicate an abundant supply of fine material or trapping of sediment by macroalgae. These samples were taken in July, a time when macroalgal biomass in this area is high and thick algae mats are common (McGlathery et al 2001). Fine material (clay and silt) does not move as bedload, only as suspended load. When the critical shear stress is reached, the fine sediment is suspended, with the amount of sediment suspended limited by both the capacity of the water to suspend material and the availability of material. The availability of fine material is often limited by “bed armoring” a coarsening of the sediment at the surface because of the removal of fine sediment from an active suspension layer or by cohesion and consolidation which lead to an increase in critical shear stress with depth below the surface. The decrease in fine material near the surface in some cores suggests that if an active suspension layer exists in these areas, it is less than 2 cm thick.

Percent organic matter and mean sediment phi size were positively correlated (a larger phi size is finer sediment), with average grain size explaining 60% of the variation

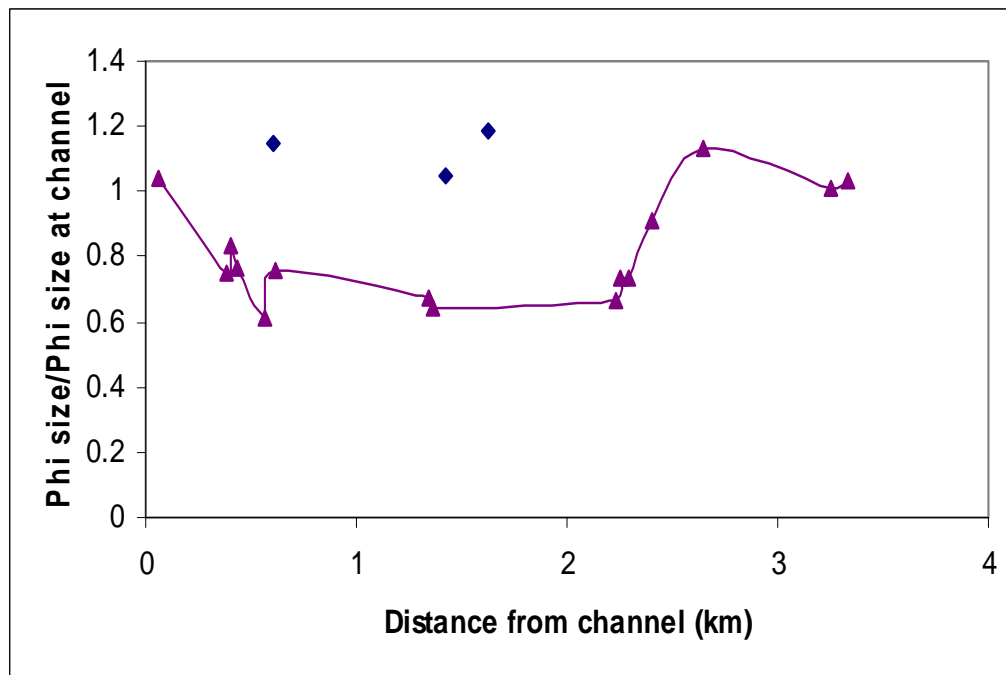


Fig. 5. Relationship of distance from the channel of the 2002 samples and grain size ( $\phi$ ) normalized to the grain size predicted by the distance from the inlet. Three points, shown in blue, did not fit the pattern exhibited by the other data.

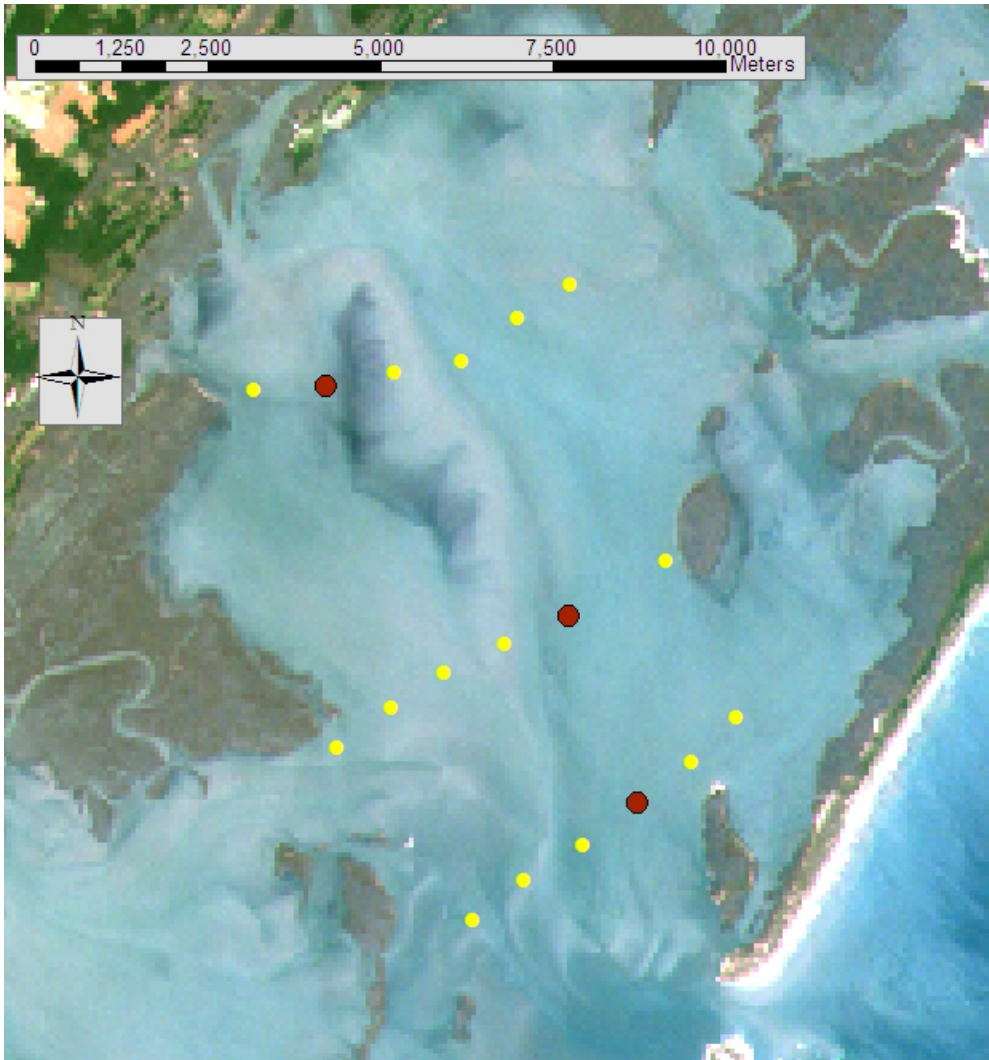


Fig 6. Location of sediment samples that do not fit the trend of coarsening away from the channel, consistent grain size on the flats and fining of grain size near the marshes. Samples shown in red do not fit the trend; those shown in yellow do.

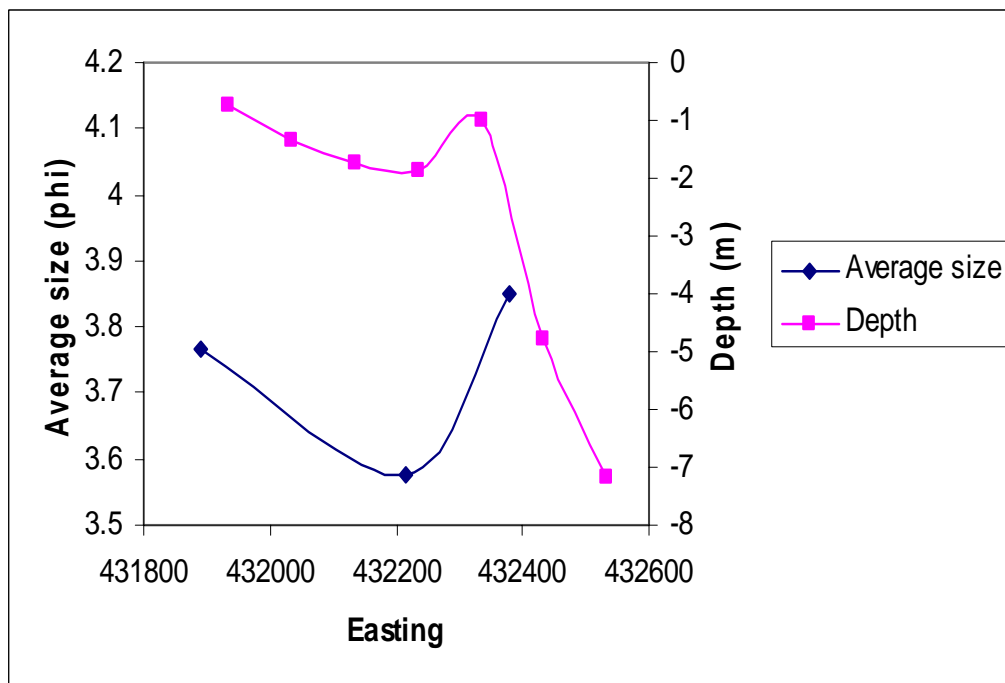
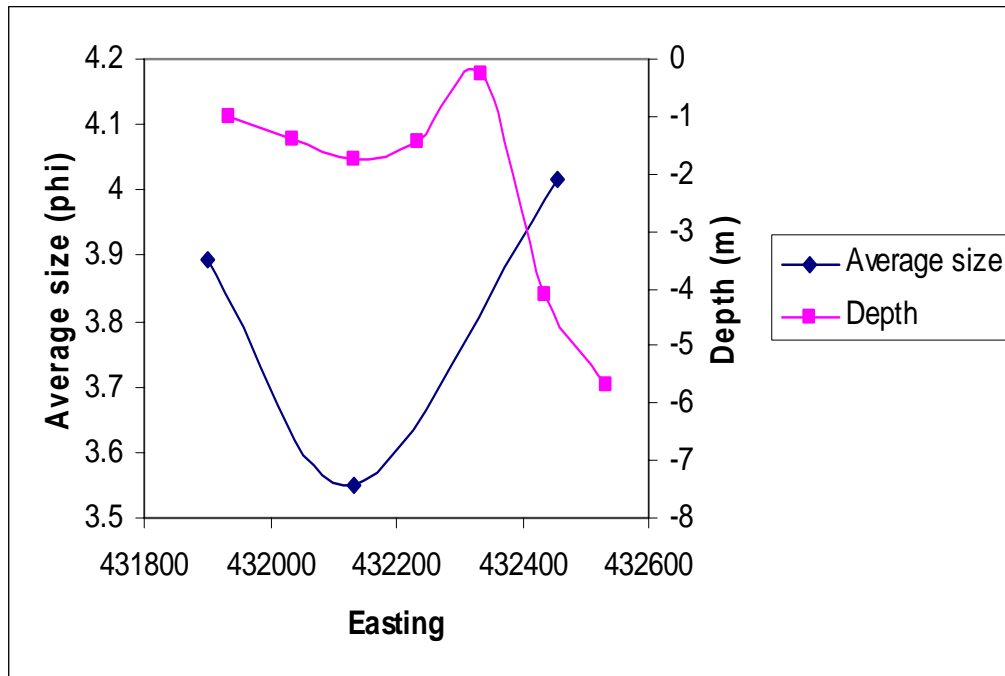


Fig. 7. Relationship of average grain size to depth at the mid-lagoon shoal sites. Easting (the east-west component of position in UTM) is used to represent distance across the shoals, which are oriented roughly north-south. The channel is east of the data shown in these graphs.

in sediment organic matter based on the August-September data (40% for the whole data set) (Fig. 9). Five points from the June-July, 2002 data were noticeably higher than the general trend of the data. These points were located near the channel (four on the west side, one on the east side) near the mid-lagoon shoal sites. Macroalgal biomass in this area is typically very high particularly in the summer months with a macroalgal crash typically in June or July (McGlathery et al 2001). Because increased organic matter was seen in sediments in an area of high benthic productivity in July but not in August, the proximity to a source of organic matter seems to have a time-limited, seasonal effect on sediment organic matter (Sfriso and Marcomini 1999, Rusch et al 2000).

The fine sediment regions of the bed in Hog Island Bay are more poorly sorted than the coarser sediment areas (Fig. 10). This poor sorting suggests flocculated deposition. In flocculated sediment deposition, the fine tail of the distribution is extended because the fine sediments are deposited as aggregates and are therefore not sorted. Flocculated sediment typically includes organic matter (Fennessy et al 1994, Dyer 1986), indicating that areas with a higher percentage of fine sediment deposited as flocs will also have higher organic matter contents.

Fine sediment generally erodes at a higher shear stress than it deposits. Given the large amount of fine sediment in Hog Island Bay, this difference between erosion stress and deposition stress and the low settling velocities of fine sediment can result in sediment remaining in suspension for long periods of time following a single high stress event. The single particle settling velocities of sediment particles from 63  $\mu\text{m}$  (transition from sand to silt size classes) to 4  $\mu\text{m}$  (transition from silt to clay) calculated using Stokes law range from 0.36 to 0.001  $\text{cm s}^{-1}$ . These settling velocities correspond to settling

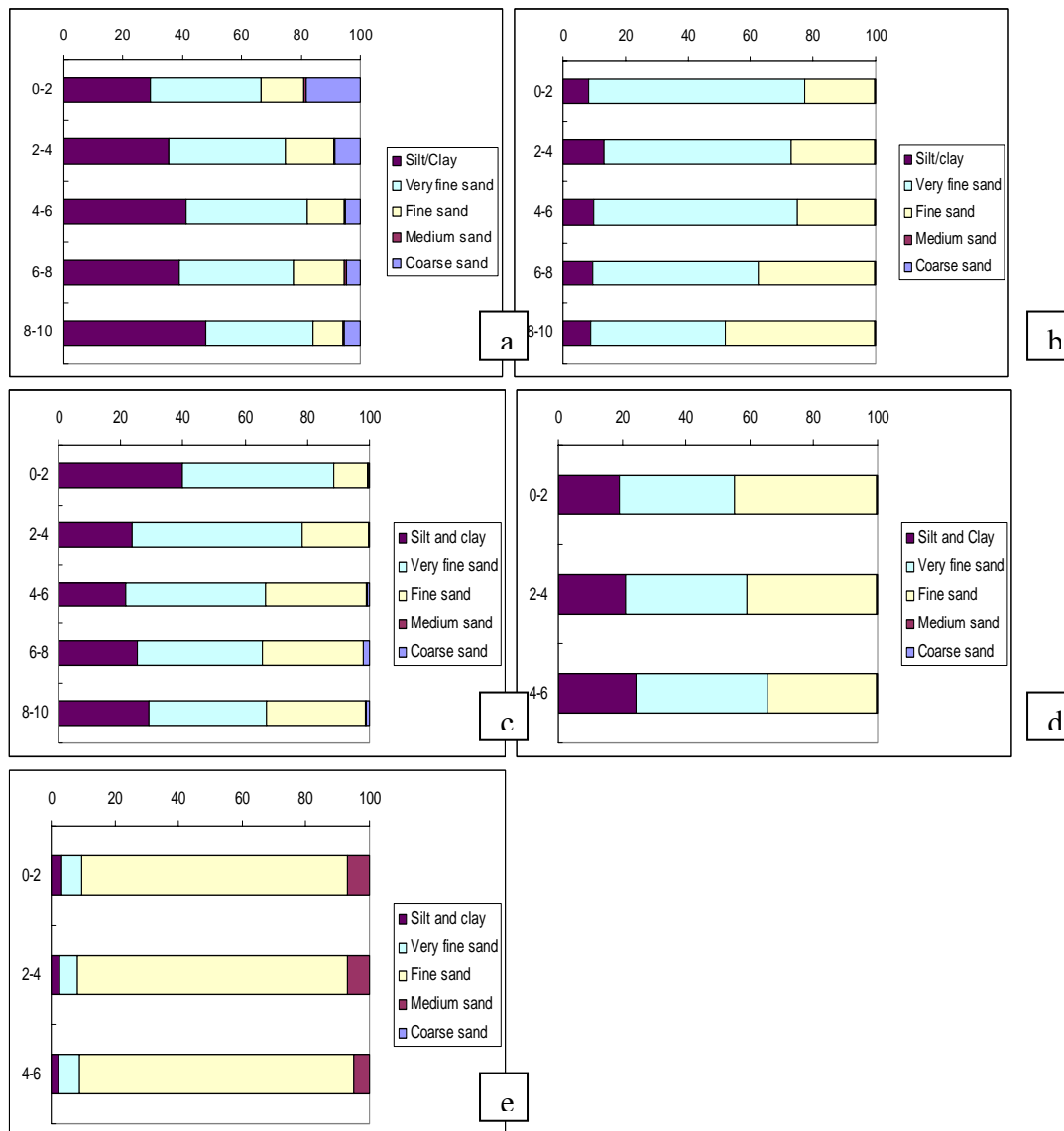


Fig 8. Changes in sediment composition with depth at five sites. The graphs are arranged with the furthest north sample first, the furthest south sample last. The vertical axis is depth in the core (cm) and the horizontal axis is percent.

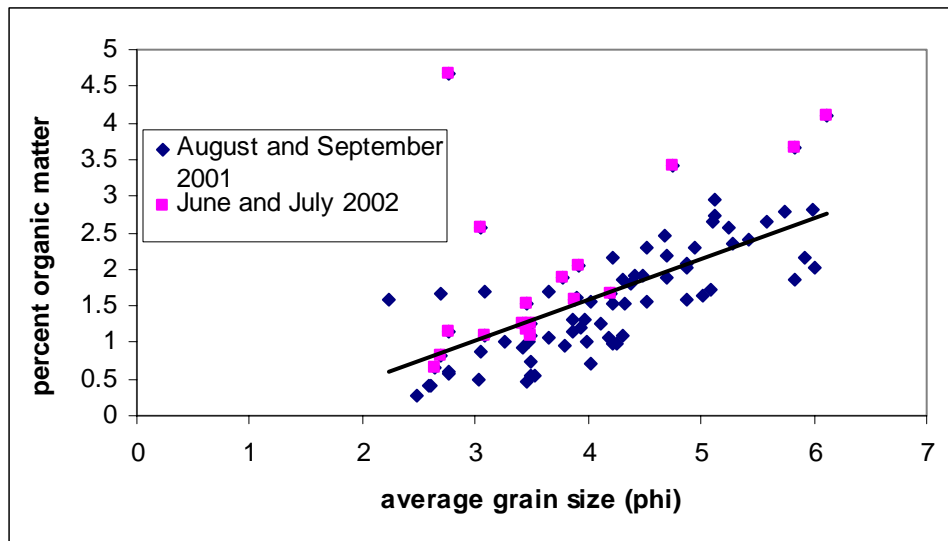


Fig. 9. Percent organic matter and average grain size.

times from about 5 minutes to 19 hours in 1 m of still water (Table 1). Even with completely still water at slack tides, if single particle settling dominates, these results show that sediment will remain in suspension for long periods of time because the settling time is long relative to the length of time the velocities will be below the suspension threshold. Because of the low settling velocities and low deposition stresses of fine sediment, the increased sediment suspension from a single high stress event can have a long duration. Blom et al (1994) found that in a shallow lake the attenuation of these fine particles is most important for light attenuation. Seagrass is sensitive not only to average conditions, but also the duration of low light events (Longstaff et al 1999; Longstaff and Dennison 1999; Moore et al 1997, Cabello-Pasini et al 2002), making quantification of the duration of suspension events important. Seagrass species are affected by light limitation as short as 3-6 days (Longstaff et al 1999). The low settling velocities and low deposition stresses mean that once the critical stress for suspension is exceeded only a moderate stress is required to maintain the sediment in suspension.

The fine sediment deposits in Hog Island Bay show characteristics of flocculation such as poor sorting and high organic contents, indicating that single particle settling velocities (Table 1) are probably underestimates. Values given for floc settling velocities vary widely, with a range of 0.02 to 3.94 mm s<sup>-1</sup> observed in two seasons in two Danish embayments (Mikkelsen 2002). This range of values is consistent with the range seen in other studies (eg, Shanks 2002, Manning and Dyer 2002, Curran et al 2003). In general, floc settling velocity is higher than single particle settling velocity (McAnally and Mehta 2002, Krank and Milligan 1992, Hill et al 2000) and is related to floc diameter (Sternberg et al 1999, Mikkelsen and Pejrup 2001) and often to suspended sediment concentration

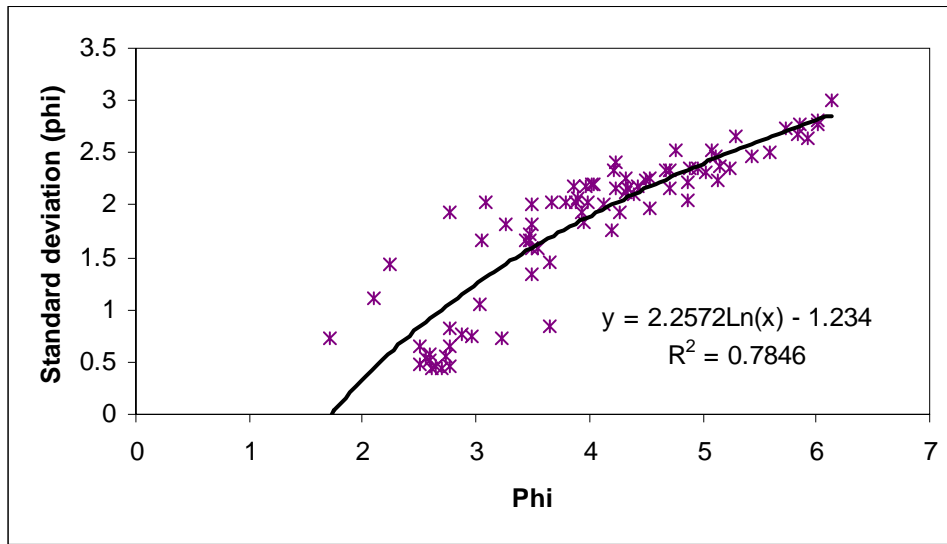


Fig. 10. Standard deviation of the sediment size against the average sediment size for all samples.

Size (um)	Size (cm)	Settling velocity(cm/s)	Time to settle 1 meter (minutes)
63	0.0063	0.36	5
30	0.003	0.08	21
15	0.0015	0.02	82
8	0.0008	0.01	290
4	0.0004	0.001	1158

Table 1. Theoretical values of settling velocity and settling time for fine sediment calculated from Stokes Law.

(Dyer et al 1996). These relationships have not been examined in Hog Island Bay, but the poorer sorting of finer sediment is suggestive of flocculation (e.g., Milliagan and Loring 1997), which may prove important for the rate of water column clearing.

The amount of fine sediment in Hog Island Bay will also affect light attenuation because on a mass basis, fine sediment attenuates more light than coarse sediment. Fine sediment has a greater surface area to volume ratio than coarse sediment resulting in greater light scattering from fine sediment (Ruffin 1998, Baker and Lavelle 1984). Flocculation may again be important, as flocculation affects the calibration of optical instruments (Mikkelsen and Pejrup 2000, Bunt et al 1999). The in-situ particle size spectra will determine light scattering because flocculation will change the surface area to volume ratio. The effects of sediment size on light attenuation is examined more fully in Chapter 3, but the need to evaluate these effects is created by the amount of fine sediment in Hog Island Bay.

## **Conclusions**

The sediment dynamics in Hog Island Bay are controlled by the Machipongo Channel. The average sediment size decreased with distance from the inlet, while organic content increased, though this relationship is somewhat dependent on seasonal productivity. Sediment size also varied with distance from the channel across the surrounding flats. The amount of fine sediment in Hog Island Bay is important because of the possibility of long durations of suspension and the greater mass specific light attenuation of fine sediment. The poor sorting of fine sediments indicated flocculated deposition of fine sediments. This flocculation will affect in situ size spectra of

suspended sediment and therefore, the duration of suspension and the extent of light attenuation.

## Chapter 3: Hydrodynamics

In addition to sediment supply, sediment suspension is controlled by the stresses acting on the sediment bed. LeHir et al (2000) list five physical forcing mechanisms for sediment transport in coastal systems: density-driven circulation, drainage, tides, wind-induced circulation, and waves. In Hog Island Bay, freshwater inflow is small, so density-driven circulation can largely be disregarded. The lack of freshwater inflow also makes modeling of the sediment concentrations easier because Hog Island Bay does not have a significant external source of sediment. The drainage process may be important in the marshes and intertidal flats (Bassoullet et al 2000), but will not be considered in this study because intertidal flats represent only 7% of the surface area of Hog Island Bay (Oertel 2001), making considerations of bed consolidation that may occur during drainage of these areas relatively unimportant. Dewatering of the porous bed layer in exposed areas is however considered in the modeling of tidal velocities for the lagoon (Zelenke 2001, Fugate 2002, Fugate and Friedrichs in prep). Christiansen et al (2000) studied sediment transport on a marsh bordering Hog Island Bay and found deposition during high tides and storms, but no tidal erosion from the marsh surface, though heavy precipitation may cause erosion from the marsh surface. The final three forcing mechanisms suggested by Le Hir et al (2000): tides, wind-induced circulation, and waves, can all be considered important in Hog Island Bay, but the time scales on which these processes act differ. The tidal currents should create a background pattern of sediment suspension with variations due to the spring-neap cycle. Storms and wave transport will be more episodic and should create peaks in suspended sediment

concentration. Because wave stress is dependent on depth, tides and waves should also have an interaction greater than just the addition of the stresses. In this chapter, movement of water in Hog Island Bay without wind is considered first, followed by a description of how wind affects the water movement and bed stresses.

### **Methods:**

The hydrodynamics of Hog Island Bay were modeled using a 2D finite element hydrodynamic model, Bellamy, (Fugate in prep) and a third generation wave model, Simulating Waves Nearshore (SWAN). Both models were forced with wind data from the NOAA CO-OPS tower in Kiptopeke, Virginia and used bathymetry data from the VCR-LTER (Oertel et al 2000). The bathymetry data were collected in 1999-2000 using Trimble 4000SE GPS Receivers, the Trimble NavBeacon XL, the Innerspace Digital Depth Sounder (Model 448), and the Innerspace DataLog with Guidance Software. Two time periods were modeled: August 2000 and November 2002. These two time periods were selected to give a range of wind conditions. The dominant storms in this area are Nor'easters which occur from October to April and frequently produce wave heights of 1.5 to 10 m on the open coast (Davis and Dolan 1993). The wind data from the two time periods modeled show the seasonality of the winds with higher wind speeds and more winds from the north in November (Fig 1).

The hydrodynamic model was used to examine the changes in water level of the tides and the depth-averaged velocities from tide and wind currents. In addition to wind data, the hydrodynamic model was forced by measured tidal elevations from NOAA stations at Wachapreague and Kiptopeke, VA, at the northern and southern end of the modeled area respectively, and run with 300 time steps per tidal cycle, allowing 6 tidal

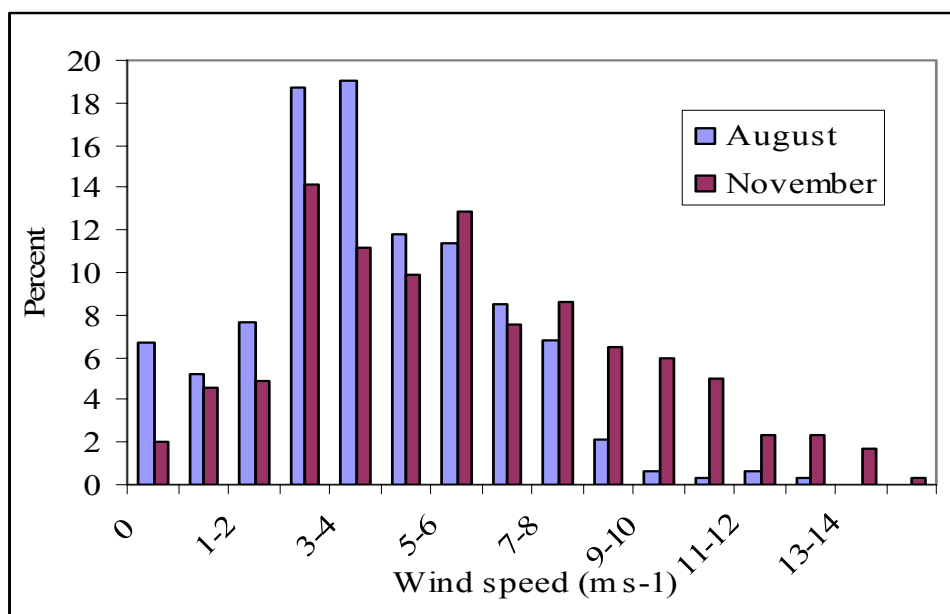
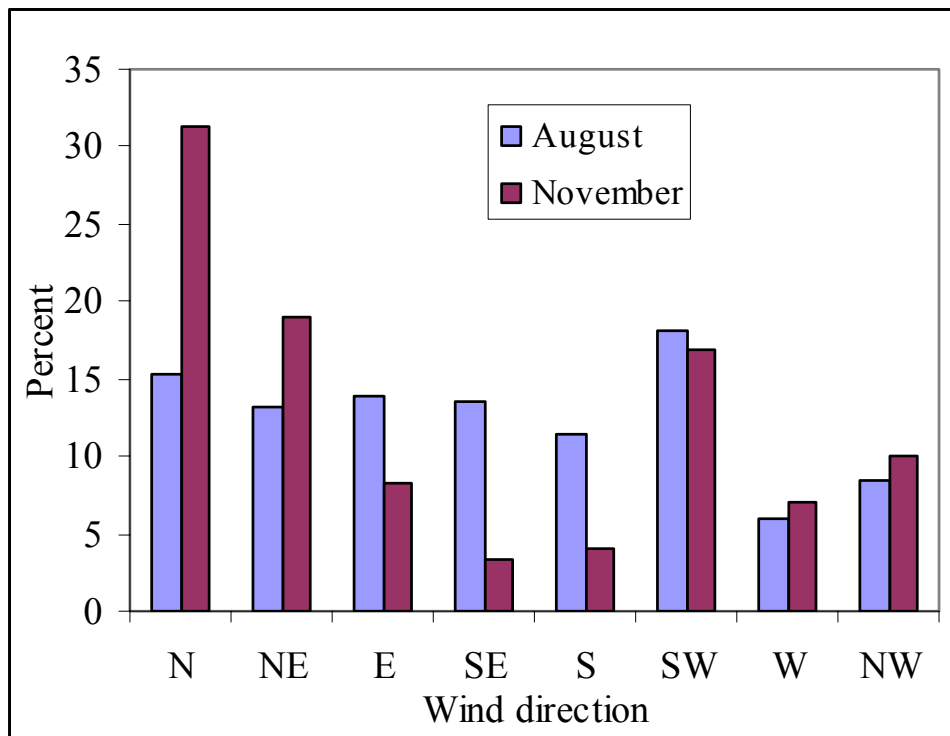


Fig. 1 Comparison of the wind direction and speed during the two modeled periods. The November period has more wind from the north and higher wind speeds.

cycles for equilibration before output was saved (Fugate and Friedrichs in prep). The model includes Darcian diffusion in intertidal areas and includes pressure gradients, bottom stress (Ip et al 1998, cited in Fugate and Friedrichs in prep), local acceleration, wind stress, and a depth-dependent bottom friction coefficient (McLaughlin et al., 2003, cited in Fugate and Friedrichs in prep). The modeled velocity results (mean = 21.2 cm s<sup>-1</sup>, maximum=48.7 cm s<sup>-1</sup>) agree with data collected by a Sontek Acoustic Doppler Profiler (ADP) (mean = 22.0 cm s<sup>-1</sup>, maximum=49.7 cm s<sup>-1</sup>) (Fugate and Friedrichs in prep). Results of the hydrodynamic model were interpolated into a grid of 200m by 200m cells using inverse distance weighted interpolation in ArcINFO.

SWAN was used to determine wave properties: significant wave height ( $H_{sig}$ ), wave period (T), and wavelength (L). Water levels from the hydrodynamic model were used in the calculation of wave characteristics using SWAN. SWAN includes wave shoaling and wind-wave generation and has been shown to accurately represent waves in back barrier systems (Ris et al 1999). We calculated  $H_{sig}$  and T with a 50 minute time step for each cell in the Hog Island Bay grid. For this study, SWAN was run using the default bottom friction and triad wave interactions. The hydrodynamic model output occurs on 49.82 minute time steps, not the 50 minute time steps used in SWAN, resulting in a time offset of 2:20 hours at the end of the November model run, the longer model run. The data were analyzed on a cell by cell basis. All time steps with a depth lower than the following time step were considered flood tide and all time steps with a greater depth than the following time steps were considered ebb tide. Time steps in which the depth was more than 0.2m above the average depth were considered high tides; those in which the depth was more than 0.2m below the average depth were considered low tides.

*Tide Stress calculation:*

The hydrodynamic model used in this study produced vertically averaged velocities. Shear stresses were calculated from these velocities using a drag coefficient calculated from a Manning's roughness coefficient (n). The roughness coefficient was calculated as

$$n = 1/((2*(g*8)^{1/2})/h^{1/6}*\log_{10}(h*D_{84}^{-1})+1)$$

where n is the Manning roughness coefficient, h is the water depth (m), g is gravitational constant (9.8 m/s<sup>2</sup>), and D<sub>84</sub> is the grain diameter that 84% of the sediment is smaller than. The drag coefficient was then determined based on the Manning equation as

$$C_d = g * n^2 / (h^{1/3})$$

where C<sub>d</sub> is the drag coefficient. The current shear stress was calculated as

$$\tau_{bTIDE} = C_d * U_{av}^2 * \rho_w$$

where  $\tau_b$  is boundary shear stress, U<sub>av</sub> is the average velocity, and  $\rho_w$  is the density of water. The shear stress calculated in this way is non-directional and was calculated for each cell for each time step.

*Wave Stress calculation:*

The wave stress was calculated from the H<sub>sig</sub> and T modeled from SWAN. The wave orbital velocity (U<sub>om</sub>), calculated from H<sub>sig</sub> and T, is related to the wave shear stress by a friction factor (f) which was calculated based on the wave amplitude (a<sub>b</sub>). When the ratio of the wave amplitude to the roughness length (k<sub>s</sub> = 3D<sub>84</sub>) is greater than or equal to 100

$$f = 0.04 * (a_b/k_s)^{-1/4};$$

when the ratio a<sub>b</sub>/k<sub>s</sub> is less than 100 but greater than 10

$$f=0.4*(a_b/k_s)^{-3/4};$$

For ratios  $a_b/k_s$  less than 10, the friction factor was represented as a constant

$$f = 0.071 (0.4*10^{-3/4}).$$

The shear stress due to waves was then calculated as

$$\tau_{bWAVE} = \rho(f/2)(U_{om}^2).$$

The wave and current stresses were represented as scalars with no direction, so they were combined to represent total stress as

$$\tau_{bTOTAL} = (\tau_{bWAVE}^2 + \tau_{bTIDE}^2)^{1/2}$$

## **Results and Discussion:**

### *Tides without wind*

The movement of water in Hog Island Bay is dominated by the Machipongo Channel. The basic tidal movements can be analyzed using results from the hydrodynamic model for August 2000, without any wind effects. Hog Island Bay has semi-diurnal tides with a delay of about 1.5 hours from the inlet to the mainland (Fig. 2). Depictions of the average relative velocities on ebb and flood tide show lower velocities in shallow areas and farther from the inlet. Water entering and leaving the bay typically runs parallel to the channel, unless it is diverted by shallow areas, such as the mid-lagoon shoals on the west side of the channel and Eggins Marsh and Rogue Island on the east side (Fig. 3). Velocities in the channel are higher ( $0.2 - 0.3 \text{ m s}^{-1}$ ) than on the flats ( $0.05 - 0.1 \text{ m s}^{-1}$ ).

Depth controls much of the spatial variation of the tides. Average depth explained about 20% of the spatial variation in average flood and ebb velocities in the bay ( $R^2 = 0.22$ ,  $p < 0.001$  (flood),  $R^2 = 0.24$ ,  $p < 0.001$  (ebb)). Average velocities binned by depth (0.1 m

bins) showed increasing tidal velocities with increasing depth (Fig. 4a). The slope of the relationship decreased at depths greater than about 2.7 m. Most of the data points (84%) were shallower than this break point (Fig 4b). This value does not represent the percent of the lagoon less than 2.7 m, however, because the finite element mesh used in the hydrodynamic model uses more elements in shallow areas. The few data points higher than this value explain some of the scatter in the values for higher depths, because there are fewer points averaged. For points with depths shallower than 2.7m depth explained 92% of the variation in flood velocities and 94% of the variation in ebb velocities. These binned values removed the effects of distance from the inlet. The dependence of velocity on depth is caused by friction and the speed of a shallow water wave. When water depth is less than  $L/20$ , the wave speed is entirely dependent on depth. This shallow water wave speed then represents the maximum speed at which the tidal wave can move into the lagoon. Typically, the speed of the tide is limited more by friction than the shallow water wave speed (Shetye and Gouveia 1992).

In Hog Island Bay, tidal asymmetry, in terms of both duration and velocity, changes with depth and distance from the inlet. The difference in average duration of flood and ebb tides is small (less than two minutes for most of the bay), but does show a spatial pattern of longer flood tides near the inlet and longer ebb tides near the mainland (Fig 5). The difference in duration of tides has to be reflected in a difference in velocities on ebb and flood tides (Fig 6). The velocities on ebb tide are greater near the inlet, while flood tide velocities are greater near the mainland. A tidal asymmetry of faster flood tide velocities is common in estuarine systems because the peak velocities on ebb tide occur in lower depths of water and are limited by shallow water wave speed (Dronkers 1986,

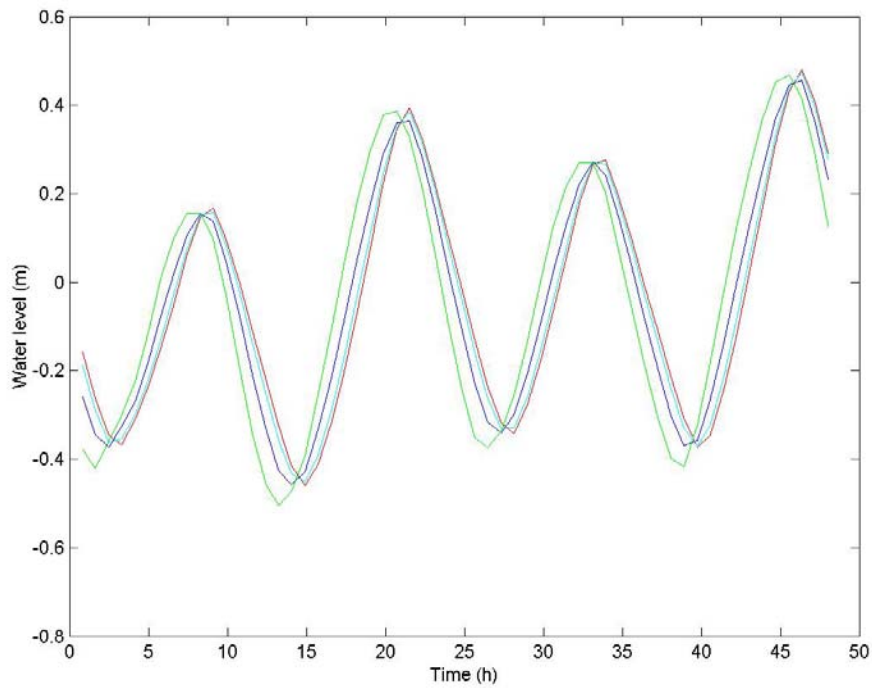


Fig. 2 a) Tidal elevation at four locations in the bay, showing that high and low tides occur earlier at the inlet. b.) Locations of the four points shown in Fig 2a). The colors correspond to those in the graph.

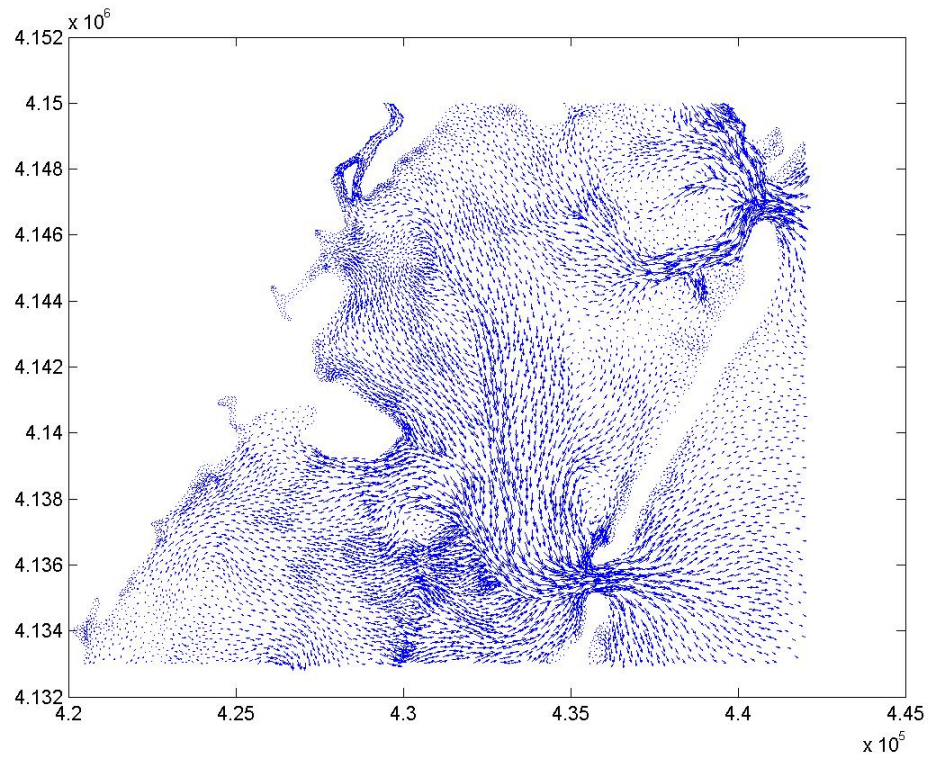


Fig. 3a) Time-averaged relative ebb tide velocities for the August model run with no wind effects.

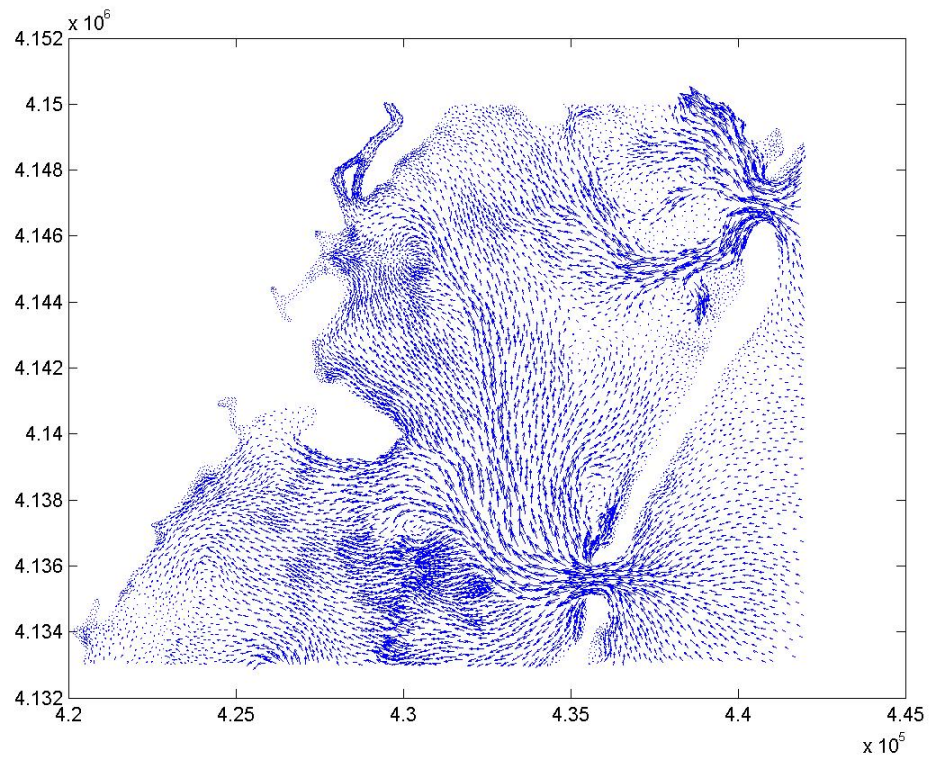


Fig 3b) Time averaged relative velocity for flood tides from the August model run with no wind effects.

Aubrey 1986). By examining the difference between flood and ebb tide velocities by depth, the transition from higher flood to higher ebb velocities occurs between 1.3 and 1.4 m. The transition from ebb to flood dominated also occurs where the width of the lagoon become restricted by the fringing marshes (Fig 5). Flood dominance is common in shallow narrow estuaries without extensive flats (Shetye and Gouveia 1992), which may explain the change in tidal asymmetry.

#### *Wind effects*

The harmonic tides presented above are modified by the effects of wind drag on the water surface. The wind can either enhance or oppose the tidal flow (Fig 7). Like average velocity and duration, the importance of wind effects on currents is depth dependent. The average difference in velocity is greatest in the shallow areas, with direction considered in determining the difference between wind and no wind conditions at each time step but not in the averaging (Fig 8). The decrease in depth near the mid-lagoon shoals on the west side on channel is mirrored in an increase in the difference in speed between the wind and no wind conditions.

Winds are also responsible for the creation of waves in the lagoon. The differences in wind conditions are seen in the wave characteristics from the two model periods. The November results showed an average significant wave height of 0.12 m and a maximum significant wave height of 0.53 m. The August results showed an average significant wave height of 0.06 m and a maximum significant wave height of 0.39 m (Fig 9). For both months, modeled wave height (Fig 9) and wave period (Fig 10) did not vary much across the lagoon as evidenced by the narrow distribution of average period and significant wave height. The average wave period in November was longer than the

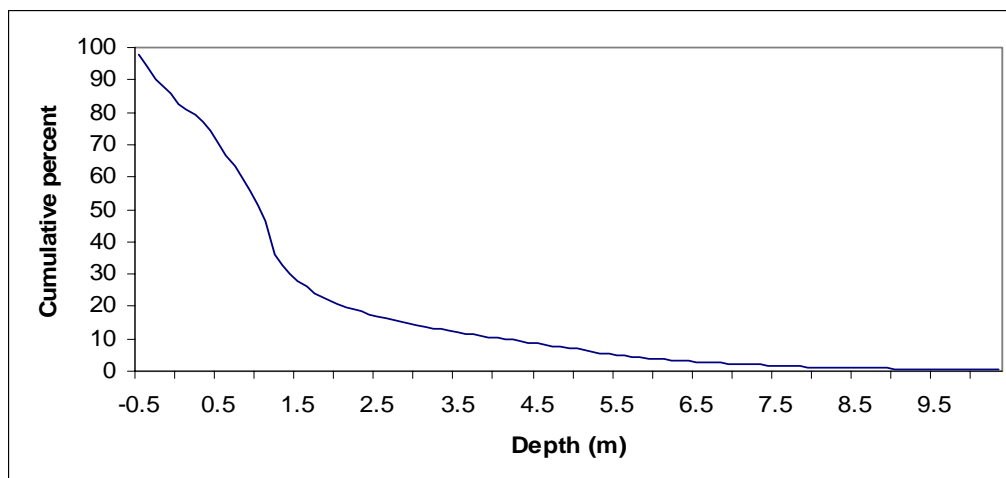
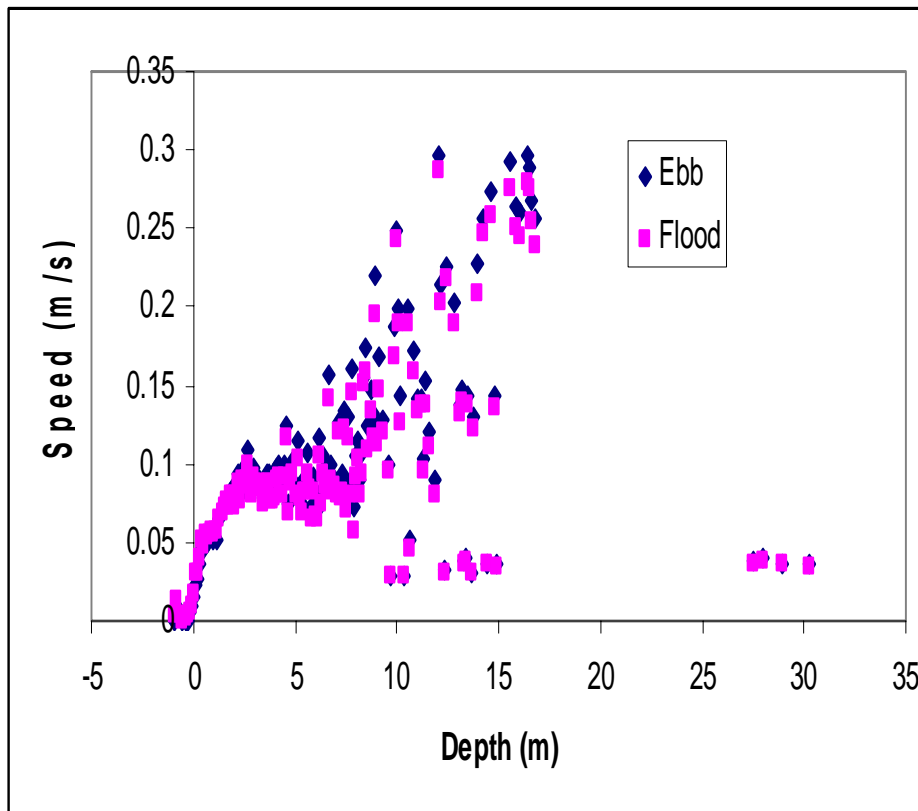


Fig 4 a.) The relationship between average depth and average ebb and flood velocities, modeled without wind forcing. b.) Cumulative distribution of average depths for the elements used to make Fig 4a. Most of the elements have depth lower than 2.7 meters (84%), but this can not be used to represent percent of the lagoon bottom at each depth because the model grid includes more elements in shallow waters.

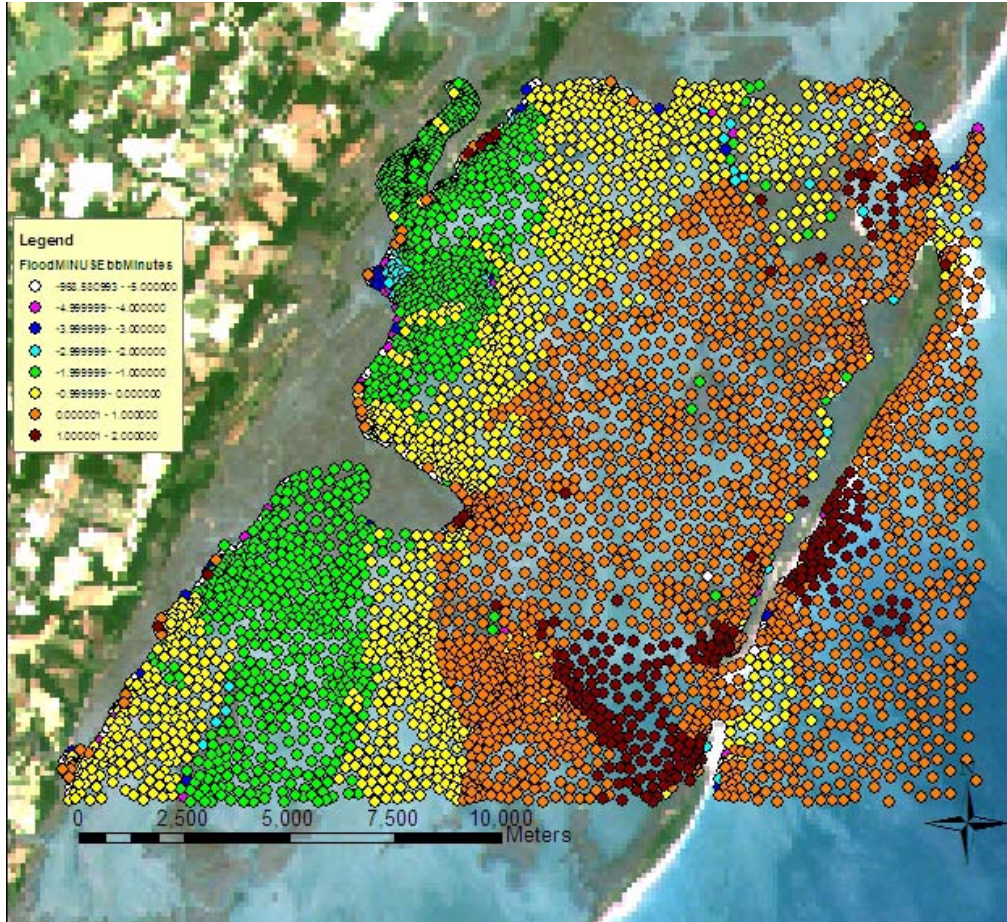


Fig 5. Average duration of flood tide minus average duration of ebb tide both in minutes. The junction between yellow and orange is the junction between longer ebb to longer flood tides.

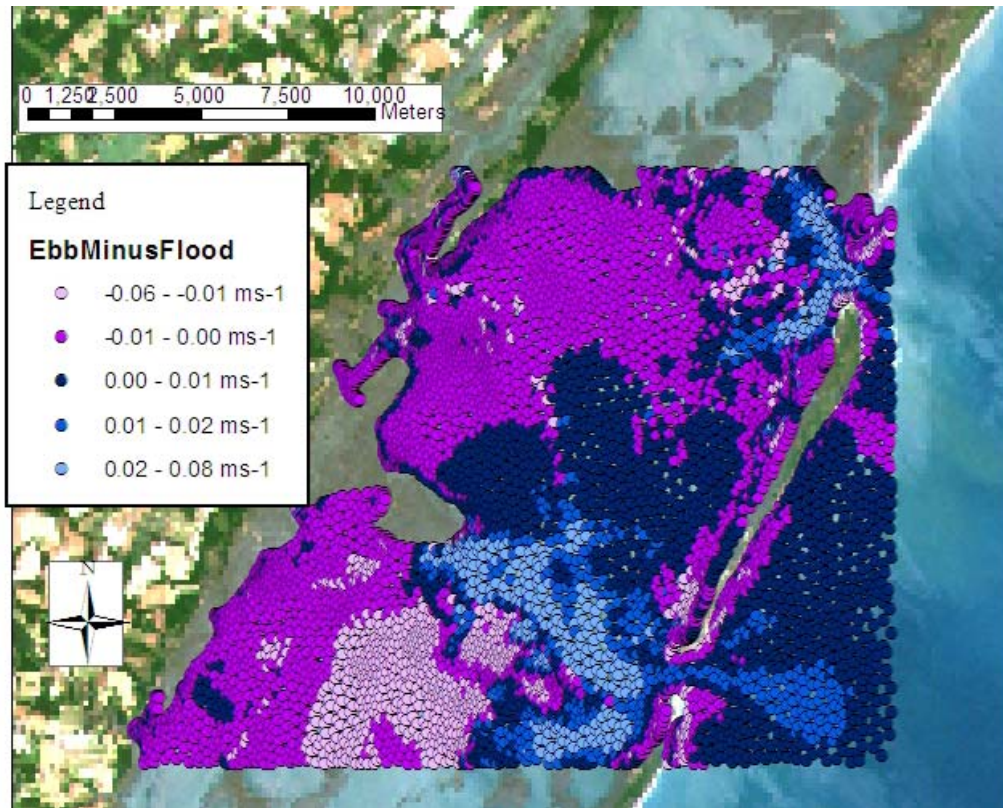
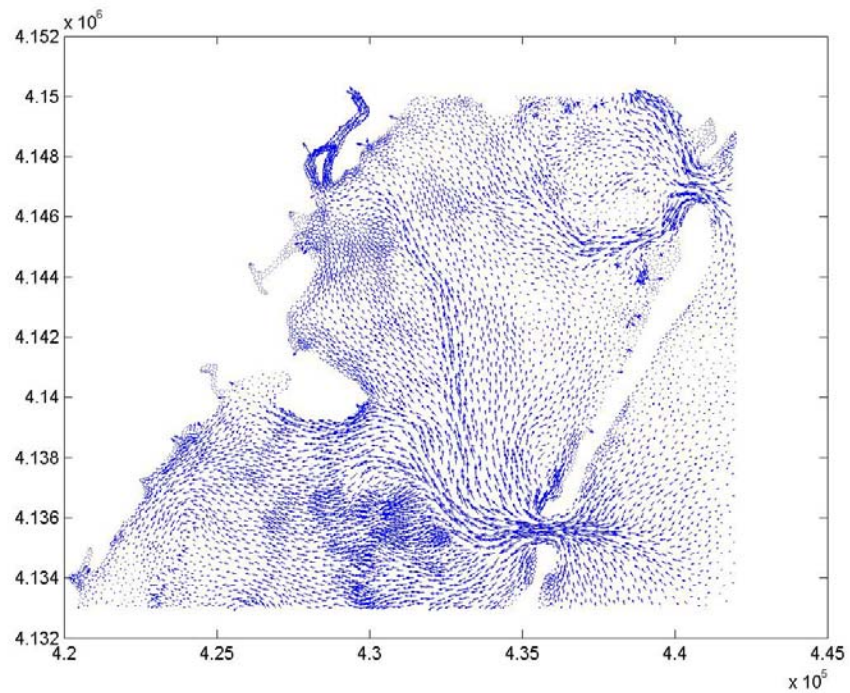
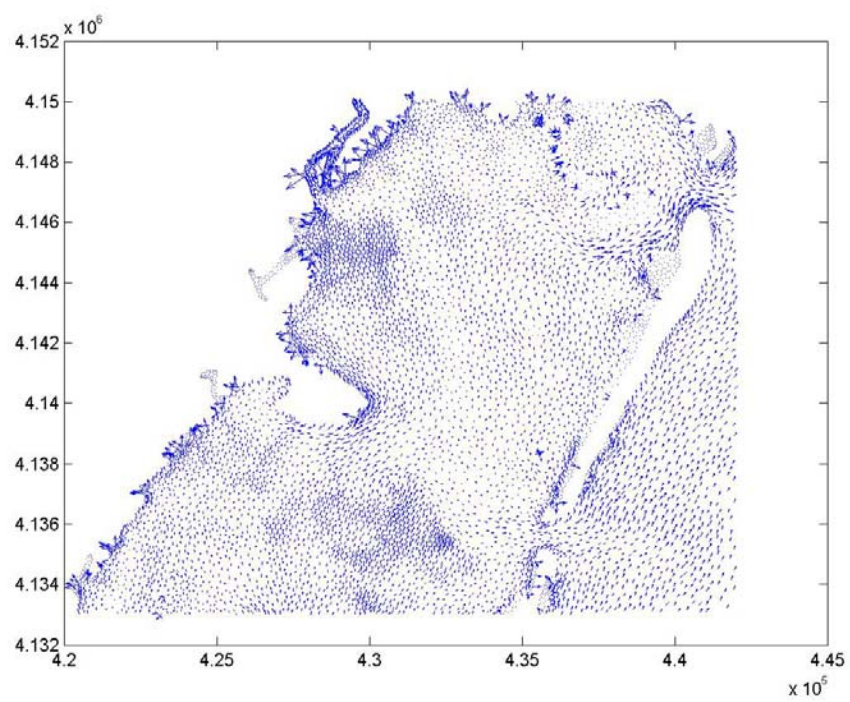


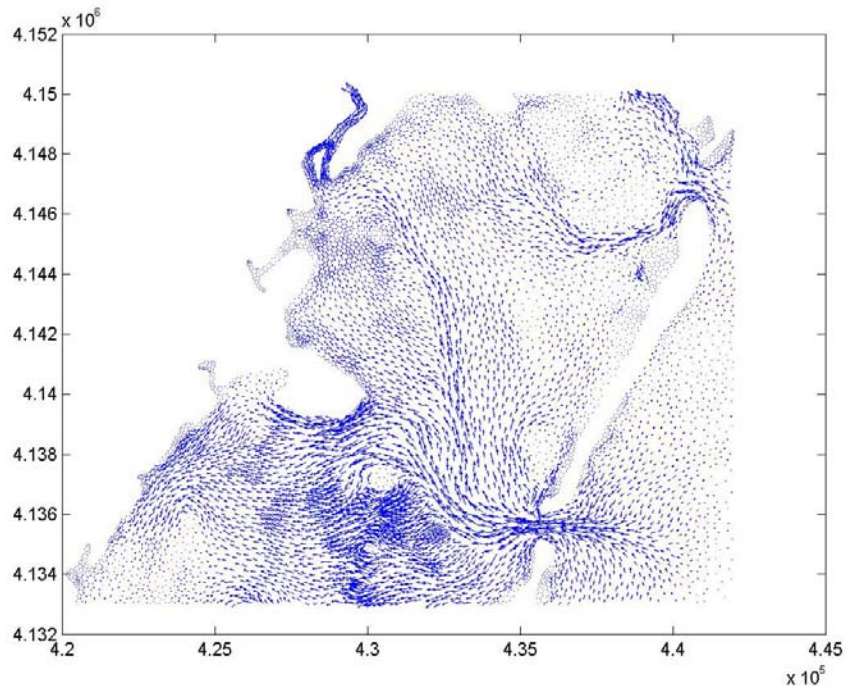
Fig 6. Difference in average speed on ebb and flood tides. Near the inlet, ebb tides show higher velocities, while flood tides show higher velocities near the mainland.



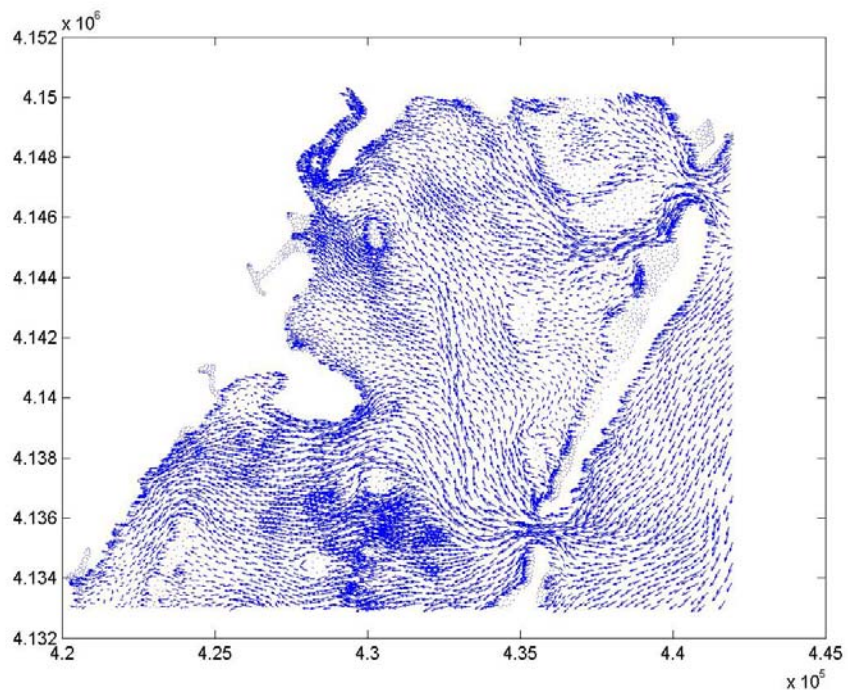
a) High tide, no wind



b.) High tide, with wind



c.) Low tide, no wind



d.) Low tide, with wind

Fig. 7. Effects of wind on tidal velocities. Fig 7a and 7c are from the August run with no wind forcing. Fig 7b and 7d are the same time steps with wind effects added.

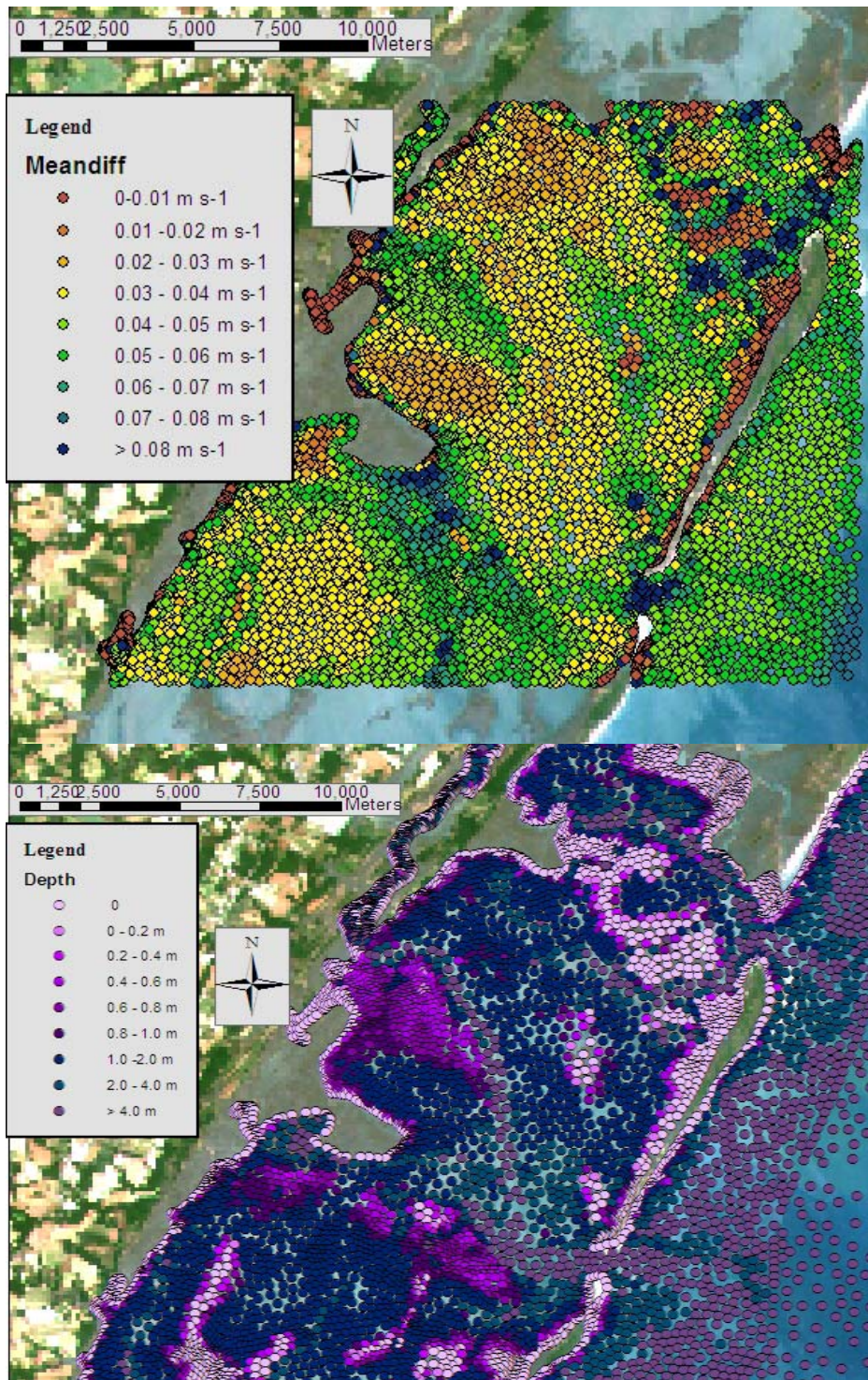


Fig. 8 a.) The time averaged difference in depth averaged velocity for the August model period calculated with and without wind. b.) Bathymetry of Hog Island Bay. The greatest wind effects are seen in the shallow areas.

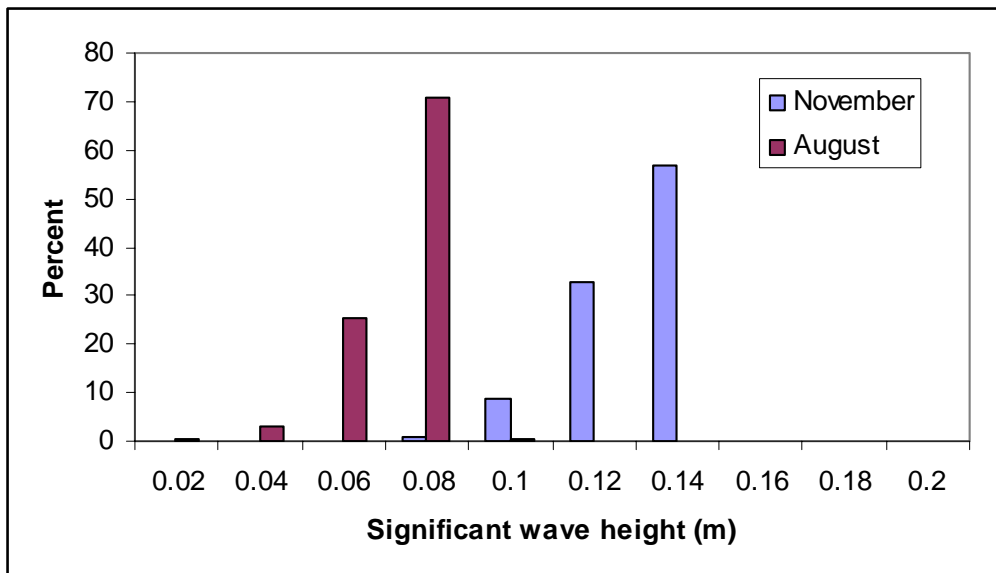


Fig 9. Percent of modeled area with time averaged significant wave height for the two model periods.

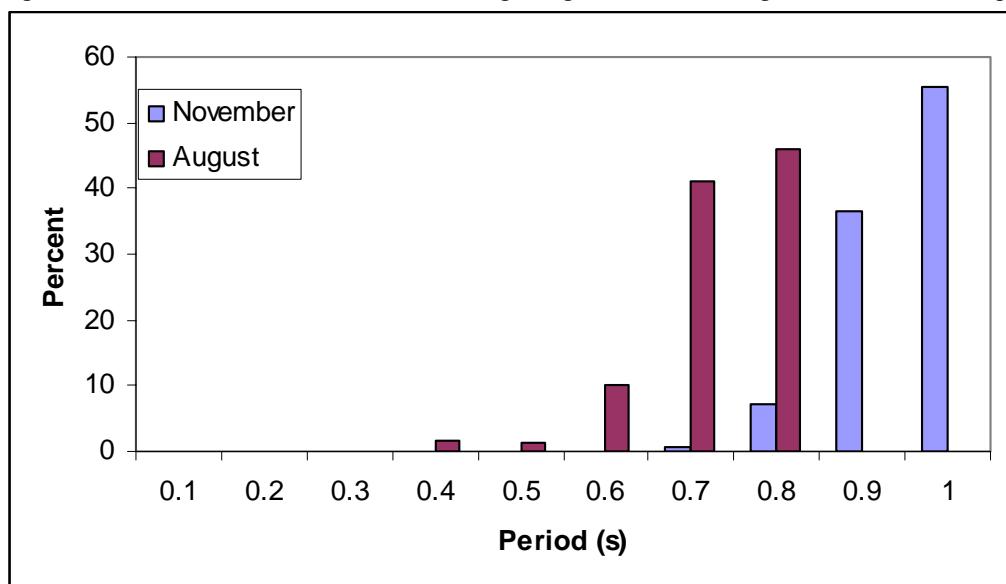


Fig 10. Percent of modeled area with time averaged wave period for the two model periods.

average wave period in August (Fig 10).

The relative importance of waves and currents is also depth dependent with the importance of wave stress increasing with shallower depths (Fig 11). In terms of sediment transport, the bed stress is the proper criteria on which to compare the relative importance of currents and waves (Le Hir et al 2000). The difference in the stress ratio at each depth between the two months illustrates that the relationship of increasing importance of wave stress holds for varying wind conditions. In low wind conditions, the tide stress is dominant at shallower depths. Based on a log-fit of the data, wave stress dominates ( $\text{Wave Stress/Current Stress} > 1$ ) in water shallower than 3.6 m in November and 0.8 m in August. From the average depths, this is 88% of the modeled surface area in November and 56% of the modeled surface area in August. The increased importance of wave stress in shallower waters is also seen with changes in the tidal stage (Fig. 12). Wave stress is always low ( $< 0.005 \text{ N m}^{-2}$ ) in the channel, but wave stress on the flats is only low during high tide. At low tide, average wave stress exceeds  $0.04 \text{ N m}^{-2}$  for 40% of the lagoon bottom (Fig 12(d)) for the November results.

The wind effects on waves and currents are greatest on the shallow flats that could be suitable habitat for seagrass. In general, the mudflats along the channel are all susceptible to wave suspension. Because of the morphology of Hog Island Bay with broad, gently sloping mudflats descending sharply to a channel, if the mudflats are not suitable habitat for seagrass, the total area available for seagrass colonization will be very limited. In addition, the hydrodynamic conditions, particularly the wave stress, are fairly uniform across the flats. Seagrasses may respond to temporary light limitation by sharing resources from shoots in areas that are not light limited (Tomasko and Dawes 1989), but

the similarity of hydrodynamic conditions in areas shallow enough for seagrass colonization indicates that light limitation will be spatially wide-spread. Similar hydrodynamic conditions across the flats should cause similar levels of light availability for a broad area making the sharing of resources by clonal seagrasses unlikely. Dring and Lüning (1994) showed that light availability at the sediment surface was highest during noon low tides. However, low tide is the time of highest wave stress on the flats in Hog Island Bay which may mitigate the increase in light caused by lower water depths at low tide if sediment suspension causes an increase in attenuation.

The hydrodynamic conditions can also be used to explain some of the trends in sediment size described in the previous chapter. The decrease in sediment size away from the inlet corresponds to the lower tidal velocities and the change to flood dominance near the mainland. The higher flood velocities can lead to trapping of fine sediment (Aubrey 1986, Dronkers 1986). The pattern of sediment size away from the channel may be a result of wave stress. Both wave and tide stresses are fairly consistent across the flats. The samples on the west side of the channel near the inlet are in an area of low wave stress, but the tidal velocities in this area are high. The three points that do not fit the trend of the rest of the data are also explained by the hydrodynamics. The farthest north point is directly behind the mid-lagoon shoals in an area of relatively low velocity. The other two points are in also in areas of low tide velocities created by Rogue Island and Eggins marsh. Links between average tidal velocity and sediment grain size are often mentioned, but rarely quantified (Le Hir et al 2000), and may explain the finer grain sizes in these areas.

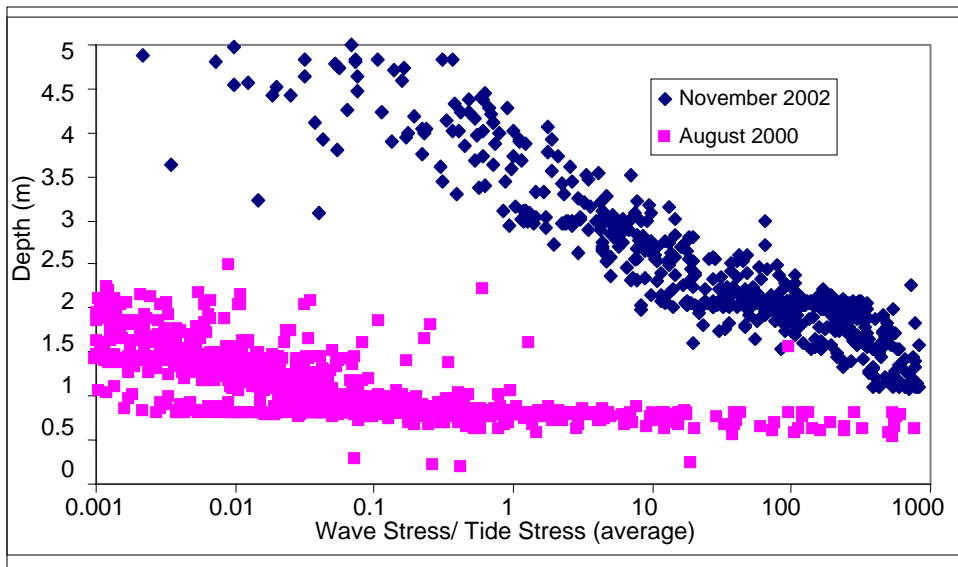
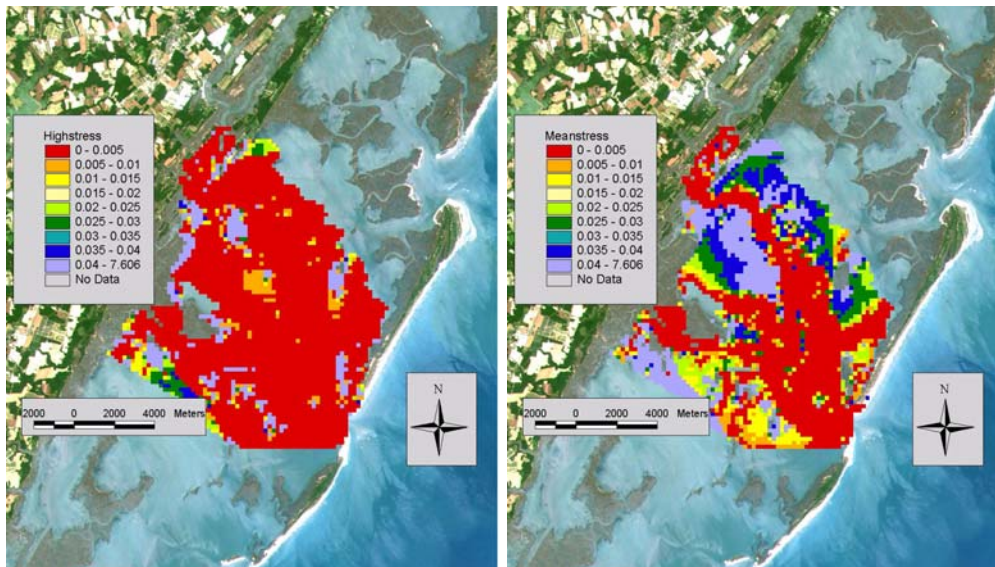
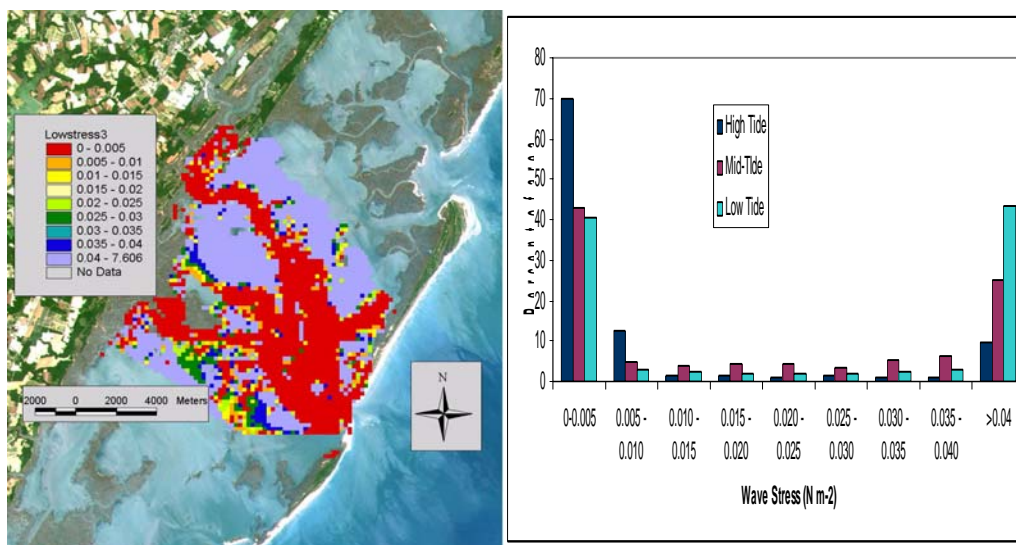


Fig 11 The relative importance of wave and current stresses, represented as a ratio, for a range of depths. Waves are overall more important in November, but both data sets show that wave stress becomes increasingly important as depth decreases.



a.) High tide

b.) Mid-tide



c.) Low tide

d.) Histogram of results

Fig. 12. Time averaged wave stress was calculated for three tidal stages, high, mid and low. The wave stress increases with lower tidal stage.

**Conclusion:**

The effects of the driving forces of water motion in Hog Island Bay, lunar tides and winds, are related to water depth. Average tidal velocities are higher in the deeper water, but wind effects are more important in shallow water. Because seagrass grows in shallow water, the wind effects on both waves and tides will be important for sediment suspension in areas of potential seagrass habitat. Monitoring of light availability during fair weather will not accurately represent the suitability of these areas for seagrass growth.

## Chapter 4: Light attenuation

While light availability at a single point in time and space can be easily measured with a secchi disk or light meter, to understand light attenuation, the impact of water column components on light availability must be addressed. The primary agents of attenuation in aquatic mediums are water, gelbstoff (dissolved organic matter), phytoplankton, particulate organic matter, and particulate inorganic matter. Suspended sediment absorbs light poorly but scatters light effectively and fairly evenly across all wavelengths. Absorption has a more direct effect on attenuation because it removes photons through energy transfer. Most particle scattering occurs in the forward direction, making the primary effect of scattering an increase in pathlength, which increases the likelihood of absorption (Kirk 1983). The organic components (gelbstoff, chlorophyll, and particulate organic matter) all absorb light with a wavelength specific pattern.

The factors affecting light attenuation in the water column can be divided into inherent and apparent optical properties. The inherent optical properties are solely properties of the medium and include the absorption coefficient ( $a$ ), the scattering coefficient ( $b$ ) and the attenuation coefficient ( $c$ ). The attenuation coefficient ( $c$ ) is the sum of the absorption coefficients ( $a$ ) and scattering coefficients ( $b$ ) of all the components of the water column. The apparent optical properties are affected both by the incident light field and by the properties of the medium. The diffuse attenuation coefficient ( $K$ ) as defined by the Lambert-Beer law is an apparent property of the water column. The Lambert-Beer law states that for the diffuse attenuation coefficient defined:

$$K = -d(\ln E) / dz$$

where  $E$  is irradiance and  $z$  is depth,  $K$  is the sum of the diffuse attenuation coefficient of each component:

$$K = \sum K_i$$

from 1 to  $i$  where  $i$  is the number of components affecting light attenuation indicating that each component of the water column (i.e. particulate inorganic matter, water, etc.) attenuates light independently and the total attenuation is additive. Because it is an inherent optical property, the attenuation coefficient ( $c$ ) does not vary with solar angle or cloudiness, and is therefore easier to predict than  $K$  from water quality measurements. However,  $K$  is a better representation of the light actually reaching depth.  $K$  can be defined for different types of irradiance, with scalar irradiance ( $K_0$ ) and downwelling ( $K_d$ ) irradiance the two most commonly used. Scalar irradiance is defined as the total irradiance reaching a point from all angles. Downwelling irradiance is the irradiance on the upward face of a horizontal plane. In studying photosynthetic capabilities and requirements of aquatic plants, scalar irradiance may be the more appropriate measure because the photosynthetic cells of aquatic primary producers can often receive radiation from many angles (Kirk 1983).

Modeling  $K$  has proven difficult because of the need to include properties of the light field as well as properties of the water. While absorption ( $a$ ) and scattering ( $b$ ) are additive with respect to the beam attenuation coefficient ( $c$ ), they are not strictly additive with respect to  $K$ . Gordon (1989) suggests a correction that removes the effects of the solar angle and allows representation of  $K$  as an inherent optical property for most waters. Using a modified version of this correction, Gallegos (2001) was able to predict  $K_d$  values with errors of only 8%. For all approaches it is important to realize the

limitations of any predictive equation. This chapter addresses three important issues necessary to describe light availability for submerged aquatic vegetation: the effects of particle size, the spectral nature of the underwater light field, and the variability in controls on light attenuation are addressed here. An equation is presented to predict light attenuation in Hog Island Bay.

## **Methods**

### *Field data*

To determine the effects of suspended sediment (organic and inorganic), gilvin, and water column chlorophyll on light attenuation, light readings and water samples were taken concurrently on October 30, 2003 at 16 points (Fig. 1). Measurements of scalar and downwelling irradiance were taken above the water surface, 0.1 m below the water surface, and 1.1 m using LI-COR 4 pi and 2 pi sensors respectively. The output from both sensors was configured to give 10 second moving averages. Three readings were taken at each location with 20 seconds between readings. Triplicate water samples were taken at the surface at each location with subsamples for particulate organic matter and particulate inorganic matter kept in clear bottles and subsamples for chlorophyll a, gilvin and determination of  $a$  and  $b$  kept in brown bottles. All samples were kept on ice until analysis. To determine the spectral pattern of the underwater light field, measurements of spectral irradiance were taken at ten sites using an Ocean Optics USB2000 Miniature Fiber Optic Spectrometer along with measurements of scalar irradiance on May 20-22, 2002. Both sampling efforts were done on clear days with low wind speeds and calm seas. To gain a larger temporal perspective, data from two longer datasets (referred to as MS and WQ) from the VCR-LTER were also used. The MS dataset includes data from 8

points for a year. The WQ dataset includes monthly or bi-monthly data at ten sites from July 1992 to February 1997. Both datasets are designed to include points from near the mainland and the islands.

#### *Lab analysis*

##### Chlorophyll analysis:

Chlorophyll analysis for the samples collected in October 2003 was performed on 200 ml water samples filtered within 24 hours of collection onto Whatmann GF/F filters with a nominal retention of 0.7 microns. The filters were placed in aluminum foil and frozen to avoid photodegradation until analysis. Prior to analysis, the samples were extracted in a 45:45:10:0.1 dimethyl sulfoxide, acetone, deionized water, diethylalanine solution overnight. Chlorophyll concentration was determined based on fluorescence read on a Shimadzu RF-5301PC spectrofluorophotometer. Chlorophyll concentrations for the MS and WQ data sets were both determined using spectrophotometers on samples extracted with 90:10 acetone and deionized water solution (MS water column chlorophyll) or 45:45:10 acetone, methanol, and deionized water solution (WQ water column chlorophyll and MS benthic chlorophyll). For all data sets, total suspended solids was determined by filtering 300-800 ml water samples onto pre-combusted, pre-weighed Whatmann GF/F filters with a nominal retention of 0.7 microns. Mineral (PIM) and organic (POM) components were determined by weight difference after combustion at 500° C for eight hours.

##### Determination of the inherent optical properties:

Laboratory methods were used to estimate the inherent optical properties of the samples. Scattering (*b*) was determined using a Hach turbidimeter. The turbidity in

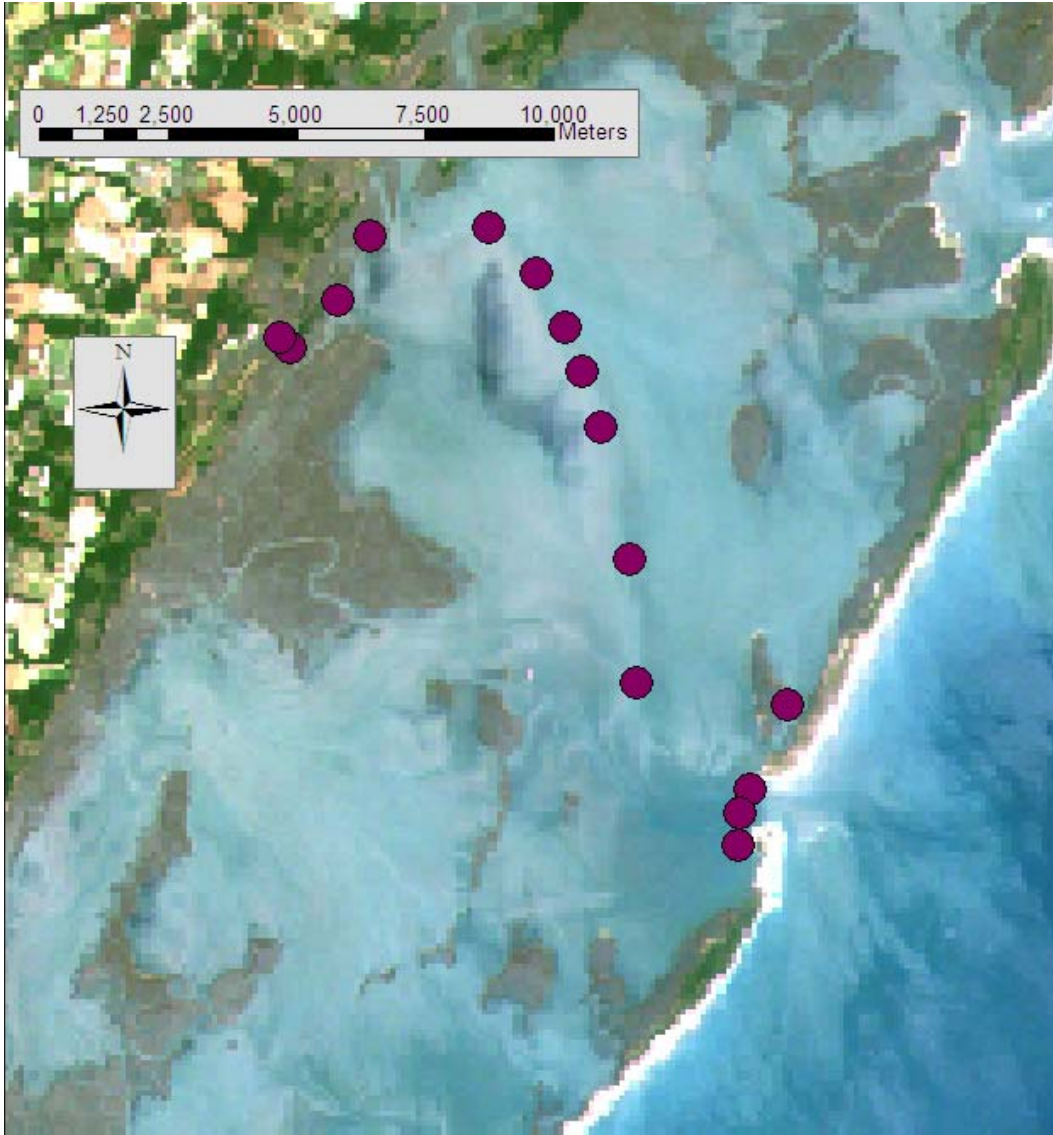


Fig. 1 Sample locations from October 30, 2003. The GPS location of one point near the mainland was not recorded. Sampling began at the islands at 11:00 and ended in the mainland creeks at 12:45.

NTU's of the sample was used as the scattering coefficient because studies have shown a one to one relationship between these two quantities (Gallegos 2001). Absorption ( $a$ ) was measured using a Hewlett-Packard scanning spectrophotometer and averaged over the range of photosynthetically active radiation (PAR) (400-700 nm). The spectrophotometric method more accurately measures total attenuation ( $c$ ) because of the small reception angle. Absorption was calculated by subtracting the scattering coefficient after the spectrophotometer results were converted from base 10 to natural logarithms (Kirk 1983). The samples were then filtered through a 0.2 micron filter and absorption at 440 nm was measured to represent dissolved organic matter (Gallegos 1996, Gallegos 2001, Kirk 1983). The contribution of each component to  $a$  and  $b$  was determined through multiple linear stepwise regressions. These values were then used with the form of the equations suggested by Bannister and Kirk to determine  $K_0$  in the form

$$K_0 = (a / \mu_0) * [1 + (C_1 \mu_0 - C_2)(b/a)]$$

where  $\mu_0$  is the cosine of the zenith angle of light in the water column and  $C_1$  and  $C_2$  are constants (Bannister, 1990). This equation simplifies to a linear regression of  $a$  and  $b$  for a constant  $\mu_0$ . The cosine of the zenith angle in the water column was calculated using 1.33 as the ratio of the refractive index of water to air in Snell's Law (Kirk 1983). Solar position was calculated from the position and time of sampling using the NOAA solar position calculator ([http://www2.arnes.si/~gljsentvid10/nebes\\_pod/legasonca.html](http://www2.arnes.si/~gljsentvid10/nebes_pod/legasonca.html)).

Measured values of  $a$ ,  $b$ , and  $K_0$  were used with the calculated value of  $\mu_0$  to determine the values of  $C_1$  and  $C_2$ .

### Spectrophotometer analysis

To determine how sediment size affects the light attenuation due to suspended sediment, two sediment samples from Hog Island Bay were wet-sieved to produce 4 size classes (63-75  $\mu\text{m}$ , 45-63 $\mu\text{m}$ , 38-45  $\mu\text{m}$ , and <38 $\mu\text{m}$ ). The sediment in these size classes was then suspended in deionized water and then diluted by 10% intervals to make 10 subsamples for each size class from each sediment sample, a total of 80 samples.

Absorbance for wavelengths between 200-900 nm was measured using a Hewlett-Packard scanning spectrophotometer for 3 analytical replicates of each sample. The 3 scans were averaged and linear regressions of absorbance averaged over the PAR range (400-700 nm) as a function of concentration were calculated. The slope of these regressions is the concentration specific absorbance due to suspended sediment in that size class. Concentration was determined by drying and weighing 5 replicates of a known volume (20ml) of the 100% suspension, then calculating the concentrations of the dilutions from this value. An equation was constructed through non-linear regression relating the average sizes to the concentration specific absorbance.

### **Results and discussion:**

#### *Equation to predict light availability from water column components*

Both  $K_0$  and  $K_d$  were primarily influenced by scattering. In a multiple linear stepwise regression, scattering, as measured on the turbidimeter, was the only significant variable and explained 94% ( $p < 0.0001$ ) and 96% ( $p < 0.0001$ ) of the variability

respectively. The slope of the regression was lower for scalar irradiance (0.08) than for downwelling irradiance (0.14). Both scattering and absorbance depended only on suspended sediment concentration ( $r^2 = 0.86$  and  $0.25$ ), which varied from 15 to 47 mg l<sup>-1</sup> in the sampled data. Chlorophyll concentrations, which ranged from 1.3 to 9.0 µg l<sup>-1</sup>, showed no relationship with  $K_d$  and a negative relationship with  $K_0$ . Both  $K_0$  and  $K_d$  are related to absorbance ( $r^2 = 0.23$  and  $0.34$ ), but the relationship with scattering explains so much of the variation that this relationship is not significant in the multiple stepwise regression.  $K_0$  ranged from 0.84 to 1.76 m<sup>-1</sup> and  $K_d$  ranged from 0.47 to 2.91 m<sup>-1</sup>.

Because the light measurements were taken over a period of a few minutes, changing sky conditions could affect their values. To account for this, K values with a standard deviation greater than 20% of the measured value were not used in the regressions.

Multiplication by the cosine of the underwater zenith angle ( $\mu_0$ ), the correction suggested by Gordon (1989) makes the regression applicable across seasons because it removes the effect of solar angle. Based on these results, the best way to predict light attenuation in Hog Island Bay is simple linear equations:

$$K_0(\mu_0) = 0.032 * \text{TSS}(\text{mg l}^{-1}) + 0.090 \quad (r^2 = 0.84, p < 0.001)$$

$$K_d(\mu_0) = 0.055 * \text{TSS}(\text{mg l}^{-1}) - 0.40 \quad (r^2 = 0.93, p < 0.001)$$

These values are similar to those seen in other systems (ex. Gallegos 2001 (0.08 mg l<sup>-1</sup> m<sup>-1</sup>), Dixon and Kirkpatrick 1995 (0.115 mg l<sup>-1</sup> m<sup>-1</sup>), Stefan et al 1983 (0.043 mg l<sup>-1</sup> m<sup>-1</sup>)), though the intercept is not typical. The intercept should represent light attenuation by water, gilvin and chlorophyll, making the negative intercept in the regression for downwelling irradiance physically incorrect. This problem illustrates that these are strictly empirical relationships.

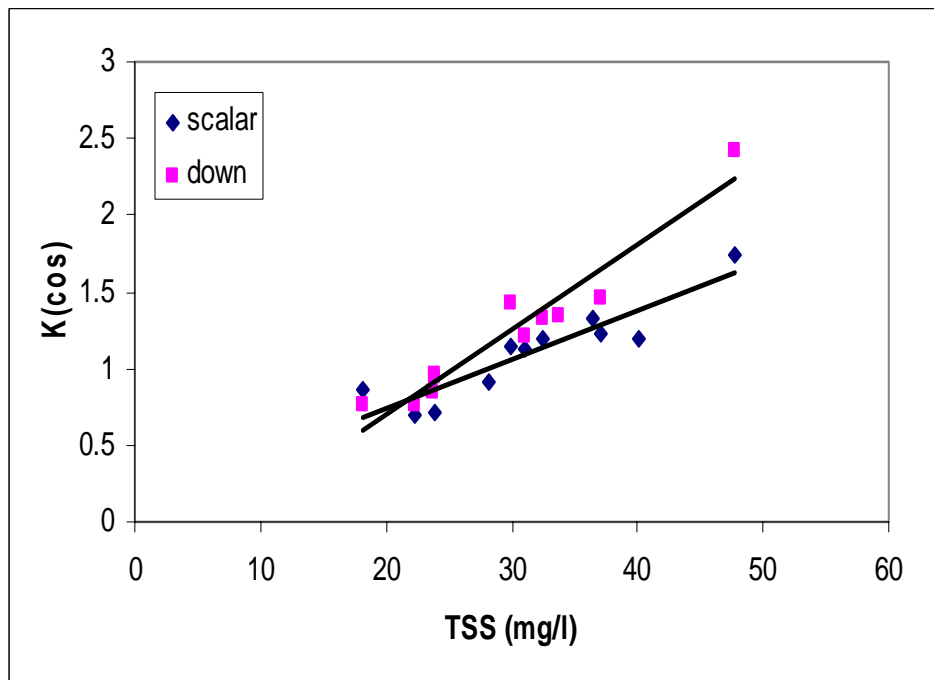


Fig. 2 Relationships between suspended sediment concentration and scalar and downwelling light attenuation.

*Spectral characteristics of light at depth:*

Though chlorophyll concentrations in Hog Island Bay are low, the spectral pattern of light at depth in Hog Island Bay showed attenuation by dissolved organic matter and chlorophyll. While the scattering due to suspended sediment is relatively insensitive to wavelength, absorption and scattering by the other water column components is wavelength specific. Because of this, the underwater light field bears the spectral “signature” of the water column components. In Hog Island Bay, the lowest attenuation in the PAR range was typically at 550 – 570 nm and the highest overall attenuation was above 700 nm with the highest attenuation in the PAR range at 400 - 440 nm (Fig. 2), a pattern that matches chlorophyll attenuation (Gallegos 2001, Kirk 1983). Maske and Haardt (1987) determined a range of 1 to 1.5 for the ratio of absorbance of blue to red light (440nm and 675 nm) by phytoplankton with absorption by detritus removed. The ratios of blue to red light attenuation from field samples in Hog Island Bay where detritus could not be removed ranged from 1.3 – 4.2, with the highest ratio occurring in one of the creeks. Because attenuation for gilvin is high for shorter wavelengths (Kirk 1983), the higher ratio may be caused by the presence of gilvin, which would increase the attenuation at 440nm more than at 675 nm. In Hog Island Bay, chlorophyll levels are relatively low, but levels of dissolved organic matter are high (McGlathery et al 2001), which should lead to greater attenuation at short wavelengths. Though all light in the wavelengths 400 to 700 nm is considered photosynthetically active, the usefulness of these different wavelengths varies, making light quality important in addition to measures of light quantity. The seagrass species *Thalassia testudinum* and *Zostera marina* show low absorption in the range from 525 -650 nm, a pattern typical of plants dominated by chlorophyll a and b (Zimmerman 2002). Light in the range that is least attenuated in Hog

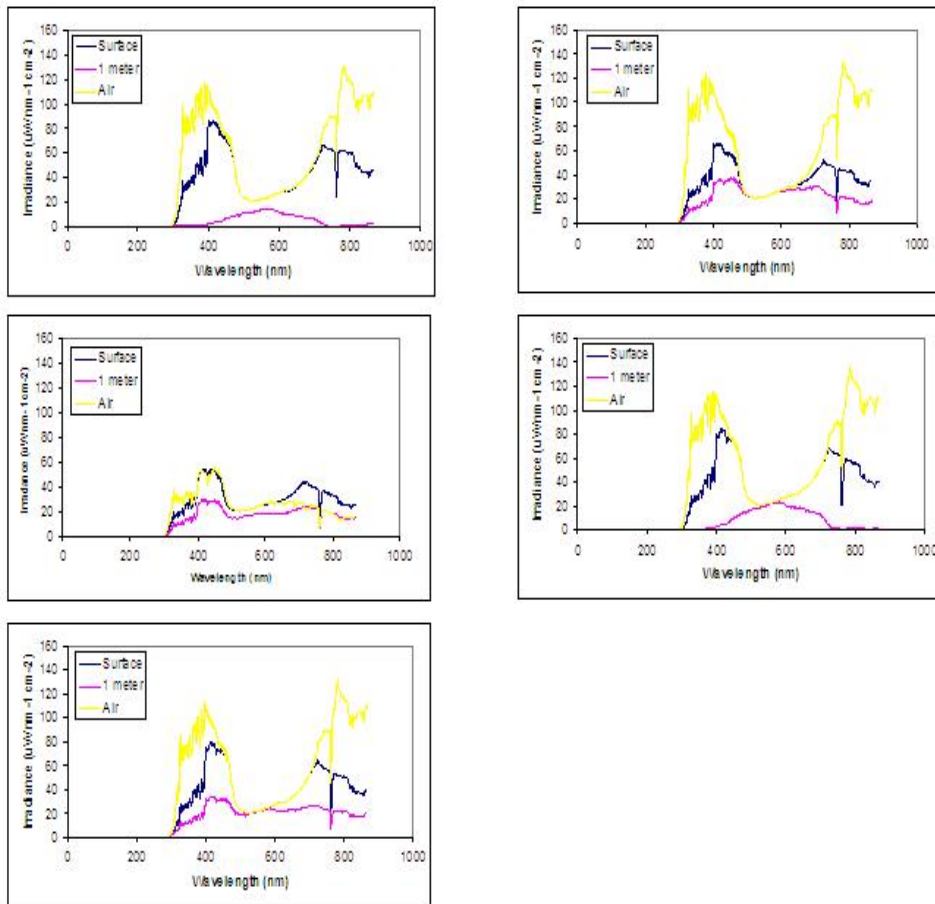
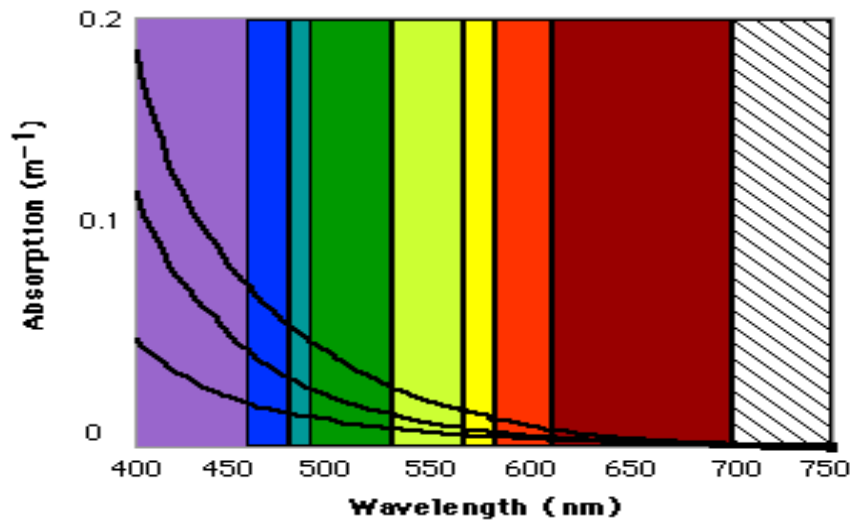
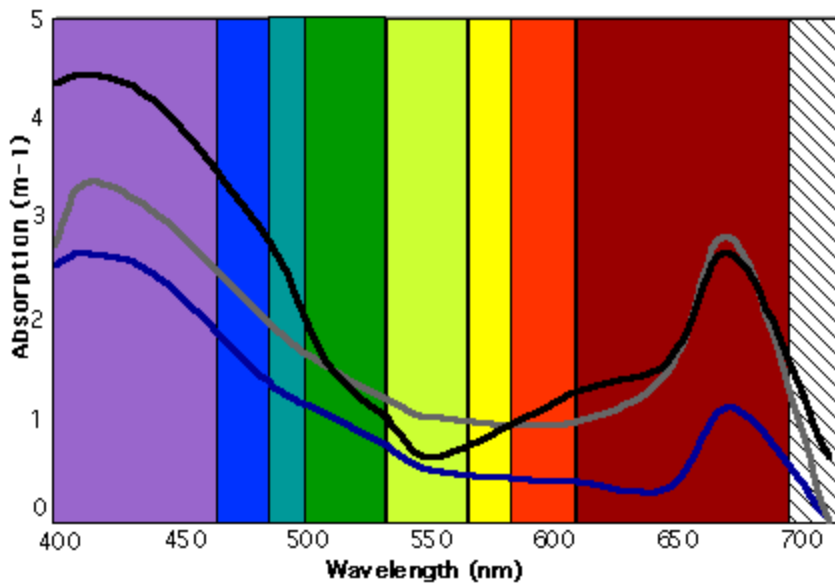


Fig 2a Sample spectra from May 20, 2002. These graphs show the downwelling light field at five locations in Hog Island Bay measured in air, just below the water surface, and at one meter depth. Each line is the average of three individual measurements, each of which averages 200 scans.



dissolved organic matter



phytoplankton

Fig 2b. Graphs from Gallegos at Smithsonian Environmental Research Center showing the spectral patterns of attenuation of different water column components. Taken from [http://www.serc.si.edu/water\\_quality/water\\_quality\\_html/hydrops.htm#optics](http://www.serc.si.edu/water_quality/water_quality_html/hydrops.htm#optics).

Island Bay is also the least useful for these seagrasses. Because chlorophyll is the light gathering component in SAV, high levels of chlorophyll attenuation could limit SAV growth even if the average light availability for the PAR range is sufficient for growth.

*Variability in controls on light attenuation:*

Multiple stepwise regressions of particulate inorganic matter (PIM), particulate organic matter (POM) and chlorophyll a (cha) with  $K_d$  calculated from secchi depth for the LTER water quality data by month and site show that the importance of these different components for light attenuation varies seasonally and spatially (Tables 1 & 2). Secchi depth was converted to  $K_d$  based on the relationship  $K_d = 1.44/Z_{SD}$  (Holmes 1970). Particulate inorganic matter, a predictor in eleven of thirteen significant regressions, is the dominant control on light attenuation in Hog Island Bay. The concentration specific attenuation, the slope of the regression, is in agreement with published values (ex. Gallegos 2001 ( $0.08 \text{ mg l}^{-1} \text{ m}^{-1}$ ), Dixon and Kirkpatrick 1995 ( $0.12 \text{ mg l}^{-1} \text{ m}^{-1}$ ), Stefan et al 1983 ( $0.043 \text{ mg l}^{-1} \text{ m}^{-1}$ )).

Chlorophyll a is only a significant predictor of light attenuation in June, July and September and at two sites (CSM and PCM). Seasonality of controls on light attenuation had been noted in other systems with DOC the dominant control on attenuation in lakes of the Mackenzie Delta (Squires and Lesack 2003) and a summer-time association of total nitrogen with chlorophyll biomass and therefore Secchi depth in Danish coastal waters (Nielsen et al 2002). This result indicates that chlorophyll a is more important in the summer and near the mainland (Fig 3), consistent with the finding of McGlathery et al (2001) that phytoplankton production is only a significant contributor to total production in the bay during summer following the decline of the macroalgae. The

decreased importance of chlorophyll in winter and fall may explain why light attenuation was dependent solely on suspended sediment in the field data from this study.

The intercept in all regressions is higher than the normally accepted value of  $0.0348 \text{ m}^{-1}$  (Lorenzen 1972). The high intercept may have resulted from the definition of secchi depth used to convert to  $K_d$ . However, seasonality is evident in the intercept, with higher values from July to October. Dissolved organic substances are the light attenuating water column components not included in these regressions, indicating a fluctuation in the concentration of dissolved organics. These data also show the difficulty of constructing equations to predict light attenuation based on field data. The negative slopes of chlorophyll in July and for the field data from this study and POM for the NC and CSH sites indicate that the effect of chlorophyll and particulate organic matter on light availability can be overshadowed by higher production in high light conditions.

Using monitoring data to predict light attenuation is also problematic because water column chlorophyll may be partially suspended benthic chlorophyll. If water column chlorophyll is primarily from suspension of benthic chlorophyll and the chlorophyll is transported similarly to sediment, the values of water column chlorophyll should be correlated with suspended solids. Max  $R^2$  regressions with a maximum of one independent variable selected from particulate inorganic matter, particulate organic matter, and total suspended solids (TSS) were run with water column chlorophyll concentration as the dependent variable. The regressions were run on the measurements as a whole and then on sub-sets by month and site. For the WQ data set, no site showed a significant relationship between water column chlorophyll and PIM, POM or TSS, but six dates showed weakly significant relationships ( $p < 0.15$ ) (12/15, 11/17, 10/6, 10/1, 7/28,

MONTH	PIM	POM	CHA	INTERCEPT	N
1					6
2					9
3					9
4					14
5					0
6	0.05 (0.47)		0.1 (0.11)	0.44	11
7	0.01 (0.24)	0.2 (0.46)	-0.04 (0.15)	1.1	9
8	0.06 (0.38)			1.6	9
9			85(0.97)	1.5	3
10	0.05 (0.44)			1.3	40
11					28
12	0.06 (0.52)			0.38	18

Table 1 Results of stepwise regressions of water column components (mg/l) and  $K_d$  calculated from secchi depth from pooled data at 10 sites in Hog Island Bay, analyzed by month. Partial  $r^2$  values are given in parentheses. The significance level for these regressions is 0.15.

SITE	PIM	POM	CHA	INTERCEPT	df
CSH					15
CSM			0.09 (0.23)	1.7	15
GC					16
NC	0.06 (0.26)	-0.14 (0.19)		1.4	17
OH	0.06 (0.46)			0.8	16
PCB					12
PCH	0.05 (0.35)	-0.04 (0.13)		0.59	13
PCM			0.13 (0.48)	1.6	19
QI	0.03 (0.19)			1.6	16
RB					17

Table 2 Results of stepwise regressions of water column components (mg/l) and  $K_d$  (m) calculated from secchi depth at 10 sites in Hog Island Bay. The relative importance of POM, PIM and cha varies throughout the year. Partial  $r^2$  values are given in parentheses. The significance level for these regressions is 0.15.

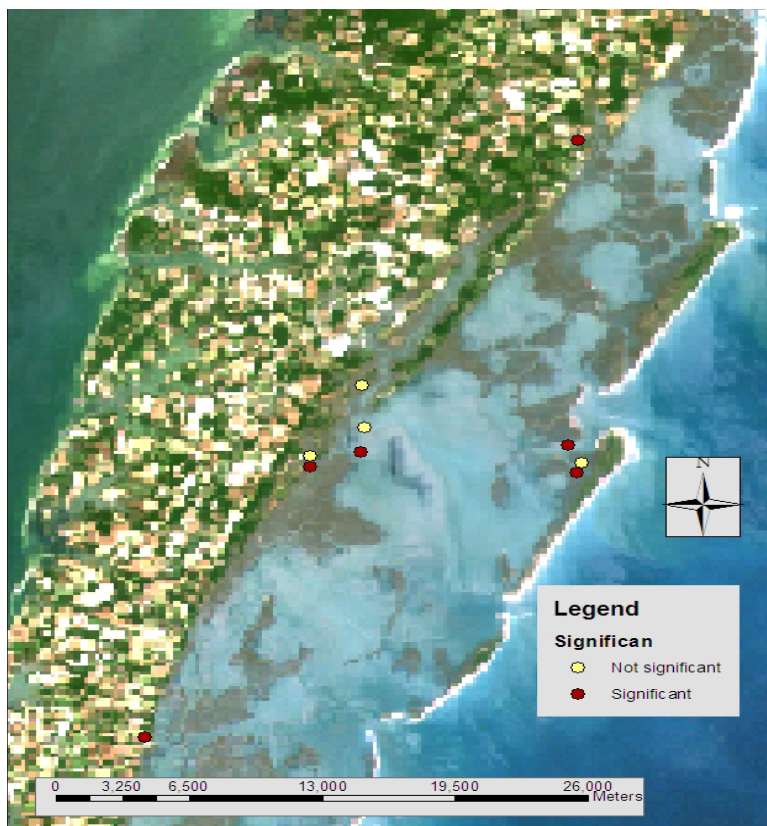


Fig. 3 Location of sampling sites for LTER water quality data. The sites that had significant ( $p < 0.15$ ) regressions between POM, PIM or cha and  $K_d$  calculated from the secchi depth are shown in yellow.

2/25). For the MS dataset, five of nine sites (Hog, Shoal 1 and Shoal 2 had strongest relationships with PIM, Cobb and Oyster Harbor had significant relationships with POM) and three months (January and October with PIM, March with POM) showed significant relationships. These results indicate seasonality in the relationship between suspended solids and water column chlorophyll. The relationship is less clear in the summer than in the winter, possibly indicating more pelagic phytoplankton in summer, a result that again is consistent with McGlathery et al (2001). While the relationships are not very strong, water column chlorophyll may be at least partially from suspension of benthic chlorophyll.

*Effect of sediment size on light attenuation:*

Absorbance was linearly related to suspended sediment concentration for each size range (Fig. 4). Linear regressions of each of four size classes for two samples (8 regressions total) gave  $R^2$  values from 0.954 – 0.998 ( $n = 8-10$ ,  $p < 0.05$ ). The lower regression coefficients were typically for larger particles sizes, possibly because of faster settling velocities resulting in lower measurement accuracy as the sample settled in the cell. A regression of the full data set yielded a non-significant relationship ( $R^2 = 0.0015$ ,  $p = 0.74$ ,  $n=74$ ), though strong, significant relationships can be found for each size class, showing that while suspended sediment contributes to light attenuation, the relationship is only linear for a small size range (Table 3).

The concentration-specific absorbance increases with decreasing sediment grain size (Fig 5, Table 3). Because fine sediment has a greater surface area to volume ratio, a volume of fine sediment will scatter more light than the same volume of coarser sediment (Ruffin 1998). Baker and Lavelle (1984) studied light attenuation by sediment using a

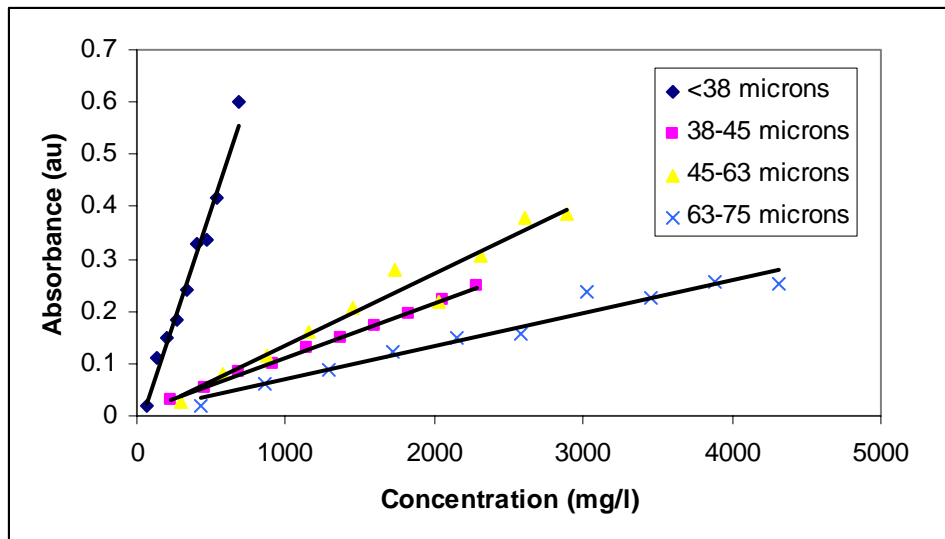


Fig. 4 Relationship between the absorbance averaged for the PAR range and the suspended sediment concentration for one sample.

beam transmissometer and found a strong linear relationship between particle concentration and beam attenuation for each size class, but found that the slope of this relationship ranged from .041 to .67 ( $m^{-1}$ ) across the range of size classes studied. The results from this study show a power relationship between average sediment grain size and absorbance (Fig 5). Average sizes for the three coarser size classes (38-45  $\mu m$ , 45-63 $\mu m$ , and 63-75  $\mu m$ ) were determined by taking a log base two average. For the finest sediment class, average grain size was calculated based on sediment size analysis of the silt and clay fraction of the original sediment sample on a Sedigraph 5100 particle size analyzer. When values from this study for absorbance at 660 nm are transformed from log base ten to log base e and from  $cm^{-1}$  to  $m^{-1}$  they can be compared directly to the values from Baker and Lavelle (1984). The results from this study show a close relationship with the theoretical slopes predicted by Baker and Lavelle (1984) using Mie theory (Fig 6). While Mie theory accurately predicted the attenuation by glass spheres, Baker and Lavelle's (1984) measured slopes from sediment suspensions were higher than the theoretical slopes, even when the particles were considered as disks, a response possibly explained by surface roughness. The agreement of the slopes measured in his study and the theoretical slopes may indicate that the particles are relatively round and smooth. While both of these studies are laboratory based, field studies have also shown the importance of grain size in beam attenuation. Mean sediment size and the standard deviation of mean particle size were statistically the strongest predictors of the beam attenuation coefficient at 670nm in a study of a lime-dredging plume (Mikkelsen and Pejrup 2000).

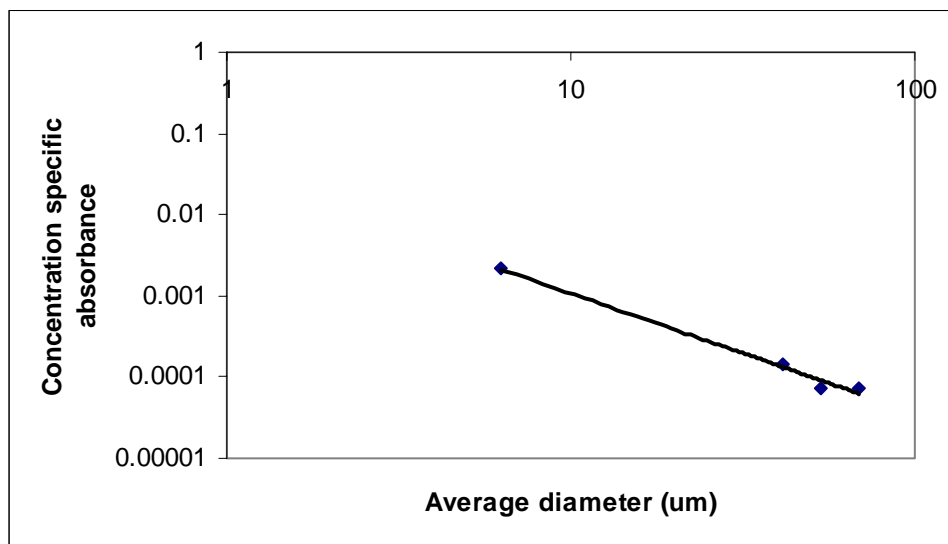


Fig 5 Relationship between the average diameter of a sediment suspension and the concentration specific absorbance as measured on a spectrophotometer.

Size class ( $\mu\text{m}$ )	slope	p	Intercept	R <sup>2</sup>	n	Average size ( $\mu\text{m}$ )
<38	0.0021	<0.001	-0.20 (p>0.05)	0.76	19	6
38-45	0.00015	<0.001	0.012 (p<0.05)	0.69	20	41
45-63	7.2E-05	<0.001	0.068 (p <0.05)	0.79	20	53
63-75	7.2E-05	<0.001	-0.0029 (p<0.05)	0.94	18	69

Table 3 Summary of statistical results of regressions of absorbance (au) and concentration ( $\text{mg l}^{-1}$ ) for sediment suspensions of limited size range.

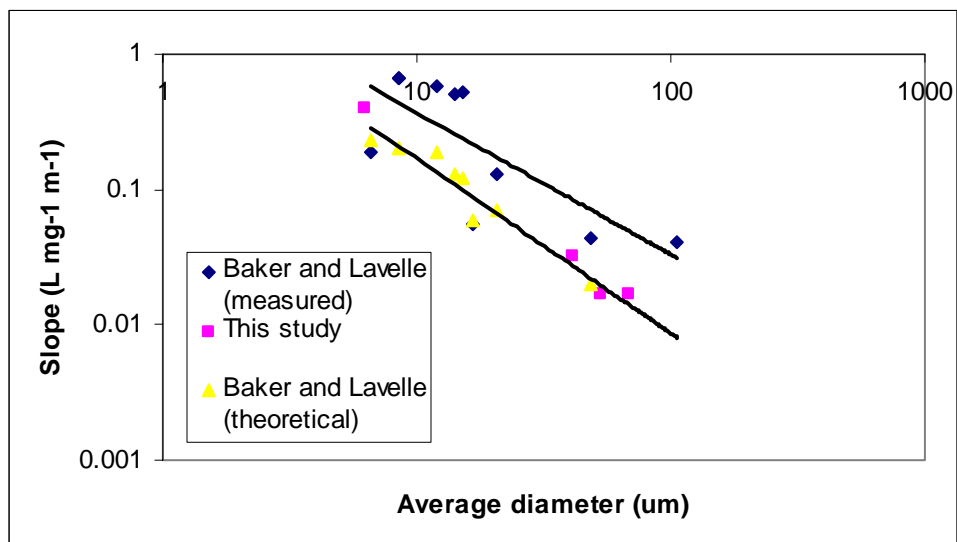


Fig 6 Comparison of concentration specific attenuation at 660 nm from this study and measured and theoretical values from Baker and Lavelle (1984). The best-fit lines shown are for the theoretical and measured values from Baker and Lavelle (1984).

Bringing together all of this information gives a picture of how light is attenuated in Hog Island Bay. The bulk attenuation as measured in October is entirely dependent on total suspended solids. However, the spectral pattern of light available at depth is determined by chlorophyll and organic matter. The sampling for these two parameters was done at different times of year which should affect the relative importance of chlorophyll and total suspended solids. Chlorophyll biomass is typically higher in May than in October with a peak in late summer (McGlathery et al 2001), and May is also a more important time for growth of seagrass (Moore et al 1997). The water quality data show that chlorophyll attenuation is more important during summer with significant relationships only in June, July and September, a result similar to that seen in the York River (Moore et al 1997). Even if the bulk attenuation is controlled by the suspended solids, the high absorbance of light in the 400- 440 nm wavelength range will limit the productivity and distribution of seagrass.

The difference between the available scalar and downwelling light is also an important consideration. Using only values with a standard deviation less than 20% of the measured value, the ratio of  $K_d$  to  $K_0$  varies from 0.87 to 1.40 (mean = 1.17). The ratio of downwelling light available to scalar light available has a range from 0.39 to 0.76 (mean = 0.58). This indicates that the ability to accept light from multiple angles almost doubles the light available to seagrass. The differences between downwelling and scalar irradiance seen here are greater than those seen by Moore et al (1997) in the York River. The suspended solids concentrations seen in this study are higher than those seen by Moore et al (1997) which should result in more scattering. Scattering should be more

likely to affect downwelling light, possibly by changing the angle of incidence of the light, spreading the light energy over a greater area.

## **Conclusions**

While many limitations exist in predicting the underwater light field from measurements of water column components, it is possible to construct an equation that predicts explains 84 -94% of the variation in light attenuation solely from the concentration of suspended solids. The equation is only applicable for a limited size range of suspended sediment, but the approach is valid for all size ranges. Supplementary data to the light attenuation equation developed in this chapter was provided to illustrate some of the limitations of this approach, but also showed that the equation is broadly applicable. Even though sediment size affects total light attenuation and chlorophyll and organic matter affect the spectral characteristics of light at depth, the slope of the equation from the October 2003 data ( $0.055 \text{ (l mg}^{-1} \text{ m}^{-1})$ ) is similar to the slopes from the equations based on the WQ dataset. Seven of the nine significant regressions had slopes of 0.05 or 0.06 ( $\text{l mg}^{-1} \text{ m}^{-1}$ ). The agreement of these values indicates that the equation may be broadly applicable despite the affects sediment size. However, when examining data from large areas or over long periods of time it may be useful to consider sediment size when calculating  $K$ , as seen in Blom et al (1994). When applying an optical model to the Rhode River and Chincoteague Bay, only coefficients relating to turbidity had to be recalibrated (Gallegos and Kenworthy 1996). In this study, the concentration specific absorbance changed 2 orders of magnitude for a 1 order of magnitude change in average sediment size (Table 1). In addition, the relative importance of the water column components as light attenuators varies spatially and

temporally. Overall, the dominant control on bulk light attenuation in Hog Island Bay is PIM. However, the spectral characteristics of the light field at depth, which are controlled by chlorophyll and organic matter, may be more important for productivity than the bulk attenuation.

## Chapter 5: Sediment suspension

Seagrass communities function in coastal and estuarine systems as a nutrient filter (Rabalais 2002, Dierberg et al 2002), nursery ground (Gullstrom et al 2002) and sediment stabilizer (Granata et al 2001, Gacia and Duarte 2001, Heiss, Smith and Probert 2000, Gacia et al 2003). However, seagrass distribution has declined in many areas frequently due to changes in water quality (Orth and Moore 1983, Hall et al 1999, Stankelis, Naylor and Boynton 2003, Duarte 2002). Light availability controls the distribution and production of seagrass and suspended particulate material is frequently a dominant control on light availability (Gallegos and Kenworthy 1996, Moore, Wetzel and Orth 1997, Havens 2003, Smith 1982). An understanding of how suspended sediment affects light availability is important to understanding seagrass distribution because sediment suspension is not adequately accounted for in the usual methods of addressing light availability. Light limitation is often studied through monitoring of light availability (ex. Koch and Beer 1996) or light availability paired with water column components that control it (ex. Moore, Wetzel and Orth 1997, Vermaat and Debruyne 1993, Havens 2003). However, these methods miss episodic sediment suspension events, the timing and frequency of which may have an important influence on seagrass distribution. The importance of storms and coincident light limitation in controlling vegetation distribution has been noted for lagoons and nearshore areas (Cabello-Pasini et al 2003) and even riparian zones (Vervuren et al 2003). However, attempts to quantitatively associate the light limitation with forcing conditions have been limited (e.g., Olesen 1996, Hanlon et al

1998). To examine the effects of sediment suspension on light availability the processes controlling sediment suspension must be addressed.

A physical processes approach is necessary to study light limitation because of the episodic nature of sediment suspension. The importance of wind for sediment suspension in shallow environments such as lakes (ex, Bailey and Hamilton 1997), lagoons (Arfi et al 1993) and even in deeper areas such as the continental shelf (ex, Wright 1999, Ogston and Sternberg, 1999) has been demonstrated. Though periods of high winds may account for a small portion of time, they can account for a large portion of overall sediment transport (ex, Janssen-Stedler 2000). Because seagrass is susceptible to even short term light limitation (Longstaff et al 1999; Longstaff and Dennison 1999; Moore et al 1997, Cabello-Pasini et al 2002), episodic events such as storm suspension are important in addition to the average conditions. Suspended sediment has been shown to be a dominant control on light availability in many shallow systems (Gallegos and Kenworthy 1996, Moore, Wetzel and Orth 1997, Havens 2003, Smith 1982), but this has not been linked to the processes suspending sediment. The need to examine the role of waves and tides in light limitation of seagrass has been recognized (e.g., Dring and Lüning 1994); this paper is a first step in filling that need. This chapter determines light availability in a shallow bay for two time periods using a process-based modeling approach.

## **Methods**

The modeling in this study was based on overlaying data layers interpolated using inverse distance weighted interpolation in the GRID module of ARC-INFO. The grid cells are 200 m on each side and the grids include 3048 active cells. The spatial extent of these layers was limited by the area covered by bed sediment samples. During August

and September 2001 and July 2002, triplicate sediment samples were taken at 82 sites in Hog Island Bay using an Ekman-style grab sampler (Chapter 2). The grain size distributions of these sediment samples were determined through wet sieving (sand fractions) and analysis on a Sedigraph 5100 particle size analyzer (silt and clay fractions). A continuous surface of average sediment grain size and percent sediment in each of ten size classes was created using inverse distance weighted interpolation in the GRID module of ARC/INFO.

*Sediment suspension calculation:*

Sediment suspension in this study was calculated using the Rouse equation (Rouse 1937)

$$C_s = C_a(z/z_a((h-z_a)/(h-z)))^{-w_s/\kappa u^*}$$

where  $C_s$  is suspended sediment concentration (unitless),  $C_a$  is a reference concentration (unitless) at reference height  $z_a$  (m),  $z$  is height in the water column (m),  $h$  is water depth (m),  $w_s$  is particle settling velocity ( $\text{ms}^{-1}$ ),  $\kappa$  is Von Karman's constant (0.4), and  $u^*$  is shear velocity ( $\text{ms}^{-1}$ ). The concentration was calculated by numerical integration from  $z_a$  to  $h$  with a depth step of 0.1 m as a partial sum of the eleven size classes. The reference concentration ( $C_a$ ) was calculated according to Smith and McLean (1977) who used a constant of proportionality ( $\gamma$ ) to relate the excess shear stress to the concentration at a reference height ( $z_a=3D_{50}$ ) near the bed. A value of 0.002 was used for  $\gamma$  in the model (Glenn and Grant, 1987; Wiberg et al, 1994). This reference concentration was calculated based on an excess shear stress from the combined wave and current stress ( $(\tau_{bTOTAL}-\tau_{cr})/\tau_{cr}$ ), but the Rouse parameter ( $-w_s/\kappa u^*$ ) was calculated using only the shear velocity from the currents. This approach mimics the ability of waves to suspend

sediment only in a near bed wave boundary layer, while current shear velocities are responsible for mixing of sediment in the water column. Calculations of the wave and current stresses are presented in Chapter 3.

The settling velocity for all size classes was determined using Stokes Law with half the sediment in size classes less than 30  $\mu\text{m}$  represented as a floc class with a settling velocity of  $0.00045 \text{ m s}^{-1}$ . This settling velocity was chosen in a manner similar to the critical shear stress, by examination of the end of sediment suspension events and the corresponding modeled shear stresses. Published values of floc settling rates vary widely, but this value is within the range of published values (Shanks 2002, Manning and Dyer 2002, Curran et al 2003, Mikkelsen 2002, Sternberg et al 1999).

The same total shear stress was used to calculate a stress-dependent surface active layer (Harris and Wiberg, 1997). Within a mixed bed, the stress required for initial motion for all size classes is similar (Wiberg and Smith, 1987), but a greater proportion of the fine sediment is suspended resulting in a coarser bed surface and “bed armoring”. Some sediment cores taken in Hog Island Bay show a reduction in fine material in the upper 2 cm of the cores (Chapter 2). The use of a stress-dependent active layer allows suspension in each size class only to a certain depth, represented by the depth of the active layer ( $\delta_{\text{mix}}$  (m))

$$\delta_{\text{mix}} = k_1(\tau_{\text{bTOTAL}} - \tau_{\text{cr}}) + k_2 D_{50}$$

with values of  $k_1=0.007$  and  $k_2=6$  used for SI units (Harris and Wiberg, 1997). Because much of the sediment in this system is very fine, sediment that was suspended was allowed to remain in suspension until a deposition stress characterized by  $10w_s=u^*$  was reached. The sediment that was retained in suspension was included in determination of

the limit by the mixing depth, so that the total volume of sediment in suspension did not exceed the volume available in the active layer.

The modeled values of sediment suspension were used to calculate light availability based on the relationships in Chapter 4. A value for  $K_d$  was determined based on the modeled value of suspended sediment concentration and values of 9 and 2  $\mu\text{g l}^{-1}$  of chlorophyll for August and November respectively, the averages for the WQ dataset, and 0.4 absorbance at 440 nm for both August and November, the average for the October 30, 2003 data presented in Chapter 4 (used to represent dissolved organic matter).

Coefficients from Gallegos (2001) were used to represent the concentration specific attenuation for chlorophyll ( $0.0154 \text{ m}^2 (\text{mg cha})^{-1}$ ) and dissolved organics ( $0.28 \text{ m}^{-1} \text{ au}^{-1}$ ) because neither of these variables had significant relationships with  $K$  in the data from Hog Island Bay. The calculated value of  $K_d$  was then used to calculate the percent light reaching the sediment surface assuming solar noon. The depth averaged value of suspended sediment concentration was used to determine  $K_d$  because the water column location of the sediment was not retained in the calculations. While  $K_0$  may be more appropriate for seagrass (Kirk 1983), the seagrass depth limits have been determined for downwelling irradiance (Duarte 1991). The equations to represent light attenuation are then:

$$K_d = \text{TSS} * 0.0665 + \text{Cha} * 0.0154 + g_{440} * 0.0308$$

A Sontek acoustic Doppler profiler was deployed and recording from November 17, 2002 to January 23, 2003, which overlapped with the November model run from November 19, 2002 to December 14, 2002. The ADP was deployed near Rogue Island in water with an average depth of 1.8 m during the deployment. The ADP was configured

with a 0.2 m blanking distance and 0.2 m cells and measured profiles every 30 minutes. The ADP was used to validate the model with critical shear stress and flocculation settling velocity the only parameters adjusted based on the ADP data. Suspended sediment concentration, assuming consistent sediment and water properties, should be generally related to the square of the strength of the acoustic backscatter signal (Holdaway et al 1999, Betteridge et al 2002). The model results were compared visually with the square of the backscatter strength at 0.75h. The critical shear stress was determined by examining the leading edge of suspension events and determining the corresponding modeled shear stress. A critical shear stress of  $0.04 \text{ Nm}^2$  determined this way was used for the entire modeled area. This shear stress is lower than that predicted by the Shields curve for the average sediment size (Soulsby 1997), but is consistent with values from other studies of muddy sediments (ex. Schaaff, Grenz, and Pinazo 2002, Ziervogel and Bohling 2003, Lund-Hansen et al 2003, Arfi et al 1993).

## **Results and Discussion**

### *Model verification and validation*

The modeled results of sediment suspension show good agreement with the backscatter signal from the ADP (Fig. 1). The correlation coefficient between the two values is 0.41 ( $p < 0.05$ ) with the ADP data sampled to match the sample timing of the model output for the entire November model period. In addition, the relative distribution of values is similar between the two data sets. The relative distributions were examined by dividing all values by the data set mean for both the model results and the ADP backscatter (Fig. 2). Because the ADP backscatter was not calibrated it can only be used

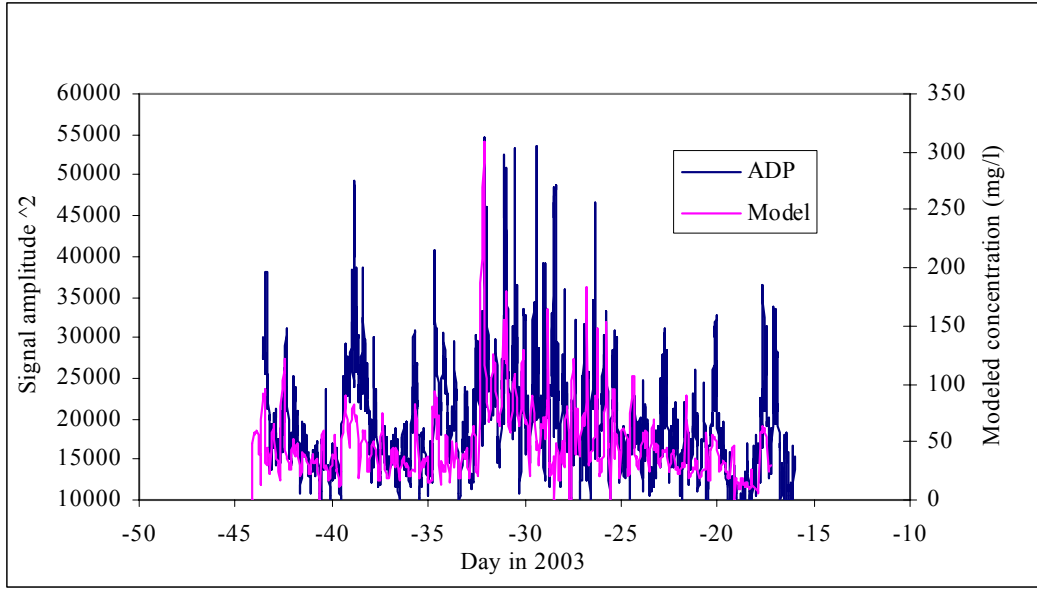


Fig 1 Comparison of model and ADP data. Signal amplitude at 0.75(depth) is used as a proxy for sediment concentration.

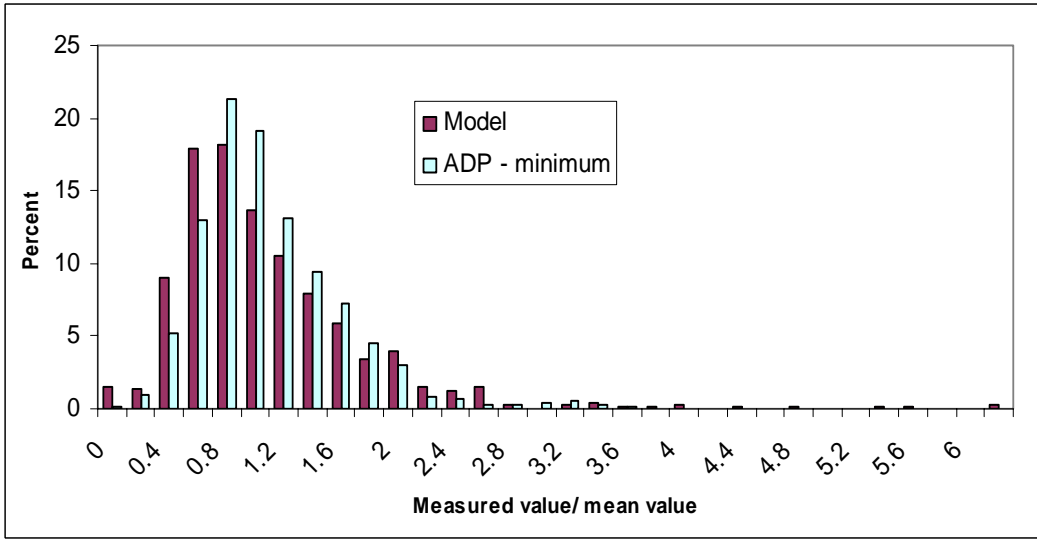


Fig 2 Comparison of the frequencies of the ADP and modeled data. Because the ADP data is not calibrated to sediment concentration, the two values are presented relative to the mean value. The minimum recorded ADP value was subtracted from all ADP measured values.

to examine the temporal pattern of in situ and modeled sediment suspension. However, surface water samples taken along two transects, one along the channel and one across the channel, on November 26, 2002 can be used to verify the suspended sediment concentrations predicted by the model. Samples from the across channel transect of seven points had an average concentration of  $26 \text{ mg l}^{-1}$  while the mean modeled value for the same transect was  $18 \text{ mg l}^{-1}$ . For the along channel transect, the average measured concentration ( $25 \text{ mg l}^{-1}$ ) is also similar to the modeled average concentration ( $18 \text{ mg l}^{-1}$ ). The model averages are both spatial and temporal averages, because all modeled values in the time period for the water sampling were averaged. In both cases the model slightly underestimates suspended sediment concentration, possibly because the time period includes a slack water period. While few water samples were taken during slack water, all of the modeled values include this time because they are averages.

The model data exhibited much greater variation than the measured data, which may be due to greater spatial resolution and a lack of advection in the model. In the lagoon, lateral mixing may smooth the distribution of sediment concentrations. The modeled wave height was fairly consistent for the along channel transect, but the tide stress is highly variable (Fig 3). The variation in concentration was largely explained by the variation in tide stress with a few peaks in concentration occurring where tide stress was low because of sediment at those sites was finer than at other sites along the transect (higher phi size) (Fig 3).

#### *Controls on sediment suspension*

Wind is an important control on sediment suspension in Hog Island Bay. The importance of wind for hydrodynamics is presented in chapter 3, but the importance of

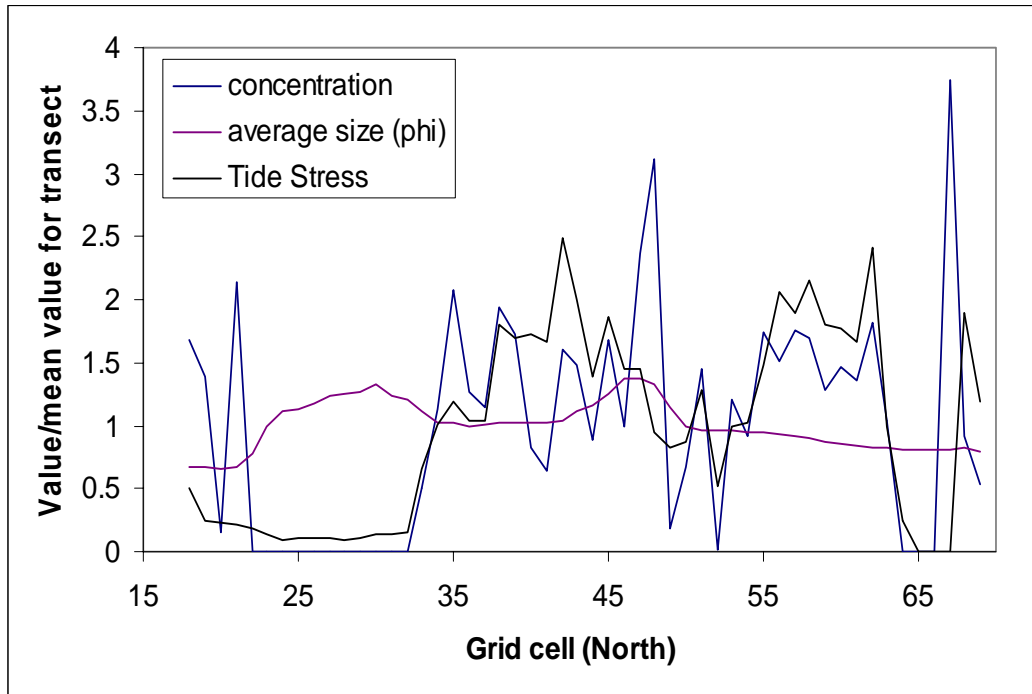


Fig 3 Variation in modeled concentration, modeled tide stress and interpolated grain size for the along channel transect on November 26, 2002. All values are presented relative to the mean for the transect.

wind for sediment suspension has to be examined to determine its role in light attenuation. The importance of wind for sediment suspension is seen in the ADP data. Wind speed binned in one meter intervals and divided into East-West and North-South components shows strong relationships with the signal amplitude squared ( $R^2=0.83$ ,  $p < 0.05$  for a second order polynomial regression of each direction Fig 4). The relationship is relatively insensitive to direction. A linear regression of wind speed and signal amplitude squared shows that, assuming signal amplitude is a measure of suspended sediment concentration, wind speed explains 29% of the variation in suspended sediment concentration. This value seems somewhat low, but that is because the effect of the wind is confounded by the tidal stage. Wave stress is also dependent on tidal stage complicating the relationship (Chapter 3). Examining the time series of wind speed and signal amplitude also shows the response of sediment suspension to wind speed (Fig 5). Wind speed forces current velocity, wave height, water elevation and sediment suspension. No time lag is evident in the response of sediment suspension to wind and all high wind events have a corresponding sediment peak. Janseen-Stedler (2000) found deposition on a tidal mudflat during calm weather and erosion during stormy weather indicating the importance of wind for sediment suspension. Arfi et al (1993) found that wind speeds greater than  $3 \text{ m s}^{-1}$  caused suspension of sediments in the Ebrie Lagoon, Cote d'Ivoire. Both of these studies show that winds are important controls on sediment suspension in shallow systems.

#### *Light availability*

The model runs for November and August, which differed only in wind forcing, show large differences in light availability. The higher wind speeds in November

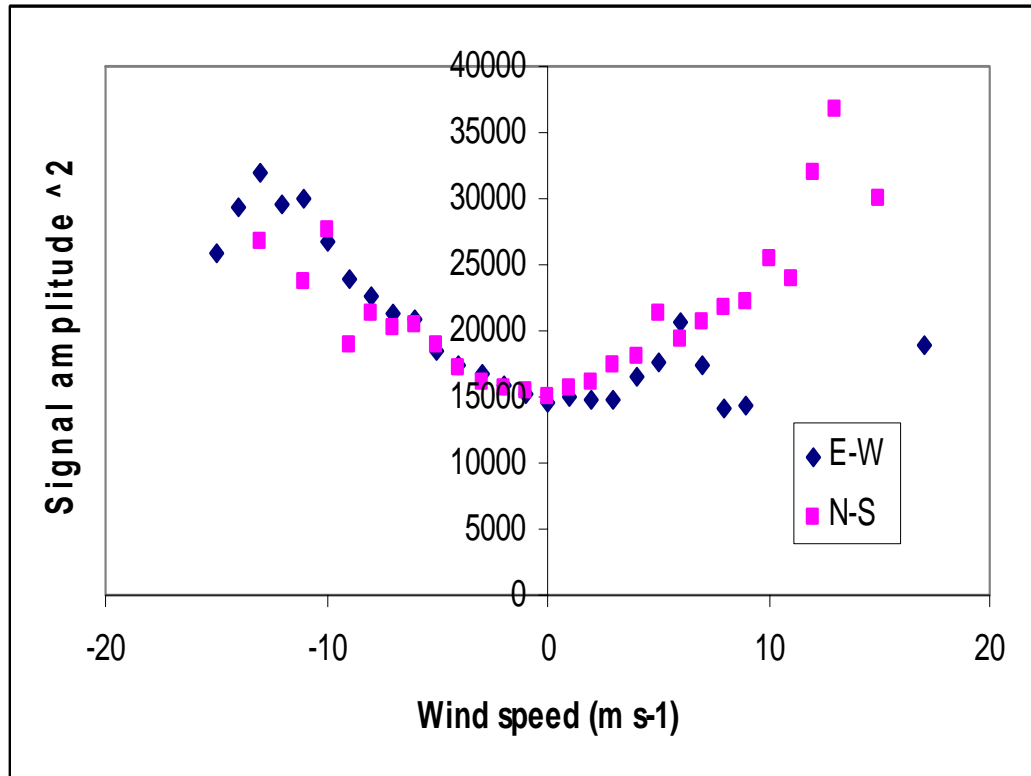


Fig 4 Relationship between binned wind speed and sediment concentration (represented by signal amplitude<sup>2</sup>). Sediment suspension is related to wind speed, but not direction.

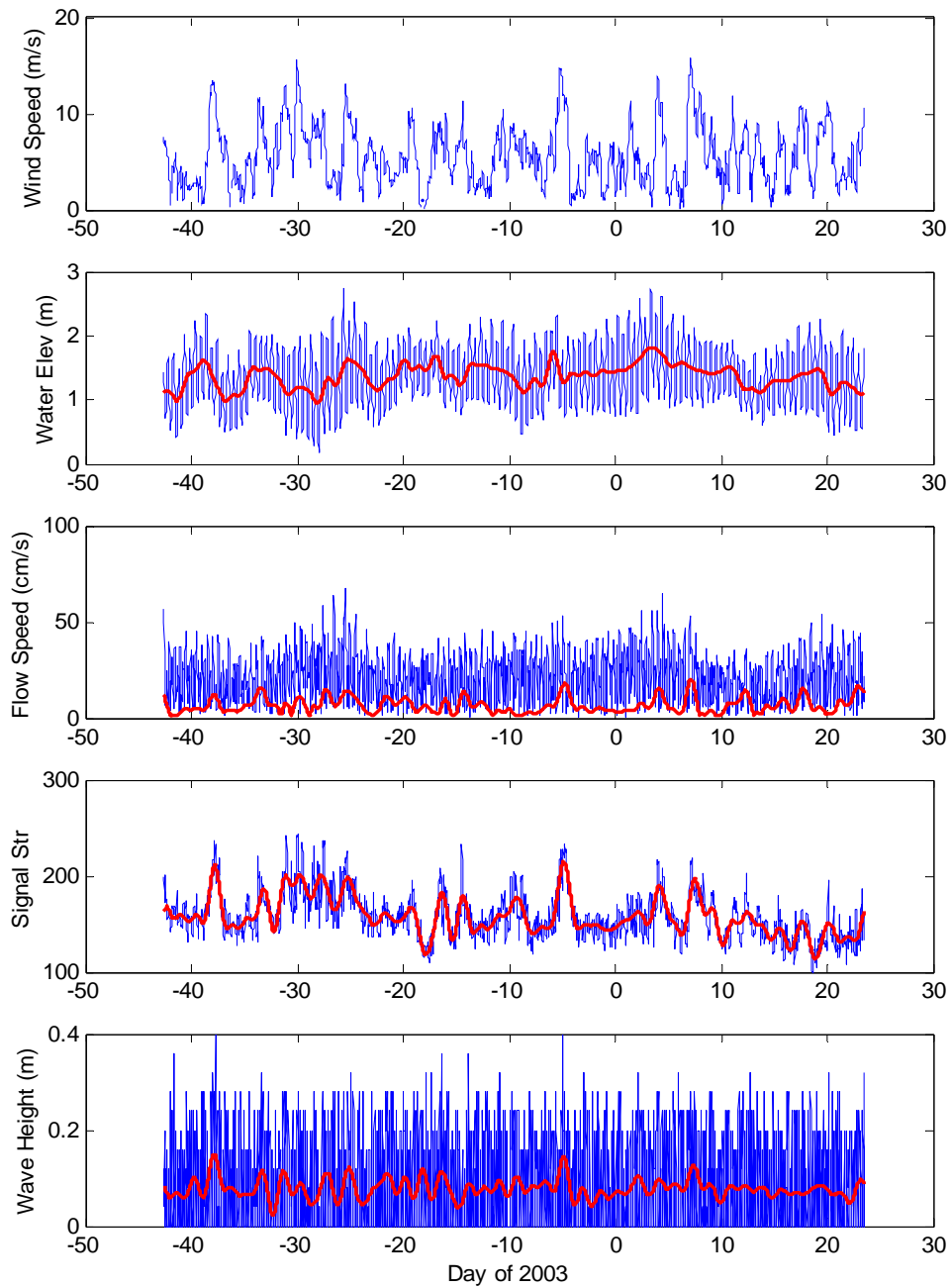


Fig 5. Wind speed measured at Kiptopeke, VA with water level, flow speed, signal strength, and wave height recorded by the ADP. The values in blue are the recorded values from the ADP; the red line is the result of a low pass filter.

resulted in more sediment suspension and lower light availability. To quantify the effects this difference in light availability can have on seagrass distribution, a criteria of 20% of surface irradiance reaching depth, a typical value used for seagrasses (Duarte 1991, Zimmerman et al 1995, Dennison et al 1993), is used to define suitable seagrass habitat. While percent light availability in this study has been calculated for both scalar and downwelling irradiance, the habitat criteria for seagrass have been established for downwelling irradiance, so that measure is used here. For the August data, 87% of the modeled sediment surface is suitable habitat based on the average light availability, with light limitation only in the channel (Fig 6a). For the November data, only 65% percent of the sediment surface is suitable habitat based on average light availability (Fig 6b), a decrease of more than 20 km<sup>2</sup>. The same trend is magnified if suitable habitat is defined only as areas that receive greater than 20% of surface irradiance 90-100% of the time. Based on this criteria, 80% of the modeled surface is suitable habitat in August, but only 14% is suitable habitat based on the November results (Fig 7). For both criteria, the area that is suitable habitat based on the November results is mostly behind Hog and Cobb Islands. In other areas of the VCR-LTER where seagrass recolonization has occurred, the seagrasses have returned in these areas behind barrier islands (Orth, personal communication). All calculations were done assuming solar noon.

The light availability at the sediment surface in Hog Island Bay changes on many time scales. The highest frequency events occur on the order of hours and include changing wind conditions and tidal depths and velocities. The tidal depths and velocities also change with the monthly pattern of the spring-neap cycle. While wind conditions change on the scale of hours, the wind conditions also follow a seasonal cycle. Finally,

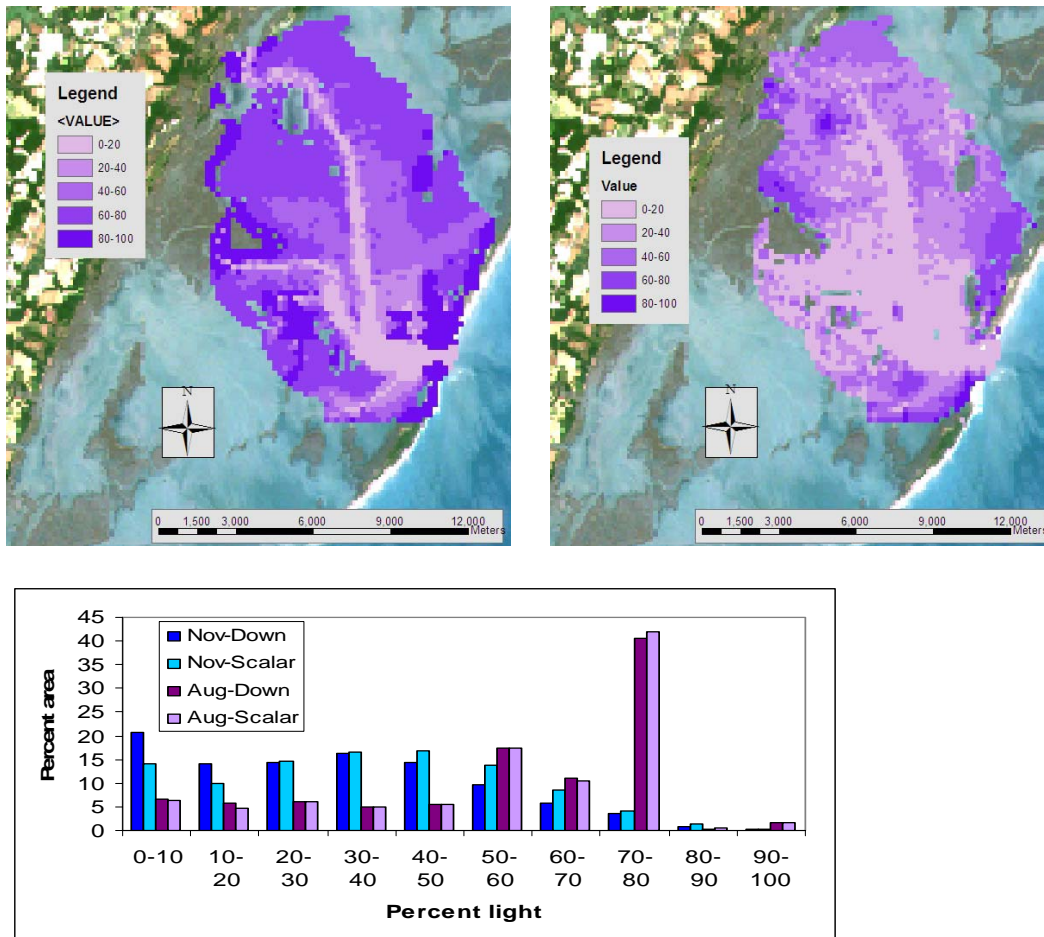


Fig 6 Depictions of modeled values of average light availability for the August (a) and November (b) model runs. The maps are made based on downwelling light. The bar graph shows results for both runs for both downwelling and scalar irradiance.

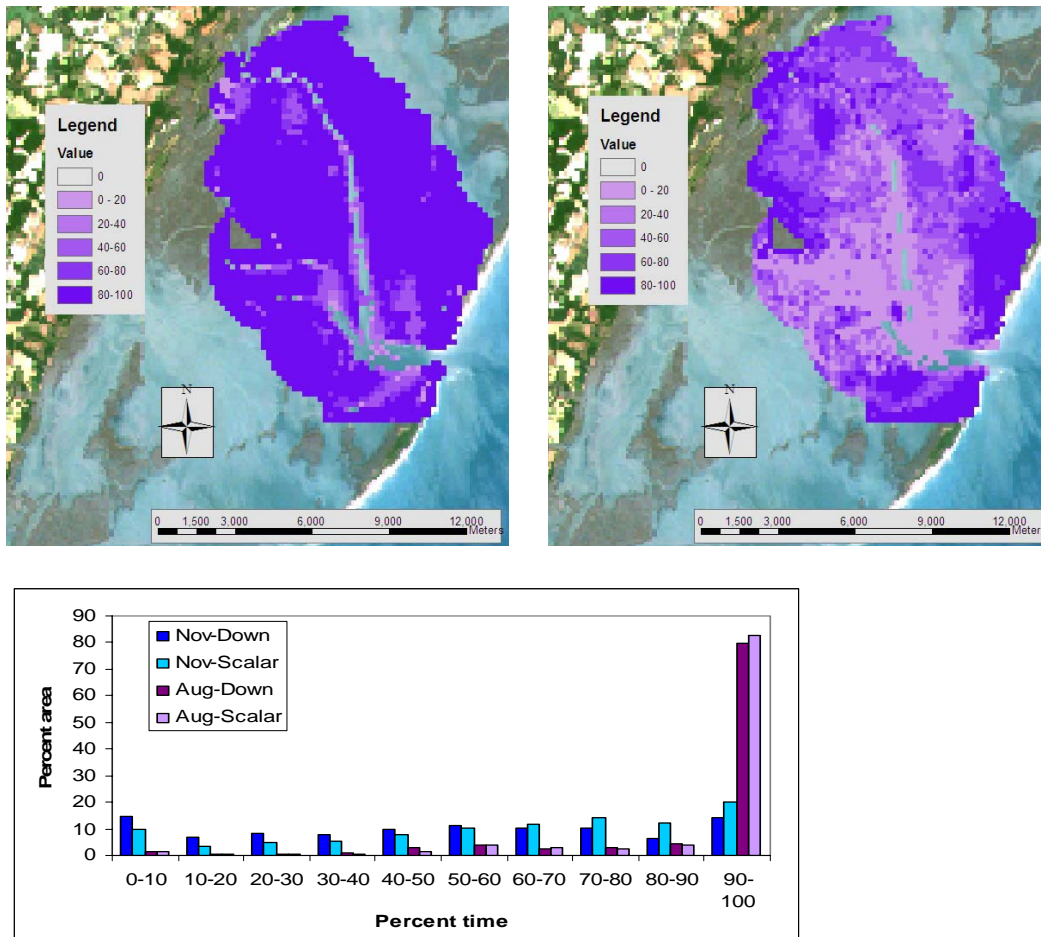


Fig. 7 Depictions of the percent of time the lagoon bottom receives greater than 20% of incident irradiance in August (a) and November (b). The maps are created using the attenuation coefficient for downwelling light. The bar graph depicts the same data with results for scalar irradiance added seasonally with changes in the solar zenith. In continuous monitoring of light availability

the light attenuation due to chlorophyll and dissolved organic carbon vary seasonally and are added to the light attenuation from suspended sediment. The incoming solar irradiance also varies hourly and in a *Halodule wrightii* meadow, Dunton (1994) found that the high variability changes in light attenuation masked the seasonal effects of changing incoming solar irradiance. The importance of these different timescales for seagrass growth is unclear. A minimum of 3-6 days of light limitation is needed to affect seagrass (Longstaff et al 1999). This finding indicates that high frequency variations in wind speed will not be important if they cause sediment suspension events shorter than this length, but because of the slow settling velocities of fine sediment particles the duration of a sediment suspension event can be much longer than the duration of the physical forcing causing the sediment suspension. Krause-Jensen et al (2003) used regression modeling of eelgrass cover with photon flux density, relative wave exposure, and salinity or different depth intervals to determine the importance of these factors in controlling eelgrass populations. They found that a large percentage of the area that seemed suitable for eelgrass had zero cover, indicating that extreme low frequency events are important in regulating seagrass distribution (Krause-Jensen et al 2003). Extreme events were also related to the light limitation that led to the die-off of a coastal population of seagrass, but these storms were considered a seasonal phenomenon (Cabello-Pasini et al 2003). The appropriate timescales for assessing all of the causes of light limitation may be the duration of the light limitation, not the duration of the forcing event.

The approach used in this study demonstrates the importance of physical forcing mechanisms in determining light attenuation. However, numerous improvements could

be made to increase the accuracy of the results. More accurate representation of chlorophyll through modeling of the productivity of phytoplankton and suspension of benthic chlorophyll will provide a better understanding of the seasonal dynamics of light availability. In addition, light attenuation was shown to be dependent on sediment grain size, but grain size was not included in the calculation of  $K$ . Finally, a single value of  $K$  was given for the entire water column in this study. Gradients in suspended sediment concentration would result in gradients in  $K$  with vertical position in the water column. The approach used to calculate suspended sediment concentrations in this study did not predict the vertical distribution of suspended sediment making this type of calculation impossible. This study has shown that a physical process approach allows extension of field data temporally and spatially to represent light attenuation more thoroughly. This study also shows the importance of considering variations in wind forcing in determining sediment suspension and concomitant light attenuation. Even if a modeling approach can not be taken, the lesson of this study that wind-forcing is important can inform the design of monitoring programs.

## **Conclusion**

Hydrodynamics and sediment transport, and therefore light availability, in Hog Island Bay are wind driven, particularly in the shallow areas. Because of this, modeled values of light availability for two time periods, characterized only by different wind conditions, show very different extents of light limitation. Changes in the concentration of other light attenuating substances, such as chlorophyll, which might lessen the difference in light availability from August to November, are considered only as monthly

averages in this approach. However, inclusion of these factors will not change that suspension of sediment from meteorological forcing is an important control on light availability in shallow systems. The spring season is the most important time period for the growth of seagrass transplants (Moore et al 1997). This time period has not been considered in this thesis but the approach shown here would be helpful to define areas for seagrass transplants based on spring conditions. The importance of considering wind conditions has been shown here.

## Chapter 6: Conclusion

This thesis furthers earlier work examining the role of physical forcing mechanisms on light attenuation. Fieldwork and process-based modeling were combined to examine light attenuation over temporal and spatial scales not possible through fieldwork alone. This approach also allowed examination not only of the extent of light limitation, but also of the controls on light attenuation. This thesis combined the physical characteristics of Hog Island Bay, the sediment characteristics (Chapter 2) and the hydrodynamics (Chapter 3) with a description of how suspended sediment and other water column components affect light attenuation (Chapter 4) to model light availability at the sediment surface for two time periods (Chapter 5).

Sediment suspension in Hog Island Bay, particularly on the shallow flats, is controlled by wind. Wind speed explains 29% of the variation in suspended sediment concentration as measured by the signal amplitude of the ADP. While this value seems small, this measure does not account for changes in wave stress caused by changing water depths which limits the ability of a linear regression in predicting suspended sediment concentration from wind speed. Visual analysis of the signal amplitude and wind stress time series show that all high turbidity events have a corresponding wind peak. The wind effect on the tides is greatest in the shallow areas and the importance of wind-driven waves also increases with depth. The average low tide wave stress exceeds  $0.04 \text{ N m}^{-2}$ , the critical shear stress determined from the ADP data, for 40% of the modeled area based on the November model results. These shallow areas are the most likely habitat for seagrass.

While the field data from this study showed that light attenuation was controlled by suspended sediment, controls on light availability in Hog Island Bay may vary seasonally. For the field data from October 2003 used in this study, total suspended solids explained 84% of the variation in scalar attenuation and 93% of the variation in downwelling attenuation. No other variables were significant in a multiple stepwise regression. Examination of monitoring data sets from Hog Island Bay showed that chlorophyll and dissolved organic matter may be important seasonally. Measurements of spectral irradiance taken in May 2002, showed the lowest attenuation from 550-570 nm and peaks in attenuation above 700nm and between 400-440 nm. This pattern is indicative of attenuation by chlorophyll and dissolved organic matter. The relative importance of chlorophyll, dissolved organic matter and total suspended solids should vary seasonally both because of the seasonality of productivity and the seasonality of wind events to suspend sediment.

The final results of this thesis are depictions of suitable seagrass habitat based on two model runs. A criteria of 20% of downwelling irradiance reaching the sediment surface was used to define suitable habitat (Duarte 1991). Based on average light conditions for the model periods, 22% less of the modeled area is suitable habitat during November, 2002 than August 2000. November is the windier period with an average wind speed of  $5.7 \text{ m s}^{-1}$ . Average wind speed for the August 2000 model period is  $3.8 \text{ m s}^{-1}$ . The decrease in suitable habitat for the November run is caused by increased sediment suspension. The model runs were only different in wind forcing and chlorophyll concentration, which was higher in August. The chlorophyll concentrations used were based on monthly averages from a long term data set from Hog Island Bay.

These results show that wind forcing of sediment suspension is important as a control on light availability.

## References

- Arfi, R, D Guiral and M Bouvy. 1993. Wind induced resuspension in a shallow tropical lagoon. *Estuarine, coastal and shelf science*. 36:587-604.
- Aubrey, DG. 1986. Hydrodynamic controls on sediment transport in well-mixed bays and estuaries. In van de Kreeke, J. (ed). *Physics of shallow estuaries and bays*. Springer – Verlag: New York, New York.
- Baba, J and PD Komar. 1981. Measurements and analysis of settling velocities of natural quartz sand grains. *Journal of sedimentary petrology*. 51(2):631-640.
- Baker, ET and JW Lavelle. 1984. The effect of particle size on the light attenuation coefficient of natural suspensions. *Journal of geophysical research*. 89:8197-8203.
- Bailey, MC and DP Hamilton. 1997. Wind induced sediment resuspension: a lake-wide model. *Ecological modeling*. 99:217-228.
- Bannister, TT. 1990. Empirical equations relating scalar irradiance to a, b/a, and solar zenith angle. *Limnology and oceanography*. 35(1):173-177.
- Barko JW and RM Smart. 1986. Sediment-related mechanisms of growth limitation in submersed macrophytes. *Ecology*. 67(5):1328-1340.
- Bassoullet, P, P Le Hir, D Gouleau, and S Robert. 2000. Sediment transport on an intertidal mudflat: field investigations and estimations of fluxes within the Baie de Marennes-Oleron (France). *Continental shelf research*. 20(12-13):16325-1653.
- Betteridge, KFE, PD Thorne and PS Bell, 2002. Assessment of acoustic coherent Doppler and cross-correlation techniques for measuring near-bed velocity and suspended sediment profiles in the marine environment. *Journal of atmospheric and oceanic technology*. 19:367-380.
- Blom G, EHS Vanduin, and L Lijklema. 1994. Sediment resuspension and light conditions in some shallow Dutch lakes. *Water science and technology*. 30(10):243-252.
- Bricaud, A and D Stramski. 1990. Spectral absorption coefficients of living phytoplankton and nonalgal biogenous matter: A comparison between the Peru upwelling area and the Sargasso Sea. *Limnology and oceanography*. 35(3):315-331.
- Bunt JAC, P Larcombe and CF Jago. 1999. Quantifying the response of optical backscatter devices and transmissometers to variations in suspended particulate matter. *Continental shelf research*. 19(9):1199-1220.
- Cabello-Pasini, A, C Lara-Turrent, and RC Zimmerman. 2002. Effects of storms on photosynthesis, carbohydrate content and survival of eelgrass populations from a coastal lagoon and the adjacent open ocean. *Aquatic botany*. 74:149-164.
- Christiansen T, PL Wiberg, and TG Milligan. 2000. Flow and sediment transport on a tidal salt marsh surface. *Estuarine coastal and shelf science*. 50(3):315-331.
- Curran KJ, PS Hill, TG Milligan. 2003. Time variation of flocculation properties in a settling column. *Journal of sea research*. 49(1):1-9.
- Davis, RE and R Dolan. 1993. Nor'easters. *American Scientist*. 81:428-439.
- Dennison, WC. RJ Orth, KA Moore, JC Stevenson, V Carter, S Kollar, PW Bergstrom, and RA Batiuk. 1993. Assessing water-quality with submersed aquatic vegetation. *Bioscience*. 43(2):86-94.
- Dierberg FE, TA DeBusk, SD Jackson, MJ Chimney, and K Pietro. 2002. Submerged aquatic vegetation-based treatment wetlands for removing phosphorus from agricultural runoff: response to hydraulic and nutrient loading. *Water research*. 36(6): 1409-1422.
- Dietrich WE. 1982. Settling velocity of natural particles. *Water resources*

- research*. 18(6):1615-1626.
- Drake DE, R Eganhouse, and W McArthur. 2002. Physical and chemical effects of grain aggregates on the Palos Verdes margin, southern California. *Continental shelf research*. 22 (6-7): 967-986
- Dring, MJ and K Lüning. 1994. Influence of spring-neap tidal cycles on the light available for photosynthesis by benthic marine plants. *Marine ecology progress series*. 104:131-137.
- Dronkers, J. 1986. Tide-induced residual transport of fine sediment. In van de Kreeke, J. (ed). *Physics of shallow estuaries and bays*. Springer-Verlag: New York, New York.
- Duarte, CM. 1991. Seagrass depth limits. *Aquatic botany*. 7:139-150.
- Duarte, CM. 2002. The future of seagrass meadows. *Environmental conservation*. 29(2):192-206.
- Dunton, KN. 1994. Seasonal growth and biomass of the subtropical seagrass *Halodule wrightii* in relation to continuous measurements of underwater irradiance. *Marine biology*. 120(3):479-489.
- Dyer, KR. 1986. *Coastal and estuarine sediment dynamics*. John Wiley and sons, Chichester, Great Britain.
- Dyer, KR, J Cornelisse, MP Dearnaley, MJ Fennessy, SE Jones, J Kappenberg, IN McCave, M Pejrup, W Puls, W vanLeussen, and K Wolfstein. 1996. A comparison of in situ techniques for estuarine floc settling velocity measurements. *Journal of sea research*. 36(1-2): 15-29.
- Fennessy, MJ, KR Dyer, and DA Huntley. 1994. INSSEV – An instrument to measure the size and settling velocity of flocs in-situ. *Marine geology*. 117(1-4): 107-117
- Fugate, DC, CT Friedrichs, IC Anderson, A Bilgili, and B Zelenke. 2002. Determining residence time for Hog Island Bay using a 2-D finite element model allowing for dewatering of intertidal flats. Abstract. American Society for Limnology and Oceanography. Ocean Sciences Meeting. February 2002.
- Fugate, DC and CT Friedrichs. Estimation of residence time in a shallow back barrier lagoon, Hog Island Bay, Virginia, USA. In prep.
- Gacia, E. and CM Duarte. 2001. Sediment retention by a Mediterranean *Posidonia oceanica* meadow: The balance between deposition and resuspension. *Estuarine, coastal and shelf science*. 52(4):505-514.
- Gacia E, C. M. Duarte, N. Marba, J. Terrados, H. Kennedy, M.D. Fortes, N.H. Tri. 2003. Sediment deposition and production in SE-Asia seagrass meadows. *Estuarine coastal and shelf science*. 56(5-6):909-919.
- Gaffey S.J. and C.E. Bronnimann. 1993. Effects of bleaching on organic and mineral phases in biogenic carbonates. *Journal of sedimentary petrology*. 63(4):752-754.
- Gallegos, CL, 2001. Calculating optical water quality targets to restore and protect submersed aquatic vegetation: Overcoming problems in partitioning the diffuse attenuation coefficient for photosynthetically active radiation. *Estuaries*. 24(3):381-397.
- Gallegos, CL and WJ Kenworthy. 1996. Seagrass depth limits in the Indian River Lagoon (Florida, U.S.A.): Application of an optical water quality model. *Estuarine, coastal and shelf science*. 42:267-288.
- Gordon, HR. 1989. Can the Lambert-Beer law be applied to the diffuse attenuation coefficient of ocean water? *Limnology and oceanography*. 34(8):1389-1409.

- Granata, T.C., T Serra, J Colomer, X Casamitjana, CM Duarte, and E Gacia. 2001. Flow and particle distribution in a nearshore seagrass meadow before and after a storm. *Marine ecology progress series*. 218:95-106.
- Gullstrom M, M de la Torre Castro, SO Bandeira, M Bjork, M Dahlberg, N Kautsky, P Ronnback, and MC Ohman. 2002. Seagrass ecosystems in the Western Indian Ocean. *Ambio*. 31 (7-8): 588-596.
- Hall MO, MJ Durako, JW Fourqurean, and JC Zieman. 1999. Decadal changes in seagrass distribution and abundance in Florida Bay. *Estuaries*. 22(2B):445-459.
- Hanlon, CG, RL Miller, and BF McPherson. 1998. Relationships between wind velocity and underwater irradiance in a shallow lake (Lake Okeechobee, Florida, USA). *Journal of the American Water Resources Association*. 34(4):951-961.
- Harris, CK and Wiberg, PL. 1997. Approches to quantifying long-term continental shelf sediment transport with an example from the Northern California STRESS mid-shelf site. *Continental shelf research*. 17(11):1389-1418.
- Havens KE. 2003. Submerged aquatic vegetation correlations with depth and light attenuating materials in a shallow subtropical lake. *Hydrobiologia*. 493(1-3):173-186.
- Hayakawa K., T Sekino, T Yoshioka, M Maruo, and M Kumagai. 2003. Dissolved organic carbon and fluorescence in Lake Hovsgol: factors reducing humic content of the lake water. *Limnology*. 4(1):25-33.
- Heiss, WM, AM Smith, and PK Probert. 2000. Influence of the small intertidal seagrass *Zostera novazelandica* on linear water flow and sediment texture. *New Zealand journal of marine and freshwater research*. 34(4):689-694.
- Hill PS, TG Milligan, and WR Geyer. 2000. Controls on effective settling velocity of suspended sediment in the Eel River flood plume. *Continental shelf research*. 20(16):2095-2111.
- Holdaway, GP, PD Thorne, D Flatt, SE Jones, and D Prandle. 1999. Comparison between ADCP and transmissometer measurements of suspended sediment concentration. *Continental shelf research*. 19:421-441.
- Holmes, RW. 1970. The Secchi disk in turbid coastal waters. *Limnology and oceanography*. 15: 688-694.
- Huettel M., H Roy, E Precht, and S Ehrenhauss. 2003. Hydrodynamical impact on biogeochemical processes in aquatic sediments. *Hydrobiologia*. 494(1-3):231-236.
- Janssen-Stedler, B. 2000. The effect of different hydrodynamic conditions on the morphodynamics of a tidal mudflat in the Dutch Wadden Sea. *Continental shelf research*. 20(12-13):1461-1478.
- Kenworthy WJ and MS Fonseca. 1996. Light requirements of seagrasses *Halodule wrightii* and *Syringodium filiforme* derived from the relationship between diffuse light attenuation and maximum depth distribution. *Estuaries*. 19(3):740-750.
- Kirk, JTO. 1983. *Light and photosynthesis in aquatic ecosystems*. New York: Cambridge university press.
- Koch EM. 2001. Beyond light: Physical, geological and geochemical parameters as possible submersed aquatic vegetation habitat requirements. *Estuaries*. 24(1):1-17.
- Koch, EW and S Beer. 1996. Tides, light and the distribution of *Zostera marina* in Long Island Sound, USA. *Aquatic botany*. 53:97-107.
- Kocum, E, GJC Underwood, and DB Nedwell. 2002. Simultaneous measurement of phytoplanktonic primary production, nutrient and light availability along a turbid,

- eutrophic UK east coast estuary (the Colne Estuary). *Marine ecology progress series*. 231:1-12.
- Krank, K. and T.G. Milligan. 1992. Characteristics of suspended particles at an 11-hour anchor station in San Francisco Bay, California. *Journal of geophysical research- oceans*. 97 (C7): 11373-11382
- Le Hir P, W Roberts, O Cazaillet, MC Christie, P Bassoullet, and C Bacher. 2000. Characterization of intertidal flat hydrodynamics. *Continental shelf research*. 20(12-13):1433-1459.
- Longstaff, BJ and WC Dennison. 1999. Seagrass survival during pulsed turbidity events: the effects of light deprivation on the seagrasses *Halodule pinifolia* and *Halophila ovalis*. *Aquatic Botany*. 65(1-4):105-121.
- Longstaff, BJ et al. 1999. Effects of light deprivation on the survival and recovery of the seagrass *Halophila ovalis* (R. Br.) Hook. *Journal of experimental marine biology and ecology*. 234:1-27.
- Lund-Hansen LC, M Laima, K Mouritsen, N N Lam, and DN Hai. 2002. Effects of benthic diatoms, fluff layer, and sediment conditions on critical shear stress in a non-tidal coastal environment. *Journal of the marine biological association of the United Kingdom*. 82 (6): 929-936
- Manning AJ and KR Dyer. 2002. The use of optics for the in situ determination of flocculated mud characteristics. *Journal of optics A- Pure and applied optics*. 4(4):S71-S81.
- Maske, H and H Haardt. 1987. Quantitative in vivo absorption spectra of phytoplankton: Detrital absorption and comparison with fluorescence spectra. *Limnology and oceanography*. 32(3):620-633.
- McAnally W.H. and A.J. Mehta. 2002. Significance of aggregation of fine sediment particles in their deposition. *Estuarine coastal and shelf science*. 54(4):643-653.
- McGlathery, KJ, IC Anderson and AC Tyler. 2001. Magnitude and variability of benthic and pelagic metabolism in a temperate coastal lagoon. *Marine ecology progress series*. 216: 1-15.
- McGlathery, K. J., A. C. Tyler, M. Thomsen, P. Berg, I. Buffam, J. Burton, S. Lawson, and J. Rosinski. Primary producer dominance and implications for nitrogen assimilation in a temperate coastal lagoon. In prep.
- Meise C.J. and L.L. Stehlik. 2003. Habitat use, temporal abundance variability, and diet of blue crabs from a New Jersey estuarine system. *Estuaries*. 26(3):731-745.
- Mikkelsen OA. 2002. Examples of spatial and temporal variations of some fine-grained suspended particle characteristics in two Danish coastal water bodies. *Oceanological acta*. 25(1):39-49.
- Mikkelsen, OA and Pejrup, M. 2000. In situ particle size spectra and density of particle aggregates in a dredging plume. *Marine geology*. 170(3-4):443-459.
- Miller M.C., IN McCave, and PD Komar. 1977. Threshold of sediment under unidirectional currents. *Sedimentology*. 24:507-527.
- Milligan TG and DH Loring. 1997. The effect of flocculation on the size distributions of bottom sediment in coastal inlets: Implications for contaminant transport. *Water air and soil pollution*. 99(1-4):33-42
- Moore, KA, RLWetzel, and RJ. Orth. 1997. Seasonal pulses of turbidity and their relations to eelgrass (*Zostera marina* L.) survival in an estuary. *Journal of experimental and marine biology*. 215:115-134.

- Murdoch A. and SD MacKnight. 1991. Bottom sediment sampling. In Murdoch, A. and S.D. MacKnight (eds). *CRC handbook of techniques for aquatic sediments sampling*. CRC Press, Boca Raton, Florida.
- Nichols, MM and RB Biggs. 1985. Estuaries. In Davis R.A. (ed) *Coastal sedimentary environments*. Springer-Verlap:New York, New York.
- Nielsen SL, K Sand-Jensen, J Borum, and O Geertz-Hansen. 2002. Phytoplankton, nutrients, and transparency in Danish coastal waters. *Estuaries*. 25(5):930-937.
- Oertel, G., CR Carlson, and K Overman. 2000. Hog Island Bay, Virginia Bathymetric Survey using Trimble DGPS and Innerspace Digital Fathometer. Online. Available: <http://www.vcrlter.virginia.edu/~crc7m/hogbay/hogbay.html>
- Oertel, GF. 2001. Hypsographic, hydro-hypsographic and hydrological analysis of coastal bay environments, Great Machipongo Bay. *Journal of Coastal Research*. 17(4):775-783.
- Ogston, AS and RW Sternberg. 1999. Sediment transport events on the northern California continental shelf. *Marine geology*. 154(1-4):69-82.
- Olesen, B. 1996. Regulation of light attenuation and eelgrass *Zostera marina* depth distribution in a Danish embayment. *Marine ecology progress series*. 134:187-194.
- Olesen, B and K Sand-Jensen. 1993. Seasonal acclimatization of eelgrass *Zostera marina* growth to light. *Marine ecology progress series*. 94:91-99.
- Orth, RJ and KA Moore. 1983. Chesapeake Bay: An unprecedented decline in submerged aquatic vegetation. *Science*. 222(4619):51-53.
- Rabalais N.N. 2002. Nitrogen in aquatic ecosystems. *Ambio*. 31(2):102-112.
- Rasheed M, MI Badran, and M Huettel. 2003. Influence of sediment permeability and mineral composition on organic matter degradation in three sediments from the Gulf of Aqaba, Red Sea. *Estuarine coastal and shelf science*. 57(1-2):369-384.
- Ris RC, LH Holthuijsen, and N Booij. 1999. A third-generation wave model for coastal regions - 2. Verification. *Journal of geophysical research –oceans*. 104(C4):7667-7681.
- Rouse, H. 1937. Modern conceptions of the mechanics of fluid turbulence. Transactions of ASCE, Vol. 102, Paper No. 1965.
- Ruffin, KK. 1998. The persistence of anthropogenic turbidity plumes in a shallow water estuary. *Estuarine, coastal and shelf science*. 47:579-592.
- Rusch A., M Huettel, and S Forster. 2000. Particulate organic matter in permeable marine sands - Dynamics in time and depth. *Estuarine coastal and shelf science*. 51(4): 399-414
- Schaaff E., C Grenz, and C Pinazo. 2002. Erosion of particulate inorganic and organic matter in the Gulf of Lion. *Comptes rendus geoscience*. 334(15):1071-1077.
- Sfriso A. and A. Marcomini. 1999. Macrophyte production in a shallow coastal lagoon. Part II: Coupling with sediment, SPM, and tissue carbon, nitrogen and phosphorus concentrations. *Marine environmental research*. 47(3):285-309.
- Sfriso A, T Birkemeyer, and PF Ghetti PF. 2001. Benthic macrofauna changes in areas of Venice lagoon populated by seagrasses or seaweeds. *Marine environmental research*. 52(4):323-349.
- Shanks, AL. 2002. The abundance, vertical flux, and still-water and apparent sinking rates of marine snow in a shallow coastal water column. *Continental shelf research*. 22(14):2045-2064.
- Shetye, SR. and AD Gouveia. 1992. On the role of geometry of cross-section in generating flood-dominance in shallow estuaries. *Estuarine, coastal and shelf science*. 35:113-126.

- Short, FT, DM Burdick, and JE Kaldy, III. 1995. Mesocosm experiments quantify the effects of eutrophication on eelgrass, *Zostera marina*. *Limnology and oceanography*. 40(4):740-749.
- Smith, W.O. 1982. The relative importance of chlorophyll, dissolved and particulate matter and seawater to the vertical extinction of light. *Estuarine coastal and shelf science*. 15:459-465.
- Squires, MM and FW Lesak. 2003. Spatial and temporal patterns of light attenuation among lakes of the Mackenzie Delta. *Freshwater biology*. 48(1) 1-20.
- Stankelis RM, MD Naylor, and WR Boynton. 2003. Submerged aquatic vegetation in the mesohaline region of the Patuxent estuary: Past, present, and future status. *Estuaries*. 26(2A):186-195.
- Sternberg, RW, I Berhane, and AS Ogston. 1999. Measurement of size and settling velocity of suspended aggregates on the northern California continental shelf. *Marine geology*. 154(1-4):43-53.
- Stickney, RR. 1984. *Estuarine ecology of the southeastern United States and the Gulf of Mexico*. College Station, Texas: Texas A & M Press.
- Vervuren, PJA, Blom, CWPM and H de Kroon. 2003. Extreme flooding events on the Rhine and the survival and distribution of riparian plant species. *Journal of ecology*. 91(1) 135:146
- Wild-Allen, K, Lane A and Tett P. 2002. Phytoplankton, sediment, and optical observations in Netherlands coastal water in spring. *Journal of sea research*. 47:303-315.
- Vanduin EHS, G Blom, L Lijklema, MJM Scholten. 1992. Aspects of modeling sediment transport and light conditions in Lake Marken. *Hydrobiologia*. 235:167-176.
- Vermaat, JE and RJ Debruyne. 1993. Factors limiting the distribution of submerged waterplants in the lowland River Vecht (The Netherlands). *Freshwater biology*. 30(1):147-157.
- Wiberg, PL and JD Smith. 1987. Calculations of the critical shear stress for the motion of uniform and heterogeneous sediments. *Water resources research*. 23(8):1471-1480.
- Wright, LD, Kim. S-C, and Friedrichs, CT. 1999. Across-shelf variations in bed roughness, bed stress and sediment suspension on the northern California shelf. *Marine geology*. 154:99-115.
- Zelenke, B, Friedrichs, CT, and Fugate, D. 2001. Determination of residence time in a shallow estuary using a two-dimensional hydrodynamic model with dewatering. Unpublished report.
- Ziervogel, K. and B. Bohling. 2003. Sedimentological parameters and erosion behaviour of submarine coastal sediments in the south-western Baltic Sea. *Geo-marine letters*. 23(1):43-52.
- Zimmerman, RC. 2002. A bio-optical model of irradiance distribution and photosynthesis in seagrass canopies. *Limnology and oceanography*. 48(1, part 2):568-585.

Appendix 1: Sieving and sedigraph  
results (percent weight by size class)

Point	Sieve size (microns)									
28	500	250	125	63	30	15	8	4	2	<2
29	0.003	0.002	0.501	0.33	0.037	0.015	0.009	0.007	0.007	0.087
30	0.008	0.003	0.095	0.487	0.143	0.078	0.043	0.037	0.03	0.072
32	0.007	0.002	0.19	0.426	0.104	0.063	0.031	0.029	0.023	0.118
33	0.002	0.001	0.265	0.446	0.103	0.064	0.028	0.019	0.016	0.015
34	0.001	0.001	0.402	0.311	0.121	0.074	0.028	0.013	0.015	0.051
35	0.004	0.001	0.106	0.435	0.1	0.08	0.043	0.035	0.035	0.15
36	0.005	0.002	0.07	0.45	0.083	0.074	0.04	0.025	0.033	0.194
37	0.004	0.003	0.146	0.431	0.116	0.075	0.034	0.026	0.029	0.147
38	0.001	0.001	0.434	0.323	0.055	0.04	0.018	0.014	0.013	0.1
39	0.021	0.002	0.329	0.33	0.062	0.054	0.023	0.015	0.015	0.133
41	0.095	0.004	0.623	0.176	0.009	0.007	0.006	0.005	0.006	0.069
42	0.23	0.008	0.502	0.155	0.01	0.011	0.008	0.006	0.007	0.006
43	0.002	0.002	0.366	0.36	0.072	0.041	0.018	0.013	0.015	0.087
44	0.001	0.004	0.663	0.227	0.016	0.009	0.004	0.005	0.005	0.086
45	0.012	0.003	0.573	0.231	0.054	0.039	0.018	0.013	0.014	0.087
46	0.003	0.003	0.245	0.431	0.096	0.061	0.028	0.021	0.022	0.105
50	0.006	0.001	0.708	0.195	0.012	0.008	0.004	0.004	0.004	0.066
51	0.007	0.001	0.196	0.488	0.092	0.049	0.025	0.019	0.02	0.101
52	0.001	0.001	0.172	0.5	0.08	0.045	0.023	0.019	0.017	0.117
53	0.007	0.002	0.145	0.479	0.107	0.051	0.023	0.021	0.018	0.129
54	0.007	0.002	0.091	0.462	0.153	0.07	0.037	0.029	0.026	0.116
55	0.014	0.003	0.166	0.459	0.124	0.06	0.031	0.024	0.023	0.093
56	0.002	0.002	0.233	0.327	0.113	0.084	0.046	0.035	0.031	0.124
57	0.007	0.005	0.094	0.314	0.158	0.149	0.062	0.04	0.037	0.13
58	0.002	0.002	0.357	0.374	0.097	0.04	0.019	0.013	0.013	0.084
59	0.001	0.001	0.42	0.409	0.032	0.012	0.006	0.005	0.007	0.069
60	0.002	0.002	0.394	0.351	0.064	0.033	0.018	0.015	0.014	0.104
61	0.004	0.002	0.064	0.465	0.132	0.075	0.042	0.033	0.032	0.151
62	0.003	0.002	0.268	0.434	0.074	0.042	0.022	0.016	0.015	0.122
63	0.03	0.002	0.137	0.41	0.099	0.089	0.047	0.032	0.029	0.122
64	0.001	0.001	0.342	0.398	0.055	0.028	0.016	0.012	0.012	0.134
65	0.005	0.002	0.223	0.437	0.095	0.045	0.026	0.016	0.017	0.108
67	0.014	0.003	0.063	0.326	0.112	0.128	0.063	0.035	0.037	0.171
68	0.003	0.003	0.047	0.385	0.101	0.09	0.052	0.042	0.042	0.21
70	0.006	0.003	0.027	0.377	0.084	0.088	0.044	0.034	0.055	0.281
71	0.01	0.002	0.192	0.309	0.099	0.077	0.046	0.034	0.038	0.207
72	0.026	0.003	0.049	0.32	0.093	0.08	0.051	0.042	0.051	0.295
73	0.021	0.005	0.073	0.34	0.071	0.082	0.05	0.038	0.048	0.27
74	0.023	0.004	0.036	0.324	0.136	0.12	0.06	0.04	0.047	0.208
75	0.023	0.004	0.04	0.349	0.155	0.118	0.063	0.044	0.047	0.149
76	0.033	0.004	0.061	0.407	0.098	0.088	0.049	0.035	0.035	0.177

77	0.011	0.002	0.124	0.424	0.172	0.077	0.037	0.024	0.028	0.23
78	0.023	0.003	0.046	0.444	0.216	0.073	0.023	0.018	0.025	0.259
79	0.017	0.002	0.069	0.523	0.224	0.068	0.04	0.024	0.029	0.083
80	0.037	0.003	0.104	0.448	0.234	0.066	0.039	0.027	0.03	0.094
81	0.018	0.003	0.289	0.454	0.144	0.027	0.01	0.007	0.007	0.087
82	0.004	0.022	0.345	0.304	0.235	0.059	0.021	0.013	0.01	0.062
83	0.01	0.008	0.508	0.249	0.11	0.036	0.015	0.011	0.01	0.096
84	0	0.016	0.793	0.121	0.038	0	0	0	0	0
85	0.001	0.015	0.738	0.211	0	0	0	0	0	0
90	0.0023	0.0784	0.8619	0.035	0.02	0	0	0	0	0
91	0.005	0.001	0.425	0.394	0.036	0.021	0.01	0.013	0.014	0.083
92	0.001	0.017	0.831	0.156	0.012	0	0	0	0	0
93	0	0.001	0.448	0.431	0.033	0.018	0.008	0.01	0.007	0.044
94	0.053	0.003	0.455	0.383	0.093	0.003	0.002	0.002	0.001	0.006
95	0.006	0.014	0.494	0.347	0.041	0.022	0.011	0.011	0.008	0.044
96	0.159	0.146	0.341	0.254	0.025	0.013	0.007	0.008	0.006	0.041
97	0.004	0.002	0.496	0.377	0.026	0.016	0.008	0.008	0.009	0.054
98	0.001	0.001	0.727	0.265	0.006	0	0	0	0	0
100	0.092	0.004	0.507	0.305	0.024	0.015	0.007	0.008	0.007	0.033
101	0.006	0.003	0.11	0.557	0.167	0.044	0.019	0.018	0.014	0.062
102	0.002	0.003	0.387	0.485	0.036	0.019	0.007	0.007	0.006	0.047
103	0.004	0.001	0.298	0.608	0.025	0.013	0.007	0.008	0.007	0.028
601	0.017	0.002	0.313	0.476	0.042	0.028	0.012	0.013	0.013	0.083
602	0.004	0.000	0.425	0.394	0.036	0.021	0.010	0.013	0.014	0.083
603	0.004	0.001	0.298	0.608	0.025	0.013	0.007	0.008	0.007	0.028
604	0.017	0.002	0.313	0.476	0.042	0.028	0.012	0.013	0.013	0.083
605	0.009	0.002	0.313	0.435	0.077	0.047	0.017	0.016	0.013	0.070
606	0.039	0.017	0.053	0.318	0.030	0.060	0.032	0.035	0.050	0.366
607	0.009	0.014	0.047	0.352	0.073	0.091	0.052	0.046	0.045	0.270
608	0.009	0.003	0.175	0.477	0.041	0.051	0.022	0.022	0.029	0.172
609	0.008	0.001	0.458	0.417	0.027	0.016	0.008	0.008	0.007	0.050
610	0.001	0.013	0.839	0.130	0.016	0.000	0.000	0.000	0.000	0.000
611	0.001	0.017	0.831	0.156	0.012	0.000	0.000	0.000	0.000	0.000
612	0.000	0.001	0.448	0.431	0.033	0.018	0.008	0.010	0.007	0.044
613	0.053	0.003	0.455	0.383	0.093	0.004	0.002	0.002	0.002	0.009
614	0.006	0.014	0.494	0.347	0.041	0.022	0.011	0.011	0.008	0.044
615	0.159	0.146	0.341	0.254	0.025	0.013	0.007	0.008	0.006	0.041
616	0.004	0.002	0.496	0.377	0.026	0.016	0.008	0.008	0.009	0.054
617	0.001	0.001	0.727	0.265	0.006	0.000	0.000	0.000	0.000	0.000
618	0.092	0.004	0.507	0.305	0.024	0.015	0.007	0.008	0.007	0.033

Appendix 2: Average sediment characteristics

<b>Point</b>	<b>Easting</b>	<b>Northing</b>	<b>Avg phi</b>	<b>AvgMicrons</b>	<b>% organic</b>
28	433009	4141413	3.6	79.7	1.1
29	433357	4141409	4.5	43.7	2.3
30	433705	4141245	4.5	43.7	1.6
32	432109	4142211	3.6	80.1	1.7
33	431887	4142328	3.9	65.3	1.2
34	433218	4143774	4.9	32.6	2.3
35	432995	4143752	5.1	29.2	2.7
36	432634	4143699	4.9	34.2	2.0
37	431780	4143724	4.0	64.2	1.3
38	431975	4143734	4.2	53.9	2.2
39	433387	4137950	3.1	118.1	1.7
41	433313	4138418	2.2	211.8	1.6
42	432952	4138639	3.9	67.4	1.6
43	433274	4139144	3.5	88.7	0.7
44	433206	4139355	3.9	68.7	1.3
45	432902	4138318	4.4	46.9	1.9
46	433448	4137650	3.3	104.1	1.0
50	433936	4141148	4.3	50.2	1.8
51	433799	4141114	4.3	49.7	1.5
52	433622	4141229	4.5	44.6	1.9
53	433343	4141421	4.7	38.4	1.9
54	432934	4141497	4.4	48.1	1.8
55	432551	4141483	4.7	38.4	2.2
56	432488	4141456	5.1	28.6	2.7
57	433246	4140016	4.0	63.1	1.0
58	433122	4139971	3.5	89.8	1.0
59	432627	4139782	4.0	61.8	1.6
60	431257	4145548	5.0	30.8	1.6
61	432810	4142027	4.3	50.8	1.1
62	432347	4142697	4.7	39.1	2.5
63	432729	4142827	4.2	54.0	1.0
64	432592	4143350	4.2	53.6	1.5
65	432019	4143687	5.1	28.6	2.9
67	432686	4144059	5.4	23.4	2.4
68	432441	4144327	5.9	16.5	2.2
70	432298	4144255	5.3	25.8	2.4
71	432593	4144160	6.0	15.7	2.8
72	432840	4144064	5.7	18.8	2.8
73	432296	4144398	5.6	21.0	2.7
74	432508	4144351	5.2	26.5	2.6
75	432758	4144303	5.1	29.6	1.7
76	431812	4144986	5.8	17.5	1.9

<b>77</b>	431989	4145048	6.0	15.5	2.0
<b>78</b>	432353	4145193	4.9	34.2	2.1
<b>79</b>	432732	4145278	4.9	34.2	1.6
<b>80</b>	435892	4136669	4.1	57.5	1.3
<b>81</b>	435791	4136873	4.3	52.5	1.0
<b>82</b>	436546	4138590	4.0	61.5	0.7
<b>83</b>	436250	4138024	2.6	165.4	0.4
<b>84</b>	435577	4136431	2.6	165.0	0.4
<b>85</b>	435580	4136053	2.5	179.0	0.3
<b>90</b>	436833	4138827	3.8	72.6	0.9
<b>91</b>	436281	4138637	2.7	154.2	1.7
<b>92</b>	436318	4138610	3.5	90.0	1.2
<b>93</b>	436195	4137484	3.0	122.2	0.5
<b>94</b>	435969	4137303	3.4	93.9	0.9
<b>95</b>	436115	4137158	2.8	147.1	0.6
<b>96</b>	435706	4136664	3.5	90.7	0.5
<b>97</b>	435631	4136637	2.8	146.9	0.6
<b>98</b>	435715	4136506	3.0	120.8	0.9
<b>100</b>	434424	4133585	4.2	54.8	1.1
<b>101</b>	434776	4133749	3.5	86.9	0.5
<b>102</b>	434528	4134220	3.5	89.5	0.6
<b>103</b>	434684	4134591	3.9	68.4	1.1
<b>601</b>	433408.4	4146063	3.8	72.6	1.9
<b>602</b>	432651	4145555	3.5	89.4	1.3
<b>603</b>	431822	4144949	3.9	68.0	1.6
<b>604</b>	430851.9	4144774	3.9	66.0	2.0
<b>605</b>	429865.3	4144572	6.1	14.4	4.1
<b>606</b>	428827	4144529	5.8	17.6	3.7
<b>607</b>	433394.8	4141227	4.8	37.0	3.4
<b>608</b>	432003.5	4136830	3.5	90.9	1.5
<b>609</b>	432745.7	4137402	2.6	160.2	0.7
<b>610</b>	433588.3	4137928	2.7	153.9	0.8
<b>611</b>	434376.6	4138529	3.5	89.3	1.1
<b>612</b>	435169	4139111	3.1	118.3	1.1
<b>613</b>	435830.9	4139780	3.4	93.0	1.3
<b>614</b>	434799.7	4142040	2.8	146.9	1.1
<b>615</b>	432459.2	4140837	3.5	90.7	1.2
<b>616</b>	431585.8	4140426	2.8	146.8	4.7
<b>617</b>	430804.6	4139919	3.0	121.3	2.6
<b>618</b>	430026.1	4139337	4.2	54.7	1.7

Appendix 3: Turbidimeter and spectrophotometer results  
10/30/03

<b>Site</b>	<b>Avg NTU</b>	<b>StDev NTU</b>	<b>Avg Abs</b>	<b>StDev Abs</b>	<b>Avg Abs(440)</b>	<b>StDev (440)</b>
<b>1</b>	19.67	1.15	0.44	0.44	0.41	0.13
<b>2</b>	15.00	2.65	0.20	0.02	0.42	0.06
<b>3</b>	20.33	0.58	0.22	0.08	0.62	0.12
<b>4</b>	11.33	0.58	0.23	0.11	0.30	0.22
<b>5</b>	11.67	1.53	0.23	0.07	0.35	0.15
<b>6</b>	11.33	1.53	0.20	0.03	0.40	0.07
<b>7</b>	13.00	3.46	0.15	0.02	0.45	0.02
<b>8</b>	13.67	0.58	0.21	0.06	0.41	0.03
<b>9</b>	8.00	1.00	0.17	0.06	0.41	0.16
<b>10</b>	8.67	3.06	0.10	0.07	0.34	0.17
<b>11</b>	10.67	0.58	0.22	0.11	0.58	0.16
<b>12</b>	7.00	1.00	0.11	0.04	0.46	0.09
<b>13</b>	4.33	0.58	0.13	0.09	0.36	0.18
<b>14</b>	5.67	0.58	0.05	0.02	0.23	0.12
<b>15</b>	6.33	0.58	0.12	0.09	0.42	0.07
<b>16</b>	8.67	0.58	0.04	0.00	0.31	0.18

Appendix 4: Concentration of water column components 10/30/03

<b>Site</b>	<b>TSS (mg/l)</b>	<b>Cha (ug/l)</b>
<b>1</b>	37.72	8.79
<b>2</b>	36.51	1.70
<b>3</b>	47.77	6.04
<b>4</b>	29.91	3.80
<b>5</b>	32.52	1.59
<b>6</b>	33.75	6.99
<b>7</b>	40.15	6.62
<b>8</b>	37.15	5.26
<b>9</b>	28.21	7.50
<b>10</b>	23.66	8.90
<b>11</b>	31.02	1.25
<b>12</b>	23.93	4.99
<b>13</b>	15.90	7.82
<b>14</b>	18.20	2.14
<b>15</b>	22.32	1.32
<b>16</b>	23.90	9.04

Appendix 5: Light attenuation 10/30/03

<b>Site</b>	<b>Avg Kscalar</b>	<b>StDev Kscalar</b>	<b>Kdown</b>	<b>StDev Kdown</b>
<b>1</b>	1.76	0.41	1.35	0.50
<b>2</b>	1.66	0.12	-0.08	2.06
<b>3</b>	2.08	0.18	2.91	0.46
<b>4</b>	1.38	0.07	1.72	0.25
<b>5</b>	1.48	0.21	1.65	0.03
<b>6</b>	1.69	0.36	1.65	0.07
<b>7</b>	1.46	0.05	0.72	2.37
<b>8</b>	1.47	0.17	1.76	0.18
<b>9</b>	1.11	0.08	2.16	1.17
<b>10</b>	0.85	0.22	1.02	0.04
<b>11</b>	1.38	0.14	1.48	0.12
<b>12</b>	0.86	0.05	1.15	0.19
<b>13</b>	0.90	0.18	0.04	0.66
<b>14</b>	1.04	0.10	0.91	0.09
<b>15</b>	0.84	0.05	0.92	0.08
<b>16</b>	1.42	0.31	1.15	0.20